LONG-LEGGED PURSUIT CARNIVORANS (AMPHICYONIDAE, DAPHOENINAE) FROM THE EARLY MIOCENE OF NORTH AMERICA

ROBERT M. HUNT, JR.

Department of Geosciences
University of Nebraska
Lincoln, NE 68588-0514
(rhunt2@unl.edu)

BULLETIN OF THE AMERICAN MUSEUM OF NATURAL HISTORY
CENTRAL PARK WEST AT 79TH STREET, NEW YORK, NY 10024
Number 318, 95 pp., 39 figures, 7 tables
Issued March 17, 2009

Copyright © American Museum of Natural History 2009

ISSN 0003-0090

The amphicyonid carnivoran *Daphoenodon* (*Borocyon*) *robustum* from the early Miocene Runningwater Formation, northwestern Nebraska (paratype cranium, UNSM 25686, Marsland Quarry; mandible, UNSM 25684, Hemingford Quarry 7A).

CONTENTS

Abstract 4
Introduction 4
Abbreviations 5
Late Paleogene and Early Neogene Amphicyonids of North America 5
Early Miocene Daphoenines 7
Discovery of North American *Borocyon* 9
Geographic and Stratigraphic Distribution of North American *Borocyon* 11
Systematics 14
Daphoenodon (*Daphoenodon*) Peterson, 1909 14
Daphoenodon (*Borocyon*) Peterson, 1910 14
Daphoenodon (*Borocyon*) *robustum* Peterson, 1910 14
Daphoenodon (*Borocyon*) *niobrarensis* Loomis, 1936 21
Daphoenodon (*Borocyon*) *neomexicanus*, new species 23
Craniodental Osteology 31
Postcranial Osteology 36
Gait and Stance 71
Dentition and Feeding 75
Conclusions 82
Acknowledgments 83
References 84
Appendix 1. Limb Bone Lengths and Proportions (Carnivoran) 88
Appendix 2. Metapodial Lengths (Amphicyonidae) 91
Appendix 3. Metapodial Lengths (Canidae, Felidae, Ursidae, Hyaenidae) 93
Appendix 4. Comparative Lengths of Carnivoran Paraxonic Metapodials 95

ABSTRACT

In the early Miocene, endemic North American amphicyonids of the subfamily Daphoeninae evolved a lineage of large beardogs adapted for prey pursuit over open terrain. Three species comprise this lineage, here placed in the genus *Daphoenodon*, subgenus *Borocyon* Peterson, 1910, the sister subgenus to the daphoenine beardog *Daphoenodon* (*Daphoenodon*). These species (*Borocyon robustum*, *B. niobrarensis*, *B. neomexicanus*, n. sp.) are distinguished by limbs modified for fore–aft motion and parasagittal alignment contributing to a lengthened stride. These adaptive features are most evident in the terminal species, *B. robustum*, where the forelimb is conspicuously elongated.

The species of *Borocyon* increase in body size from small *B. neomexicanus*, known only from the latest Arikareean of northern New Mexico, through earliest Hemingfordian *B. niobrarensis* from western Nebraska and southeast Wyoming, to *B. robustum*, likely the keystone predator of its guild. *Borocyon robustum* (~100–150 kg) was the most widely distributed, occurring during the early Hemingfordian from the Pacific Northwest through the Great Plains to the Florida Gulf Coast. Regional aridity prevalent in the North American midcontinent during the Arikareean may have contributed to the emergence of *Borocyon* by providing an appropriate niche for a long-legged, open-country predator.

The skeleton of *Borocyon robustum*, based on composite elements acquired over many decades, reveals a carnivoran unlike any living pursuit predator. The species displays a mosaic of postcranial features that parallel limb elements of both highly evolved cursors (*Canis lupus*, *Acinonyx jubatus*) and large, ambush felids (*Panthera leo*, *P. tigris*). Skeletal traits contributing to its efficient locomotion include: proportionately lengthened forelimbs, the parasagittal radioulnar articulation with the humerus, an elongate radius and ulna, a modified carpal structure, and paraxonic elongate metapodials of the fore- and hindfoot, as well as details of the anatomy of femur, tibia, and proximal tarsals. These postcranial features indicate a large digitigrade predator with a number of anatomical parallels in the forelimb to running pursuit predators such as the wolf, but there are also musculoskeletal adaptations of the shoulder and hindlimb that compare with those of large, living felids.

Skull, dentition, and mandibular anatomy are similar to those of living wolves. However, *Borocyon robustum*, on average a much larger carnivore, placed even greater emphasis on a pattern of dental occlusion and toothwear suggesting both carnivory and durophagous habits. Physiological attributes of *Borocyon* that may have contributed significantly to its adaptive program as a pursuit predator remain unknown.

INTRODUCTION

Long-legged pursuit carnivorans are not represented among Paleocene and Eocene species of the Order Carnivora. In North America it is not until the late Oligocene/early Miocene that carnivorans evolve multiple lineages with elongated fore- and hindlimbs. Presumably limb elongation increased stride length, contributing to a more energy-efficient gait. This initial experiment attained a climax in the early Miocene when Arikareean temnocyonines and early Hemingfordian daphoenines developed striking anatomical parallels in limbs and feet relative to long-legged carnivorans common in late Cenozoic and Recent faunas.

A seasonally arid climate in the North American mid-continent in the early Miocene apparently contributed to the emergence of long-legged carnivorans. The development of widespread grasslands east of the Rocky Mountains favored larger carnivores adapted for open-country predation. Following the extinction of temnocyonines in latest Arikareean time, Eurasian digitigrade hemicyonine ursids (*Cephalogale* and its contemporary *Phoberocyon*) made a brief appearance in the early Hemingfordian of North America. However, the most spectacular response to these environmental conditions arguably took place among endemic daphoenine amphicyonids, a group characterized for most of its history by "normal" limb proportions. By the end of the early Miocene the daphoenines produced an enormous long-legged predator, *Daphoenodon* (*Borocyon*) *robustum*, the largest New World pursuit carnivoran evolved up to that time. This species and its lineage are the subject of this report.

ABBREVIATIONS

ACM	Amherst College Museum of Natural History, Amherst, Massachusetts
AM	Division of Mammalogy, American Museum of Natural History, New York
AMNH	Division of Paleontology, American Museum of Natural History, New York
CM	Division of Vertebrate Fossils, Carnegie Museum of Natural History, Pittsburgh
CNHM	Department of Geology, Field Museum of Natural History, Chicago
F:AM	Frick Collection, American Museum of Natural History, New York
FMNH	Field Museum of Natural History, Chicago
KU	Vertebrate Paleontology, University of Kansas, Lawrence
UCMP	University of California Museum of Paleontology, Berkeley
UF	Florida Museum of Natural History, University of Florida, Gainesville
UNSM	Vertebrate Paleontology, University of Nebraska State Museum, Lincoln
USNM	United States National Museum, Washington, D.C.
UW	Vertebrate Paleontology, University of Wyoming, Laramie
YPM-PU	Yale Peabody Museum (Princeton University collection), New Haven
ZM	Division of Mammals, University of Nebraska State Museum, Lincoln

LATE PALEOGENE AND EARLY NEOGENE AMPHICYONIDS OF NORTH AMERICA

The transition from Paleogene to Neogene mammal faunas in North America was marked by a turnover event within the large carnivore guild (Hunt, 2002a, 2004), an event in which amphicyonids play a prominent role (fig. 1).

Oligocene amphicyonids of North America include only species belonging to the endemic subfamily Daphoeninae and to the dentally and postcranially specialized Temnocyoninae. No Oligocene daphoenine attains large size—all are <20 kg in Orellan and Whitneyan faunas and are assigned to the genera *Daphoenus* and *Paradaphoenus* (Hunt, 1996, 2001). Their lower limb segments and feet are normally proportioned and lack elongation. A terminal and largest species of Oligocene *Daphoenus* (~20–25 kg, basilar skull length 24 cm, lacking a postcranial skeleton) co-occurs with the first appearance of temnocyonines in earliest Arikareean interval Ar1. Temnocyonines of moderate size (~20–30 kg, basilar lengths of 24–28 cm) are known in the early Arikareean (Ar1–Ar2 intervals fide Tedford et al., 2004), but pronounced specialization of the limbs and feet is not seen until the temnocyonine *Mammacyon obtusidens* appears in Ar2.

By the late Arikareean (Ar3–Ar4, early Miocene), all temnocyonine genera included at least one species with elongate limbs and, in all species where limb elements are adequately represented, the limbs and feet reflect similar anatomical specializations for a parasagittal gait incorporating an increase in stride length. Elongation of the lower limbs and feet is now documented in four Arikareean temnocyonine skeletons: *Temnocyon ferox* from the John Day Formation (Oregon); *Mammacyon obtusidens* from the Monroe Creek beds (South Dakota); a terminal species of *Mammacyon*, as yet unnamed, from north of Keeline (Wyoming); and a new genus and species from Stenomylus Hill at Agate National Monument (Nebraska).

With the extinction of temnocyonines at the end of the Arikareean, the niche for long-limbed predatory carnivorans in North America again became available. Mid-sized hemicyonine ursids entered the New World at this time (in Ar3–Ar4) and by the early Hemingfordian were represented by digitigrade yet short-lived species of *Cephalogale* and *Phoberocyon* (both extinct without descendants by the later Hemingfordian). However, the principal response to this ecological

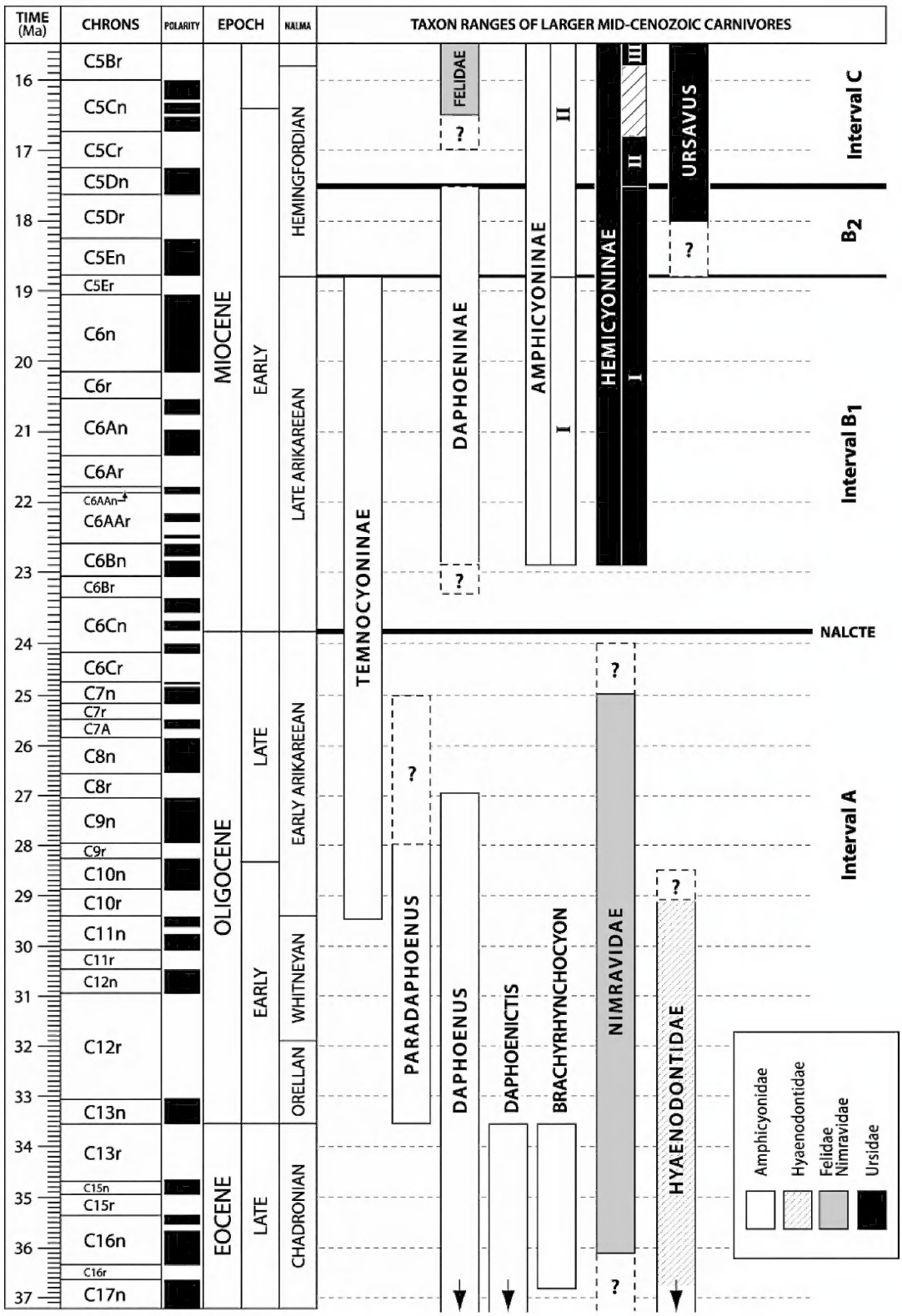
TIME (Ma)
CHRONS
POLARITY
EPOCH
NALMA
TAXON RANGES OF LARGER MID-CENOZOIC CARNIVORES
C5Br
C5Cn
C5Cr
C5Dn
C5Dr
C5En
C5Er
C6n
C6r
C6An
C6Ar
C6AAn
C6AAr
C6Bn
C6Br
C6Cn
C6Cr
C7n
C7r
C7A
C8n
C8r
C9n
C9r
C10n
C10r
C11n
C11r
C12n
C12r
C13n
C13r
C15n
C15r
C16n
C16r
C17n
MIOCENE
OLIGOCENE
EOCENE
EARLY
LATE
EARLY
LATE
HEMINGFORDIAN
LATE ARIKAREEAN
EARLY ARIKAREEAN
WHITNEYAN
ORELLAN
CHADRONIAN
FELIDAE
DAPHOENINAE
AMPHICYONINAE
HEMICYONINAE
URSAVUS
TEMNOCYONINAE
PARADAPHOENUS
DAPHOENUS
DAPHOENICTIS
BRACHYRHYNCHOCYON
NIMRAVIDAE
HYAENODONTIDAE
NALCTE
Interval C
B2
Interval B1
Interval A
Amphicyonidae
Hyaenodontidae
Felidae
Nimravidae
Ursidae

vacuum is found among species of the early Miocene amphicyonid *Daphoenodon*, which first appeared in the North American midcontinent in interval Ar3.

At first, *Daphoenodon* includes species with normally proportioned limbs. The late Arikareean *Daphoenodon superbus* from the carnivore dens at Agate National Monument (Peterson, 1910; Hunt et al., 1983) demonstrates this plesiomorphic state of the lower limb segments and feet. Here I employ as a subgenus of *Daphoenodon*, O.A. Peterson's (1910) nomen *Borocyon*, to designate a derived lineage of remarkable long-legged amphicyonids, the terminal species enormous, with skull and skeleton exceeding in size those of the largest living wolves (*Canis lupus*). The hypodigm of this terminal species includes O.A. Peterson's fragmentary holotype of *Borocyon*, *B. robustum* Peterson, 1910. The earliest record of *Borocyon* is restricted to the latest Arikareean of New Mexico. By the early Hemingfordian the lineage had spread across the continent from the Pacific Northwest through the Great Plains to the Florida Gulf Coast (fig. 2). *Borocyon* is known only from the latest Arikareean and early Hemingfordian in North America, becoming extinct at ~17.5 Ma.

EARLY MIOCENE DAPHOENINES

The North American fossil record of early Miocene amphicyonids is best represented in Arikaree and Hemingford Group sediments of western Nebraska and southeastern Wyoming. Here fine-grained volcaniclastic sandstones of the Harrison and Anderson Ranch Formations (Ar3–Ar4: late to latest Arikareean) and fluvial sands and gravel of the Runningwater Formation (early Hemingfordian) yield a succession of species represented by well-preserved craniodental and postcranial remains, in some cases including sufficient numbers of individuals to assess population variation in these carnivores. These beardogs fall into the three North American subfamilies: daphoenines, amphicyonines, and temnocyonines. Daphoenines had been present in North America since the late Eocene and are considered endemic; amphicyonines are early Miocene immmigrants from Eurasia; temnocyonines first appear in the Oligocene and become extinct by the end of the Arikareean in the early Miocene.

Although a number of amphicyonid species have come from Arikareean localities in western Nebraska and southeastern Wyoming, only temnocyonines show marked specialization of the limbs at this time. The daphoenines *Daphoenodon* (*Daphoenodon*) *superbus* from the Anderson Ranch Formation of western Nebraska (Peterson, 1910) and its probable ancestor *D.* (*D.*) *notionastes* from Florida (Frailey, 1979), the oldest currently recognized species of the genus, are both short-limbed animals, known from reliably associated cranial and postcranial material. A larger, latest Arikareean form from southeastern Wyoming, *D.* (*D.*) *falkenbachi* (Hunt, 2002b), seems to be directly descended from *D.* (*D.*) *superbus*. Although represented only by fragmentary postcranial material, it possibly had achieved an incipient limb elongation, but the defining skeletal elements, particularly its forelimb, have not been recovered. Other late and latest Arikareean amphicyonids (*Ysengrinia americana*, *Adilophontes brachykolos*) are short-limbed carnivores (Hunt, 2002a, 2002b), and their skeletons indicate an attack strategy more likely relying on a rush from cover followed by a short pursuit.

←

Fig. 1. Temporal range diagram of late Eocene, Oligocene, and early Miocene North American Carnivora, illustrating the large carnivoran turnover event (NALCTE) in proximity to the Oligocene–Miocene boundary. Following NALCTE, interval B_1 is characterized by persistence of temnocyonine and daphoenine amphicyonids at the time of the first New World appearance of amphicyonines and hemicyonine ursids. Interval B_2 is typified by extinction of temnocyonines, presence of large daphoenines (*Borocyon robustum* and *B. niobrarensis*), and appearance of the ursid *Ursavus*. Interval C features the extinction of daphoenines, appearance of the first felids, and the presence of advanced amphicyonines, hemicyonines, and *Ursavus*.

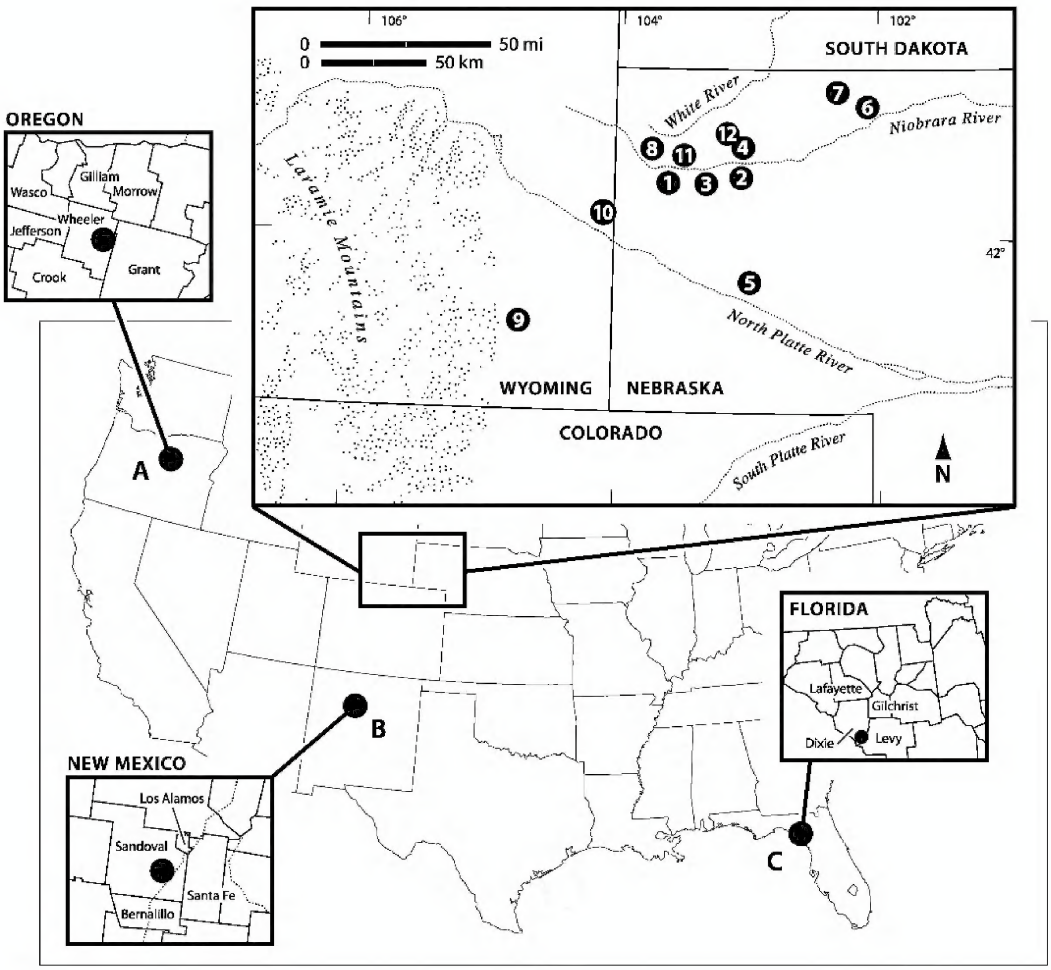

Fig. 2. Geographic distribution of the daphoenine amphicyonid *Borocyon* in North America. **A**, *Borocyon robustum*, UCMP Locality PG-36, Rose Creek Mbr., upper John Day Fm., Oregon; **B**, *Borocyon neomexicanus*, Standing Rock Quarry, Piedra Parada Mbr., Zia Sand, New Mexico; *Borocyon robustum*, Blick Quarry, Chamisa Mesa Mbr., Zia Sand, New Mexico; **C**, *Borocyon* cf. *B. robustum*, sinkhole or fissure in Suwanee River, Florida. Inset shows localities in western Nebraska and Wyoming: **1**, *B. robustum* holotype, Whistle Creek area, Sioux Co.; **2**, Hemingford Quarries 7A, 7B, 12A, and 12D, Box Butte Co.; **3**, Marsland, Hovorka, and Shimek Quarries, Box Butte Co.; **4**, Dunlap Camel Quarry, Dawes Co.; **5**, Bridgeport Quarries, Morrill Co.; **6**, Aletomeryx Quarry, Cherry Co.; **7**, UNSM Locality Sh-101B, Sheridan Co.; **8**, Northeast of Agate, Sioux Co.; **9**, Horse Creek Quarry, Laramie Co.; **10**, Merycochoerus Butte, Goshen Co.; **11**, Skavdahl Ranch, Sioux Co.; **12**, Red Horse Quarry, Dawes Co. Nos. 1–5, *B. robustum*; nos. 6–12, *B. niobrarensis*.

In 1947 Ted Galusha of the Frick Laboratory discovered a small population sample of *Daphoenodon* at Standing Rock Quarry in the early Miocene Zia Sand Formation of New Mexico (Galusha, 1966). Although clearly referable to *Daphoenodon* on craniodental traits, this remarkable latest Arikareean species had developed more elongate limbs and somewhat larger size relative to the northern late Arikareean genoholotypic species, *D. superbus*, from western Nebraska. This undescribed New Mexican daphoenine, here assigned to *Daphoenodon* (*Borocyon*) *neomexicanus*, n. sp., is known only from the sample from Standing Rock Quarry despite the presence of coeval early Miocene sediments common in the Great Plains.

The first appearance of a long-limbed species of *Daphoenodon* in the Great Plains occurs in the earliest Hemingfordian. The lower Runningwater Formation of western Nebraska and temporally equivalent sediments at Horse Creek Quarry in southeastern Wyoming yielded a larger animal than the New Mexican species, referred here to *Daphoenodon* (*Borocyon*) *niobrarensis* Loomis, 1936. This carnivore displays a moderate degree of limb elongation that foreshadows an even larger, long-limbed *Daphoenodon* from the upper Runningwater Formation, referred in this report to *Daphoenodon* (*Borocyon*) *robustum* (Peterson), 1910.

Borocyon is employed here as a subgenus of *Daphoenodon* to set apart these long-limbed daphoenines of latest Arikareean and early Hemingfordian age from the plesiomorphic subgenus *Daphoenodon* with "normally" proportioned limbs. *Daphoenodon* (*Daphoenodon*) is reserved for the ancestral, short-limbed species (*D. superbus*, *D. notionastes*) that precede the long-footed daphoenines placed here in *Borocyon*. The two subgenera are united by their shared, derived basicranial anatomy, particularly by the form and relationships of the auditory bulla, which is unique to the genus *Daphoenodon*.

Borocyon is best represented in western Nebraska, where the largest animals are referred to *B. robustum* and occur in Hemingford Quarries 7A, 7B, and 12D and in the Bridgeport Quarries. *Borocyon niobrarensis* is known from only a few individuals from western Nebraska and southeastern Wyoming, and they average smaller in size than *B. robustum*. The last records of *Borocyon*, in fact of the Daphoeninae, are from the Hemingford Quarries, estimated at ~17.5 Ma.

DISCOVERY OF NORTH AMERICAN *BOROCYON*

During an expedition of the Carnegie Museum of Natural History (Pittsburgh) to western Nebraska in 1905, T.F. Olcott, a collector in the employ of the museum, discovered the fragmentary remains of a large amphicyonid carnivore (CM 1918, holotype of *Borocyon robustum*) several miles southeast of the Agate Spring Quarries in Sioux County, western Nebraska (fig. 3). Olcott's supervisor in the field, O.A. Peterson, had discovered the Agate bonebed just one year previously, in August of 1904, but had postponed major excavation until 1905.

Olcott and Peterson had arrived early, in April 1905, to begin the excavation of the waterhole bonebed on Carnegie Hill. Peterson was soon called back to Pittsburgh, leaving Olcott in charge of the quarry work from April into July. Late in July, Peterson returned and resumed oversight of the Agate excavations. Peterson (1910) also apparently excavated the carnivore dens at Beardog Hill (Carnegie Quarry 3) after his return in July, extending this work into early October (Carnegie field labels show that excavations at Quarry 3 occurred at least from August 11 to October 4). Whether Peterson remained in the field after October 4th is uncertain, but Olcott continued for at least an additional week.

Following the conclusion of the 1905 excavations in the Agate quarries, Olcott explored the terrain southeast of the quarry hills along the crest of the Agate anticline (Schramm and Cook, 1921). The south limb of the anticline is dissected by a number of deep ephemeral draws that join to form the headwater drainage of Whistle Creek. In his publication first describing *Borocyon* (CM 1918), Peterson (1910) specifically cited Whistle Creek as the locality for the holotype, and this designation agrees with information on the original field label found with the holotype of *Borocyon* at the Carnegie Museum. Written in pencil is the date of collection, October 13, 1905, followed by the accession number (2905), the designation Carnivora, and the following stratigraphic and geographic information: "upper Loup Fork (Neb. beds), 5 miles E. of Agate, 3 miles S. Niobrara River, Sioux Co., Nebr." Later, a description was added in ink: "Fragts of hind limb & foot and front of jaw". In a darker ink, at the time of Peterson's (1910) publication of the material, the department number CM 1918 and the name *Borocyon robustum* in script were added to the label.

The terrain 5 miles east of the Agate post office and 3 miles south of the Niobrara

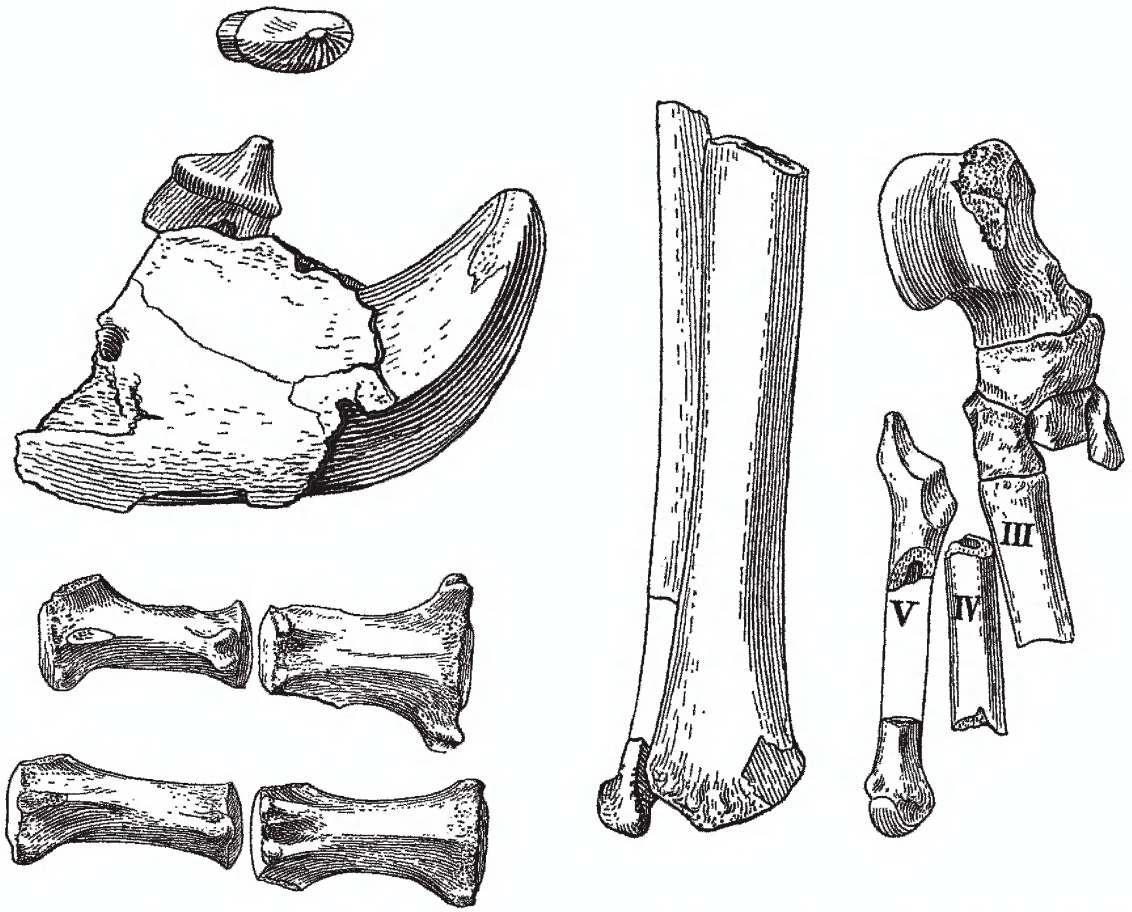

Fig. 3. Peterson's holotype of *Borocyon robustum* (CM 1918): an anterior mandible with right p2, p1 alveolus, and worn canine; two caudal vertebrae indicating a long tail; distal right tibia and fibula; partial right tarsus-metatarsus including astragalus, navicular, ecto-, meso-, and entocuneiforms, and parts of metatarsals 3, 4, and 5. Runningwater Fm., Whistle Creek area, Sioux Co., Nebraska.

River in Sioux County is situated high on the Agate anticline in proximity to the large draws making up the headwaters of Whistle Creek. These draws dissect the southeastern corner of the Whistle Creek NW 7.5-minute topographic quadrangle. Reddish-brown to buff silts, sands, and interbedded granitic gravel of the Runningwater Formation comprise much of the outcrop in this area and yield early Hemingfordian mammals. Fine reddish silty sand identical to sediment from these exposures still adheres to the *Borocyon* holotype. Peterson (1910) published the stratigraphic horizon of the holotype as "Upper Harrison" because at that time he thought that all reddish silty sands in the area belonged to that unit. Later it was realized that lower Runningwater fine-grained sands and silts in the Whistle Creek and Agate areas are reddish-brown, much like typical Upper Harrison sandstones (now Anderson Ranch Formation, Hunt, 2002b). These reddish-brown Runningwater sediments had been confused with Upper Harrison (Anderson Ranch) sediments by Peterson.

Peterson published the holotype material of *Borocyon robustum* in 1910, together with a description of the smaller plesiomorphic *Daphoenodon superbus* from the carnivore dens at Carnegie Quarry 3 at Agate. He considered the *Borocyon* holotype fully adult, based on its worn canine, remarking that it was subdigitigrade, the size of a lion, and related to *Daphoenodon*. Its foot bones were

very similar to those of *D. superbus*, but certain ones, such as the astragalus, suggested a longer footed carnivore. In this regard Peterson anticipated the elongated limbs of this amphicyonid, which prove to be its most arresting anatomical characteristic.

GEOGRAPHIC AND STRATIGRAPHIC DISTRIBUTION OF NORTH AMERICAN *BOROCYON*

Early Hemingfordian *Borocyon*

Daphoenodon (*Borocyon*) *robustum* is the terminal species of the genus in North America and is well represented by craniodental and postcranial remains. The best preserved sample was collected in the Hemingford Quarries, Box Butte County, Nebraska, worked by the University of Nebraska from 1934 to 1941 (fig. 2, localities 2, 3). The three known crania of the species, 10 nearly complete mandibles, and representative postcrania come from these sites. Several of the quarries yielding *Borocyon* in the Runningwater Formation include the youngest mammal faunas identified in that rock unit and show that this large daphoenine survived to the conclusion of Runningwater deposition in the region.

The Box Butte Formation of medial Hemingfordian age is directly superposed on the Runningwater beds over much of its outcrop area in northwestern Nebraska (Galusha, 1975). The Box Butte Formation displays a much different lithologic aspect and style of sedimentation relative to the Runningwater, and its mammal fauna is markedly distinct. No evidence of *Borocyon* or any other daphoenine amphicyonid has been found in Box Butte deposits. Amphicyonids from the Box Butte and Sheep Creek Formations (medial to late Hemingfordian) in Nebraska belong to the subfamily Amphicyoninae made up of Eurasian immigrant lineages.

Whereas most *Borocyon* fossils from the Runningwater beds are from quarries in Box Butte and Dawes Counties in northwest Nebraska, Peterson's (1910) holotype of *Borocyon robustum* is an isolated occurrence to the west in Sioux County (fig. 2, locality 1). Quarry accumulations of fossils in Runningwater exposures west of the principal quarries in Dawes and Box Butte Counties were unknown until recent discoveries by the University of Nebraska in 1997 in Sioux County. These quarries, to date only explored by preliminary excavations, have yet to produce carnivore material.

The only other locality in Nebraska where *Borocyon robustum* has been found is a waterhole bonebed in Morrill County in the southern Nebraska panhandle, approximately 70 km (~44 mi) southeast of the principal Hemingford Quarries. Here sediments of early Hemingfordian age were explored by UNSM field crews working under the auspices of the Works Progress Administration. Excavations took place during 1932–1933 and 1940, with a few fossils found in 1934–1935 and 1937. Large numbers of the early Miocene rhinoceros *Menoceras*, along with various cervoids, camels, equids, and carnivores, were collected at several closely adjacent sites in the immediate area, collectively termed the Bridgeport Quarries (fig. 2, locality 5). Several species of amphicyonids were found at these sites, including isolated teeth, edentulous mandibles, and postcranial bones of *Borocyon robustum*. The Bridgeport *Borocyon* sample closely corresponds in morphology of isolated teeth and postcranials to the Runningwater hypodigm. However, the Bridgeport specimens appear to have accumulated in the waterhole environment over a prolonged period. Most teeth of Bridgeport *Borocyon* share similar dental dimensions with Runningwater *Borocyon*, but the quarries also include small individuals that could be geologically older. Many specimens show the marks of scavenging and exhibit the dull, worn edges indicating long-term abrasion within the waterhole environment.

Borocyon robustum occurs at only two localities outside of western Nebraska. Early Miocene mammals apparently found in a sinkhole in the bed of the Suwanee River in northern Florida (fig. 2C) included this beardog, referred here to *Borocyon* cf. *B. robustum*. The species is represented by a reconstructed palate with nearly perfect dentition, a few isolated teeth, and numerous postcranial bones. The palate found in the 1980s was retained by a private collector, but

the University of Florida (UF 95092) and University of Kansas (KU 114592) have casts of the specimen. The palate and teeth belong to an individual nearly equal in size to the largest crania (UNSM 25547, 26416) from the Hemingford Quarries in the upper Runningwater Formation. However, the sample of postcranial bones, although fragmentary, shows that the Florida population averaged somewhat smaller in body size relative to the upper Runningwater *B. robustum* population. Yet the Florida beardog possesses the typical anatomical traits of the species in its teeth and postcrania. The occurrence of *Borocyon* at the Suwanee River locality is doubtless of early Hemingfordian age, based on the associated fauna.

Rare fragmentary remains of what appear to be a single individual of *B. robustum* were found in basal sands and gravel of the Rose Creek Member of the John Day Formation, Grant County, Oregon (fig. 2A). The Rose Creek Member is the youngest lithostratigraphic unit recognized in the eastern facies of the John Day Formation (Hunt and Stepleton, 2004, 2006) and is well exposed south of Kimberly, Oregon. These Rose Creek exposures represent the final episode of John Day sedimentation prior to outpouring of the Columbia River flood basalts within the geographic area in north-central Oregon first described by Merriam (1901) and later studied by Fisher and Rensberger (1972). The Rose Creek Member is biochronologically dated by an early Hemingfordian mammal fauna from a single locality (Picture Gorge 36) south of Kimberly (Hunt and Stepleton, 2006). From this locality John Rensberger and his associates collected teeth (p2–m2), an astragalus, and additional fragments of a beardog during his biostratigraphic study of the formation in 1961–1962. Later, in 1993, at the same site and very likely on the same sandstone ledge, we recovered additional teeth and fragments of this individual. Evaluation of the diagnostic Berkeley material (UCMP 76864, astragalus; UCMP 76875, lower dentition) identified it as *Borocyon robustum*, and extended the early Hemingfordian range for this daphoenine to include the Pacific Northwest, so that together with the Great Plains and Florida occurrences, the species spans the North American mid-latitudes.

Earliest Hemingfordian *Borocyon*

Early Miocene mammal faunas of earliest Hemingfordian age from the lower part of the Runningwater Formation in northwest Nebraska and from age-equivalent strata in southeast Wyoming have produced a few individuals of *Borocyon* that do not fit comfortably into the hypodigm of *B. robustum* but rather indicate a taxon slightly older than and probably ancestral to Peterson's species. These carnivores are slightly smaller than *B. robustum* in dental dimensions and show less elongation of their lower limb bones (particularly the radius, ulna, astragalus, calcaneum, and metapodials).

The first of these is the holotype of *Daphoenodon niobrarensis* Loomis, 1936 (ACM 3452) from Aletomeryx Quarry, Cherry County, western Nebraska (fig. 2, locality 6). This quarry in the lower Runningwater Formation was excavated at various times by the University of Nebraska, the Frick Laboratory of the American Museum, Yale University, and Amherst College. Here in 1934 F.B. Loomis (Amherst) discovered the associated mandibles, upper molar, and nearly complete forelimbs of a large representative of *Daphoenodon* (Loomis, 1936). The forelimbs establish the proportions of the lower limb elements relative to the humerus and scapula, and these elements prove to be less elongate than the limb elements of the *B. robustum* sample from the Hemingford Quarries. This shorter limbed amphicyonid is here designated *Daphoenodon* (*Borocyon*) *niobrarensis*. In addition to the holotype specimen, other isolated elements have been found at Aletomeryx Quarry. Of interest are two metacarpals that are also elongate and anatomically comparable to those of the holotype, but much more slender and gracile. Thus dimorphism is indicated for *B. niobrarensis*, and this condition can also be demonstrated for *B. robustum* from the Hemingford Quarries.

A second occurrence was found at the Horse Creek Quarry of the University of Wyoming in early Miocene beds deposited on

the eastern slope of the Laramie Mountains (fig. 2, locality 9). The sediments and mammal fauna of the Horse Creek Quarry were described by Cassiliano (1980), who established a lithostratigraphy for the area. At that time the Horse Creek Quarry fauna was thought to be late Arikareean in age. Subsequent examination of these mammals at the University of Wyoming, following our reassessment of Hemingfordian rocks and faunas in western Nebraska (MacFadden and Hunt, 1998), suggests that it is an earliest Hemingfordian assemblage, coincident in age with mammals of the Carpenter Ranch Formation of southeastern Wyoming (Hunt, 2005) and with the lower Runningwater faunas of Nebraska. The Horse Creek amphicyonid (UW 10004) is represented by a single individual: a mandible associated with a partial postcranial skeleton that allows limb proportions to be accurately determined. This linking of dentition with both fore- and hindlimbs is the only such association at this temporal horizon. The metacarpals and other forelimb elements are proportionally nearly identical to these elements of the *B. niobrarensis* holotype.

A third individual (F:AM 107601) comes from Sioux County, Nebraska, northeast of Agate in the lower Runningwater Formation (fig. 2, locality 8), and includes a mandible with associated ulna, innominate, calcaneum, and metacarpal. The ulna indicates that the forelimb had lengthened to the extent seen in the Horse Creek and Aletomeryx Quarry amphicyonids, and the metacarpal also corresponds to the equivalent bones of *Borocyon niobrarensis* from these quarries. This amphicyonid and the individuals from the Horse Creek and Aletomeryx Quarries are all accompanied by earliest Hemingfordian mammals, demonstrating that these beardogs are penecontemporaneous and can be assigned to a single taxon preceding *Borocyon robustum* in time. *Daphoenodon* (*Borocyon*) *niobrarensis* is employed here for this hypodigm.

A fourth occurrence consists of a partial mandible from the earliest Hemingfordian Carpenter Ranch Formation (Hunt, 2005), Goshen County, southeastern Wyoming, in proximity to the Nebraska–Wyoming state boundary (fig. 2, locality 10). It is only tentatively referred to *Daphoenodon* (*Borocyon*) due to absence of postcranials and to heavily worn teeth.

Latest Arikareean *Borocyon*

The population sample of a small *Daphoenodon* from latest Arikareean sediments at Standing Rock Quarry in northern New Mexico (fig. 2B) shares a number of derived dental and skeletal traits with the much larger species *Borocyon robustum*. Despite their smaller size, these carnivores had already developed elongated lower limbs. Although limb elongation in itself is not a sufficient criterion allying this species to *B. robustum*, the derived morphology of the radius, astragalus, and metapodials shows near identity to the large Runningwater species. Moreover, the broad skull and diagnostic form of the M2 indicate a close affinity with *B. robustum* and suggest a plausible ancestor–descendant relationship.

The stratigraphic occurrence of this species, here named *Daphoenodon* (*Borocyon*) *neomexicanus*, n. sp., is discussed by Galusha (1966), Tedford (1981, 1982), and Gawne (1981). Galusha (1966) placed Standing Rock Quarry low in the Piedra Parada Member of the Zia Sand, about 20 m above the base of the formation. Gawne (1981) indicated that the member began with widespread sheetlike channel deposits, overlain by eolian sediments that make up the bulk of the member. She envisioned the depositional setting as a semiarid to arid open plains environment.

Two slender metacarpals of a female individual of *Borocyon robustum* were found in Blick Quarry in 1949 in the Chamisa Mesa Member of the Zia Sand Formation, an early Hemingfordian site a short distance north of Standing Rock Quarry in New Mexico. These metacarpals are the only record of *B. robustum* from the American Southwest. They suggest that *Daphoenodon* (*Borocyon*) *neomexicanus* at Standing Rock Quarry, after evolving to *D.* (*B.*) *robustum*, possibly spread northward into the Great Plains, the Pacific Northwest, and eastward to the coastal plain of the Gulf of Mexico during the Arikareean–Hemingfordian transition.

SYSTEMATIC PALEONTOLOGY

Daphoenodon (*Daphoenodon*) Peterson, 1909

Amphicyon superbus Peterson, 1907.
Daphoenodon superbus Peterson, 1909.

ETYMOLOGY: From the Greek δαιοινός, "blood-reeking", and ὀδούς, "tooth", in reference to its carnivorous habit.

This is the sister subgenus of *Daphoenodon* (*Borocyon*). *D.* (*D.*) *superbus* remains the best known species of the subgenus, represented by the holotype, a nearly complete skeleton of an adult female (CM 1589), and other individuals from the carnivore dens (Carnegie Quarry 3), Agate National Monument, Nebraska (Peterson, 1910; Hunt et al., 1983).

Daphoenodon (*Borocyon*) Peterson, 1910

Borocyon robustum Peterson, 1910.

DIAGNOSIS: The subgenus *Borocyon* differs from all other New World amphicyonids by its longer distal forelimbs and by proportions of the proximal tarsals (figs. 33, 34). *Borocyon* differs from its sister subgenus *Daphoenodon* by its longer distal forelimbs and by a "folded" M2, as well as by measurements of the dentition (figs. 17, 18; tables 2, 3). It is distinguished from *Amphicyon galushai* by its unreduced premolars, more sectorial carnassials, reduction and loss of M3, "folded" occlusal surface of M2, differently proportioned proximal tarsals (figs. 33, 34), and longer distal forelimbs with much more elongate paraxonic metapodials (see text for discussion of postcranial anatomy).

ETYMOLOGY: From the Greek βορός, "devouring", and κύων,"dog".

On the reduction of the genus *Borocyon* Peterson, 1910, to the rank of subgenus:

International Code of Zoological Nomenclature (1985): Article 43— (a) A name established for a taxon at either rank in the genus group [i.e., genus or subgenus] is deemed to be simultaneously established with the same author and date for a taxon based upon the same name-bearing type (type species) at the other rank in the group, whether that type was fixed originally or subsequently. (b) When a nominal taxon is raised or lowered in rank in the genus group its type species remains the same [the neuter *-um* is retained here although *robustus* is appropriate].

Daphoenodon (*Borocyon*) *robustum* Peterson, 1910

Figures 3–8, 15, 21, 22, 24–28, 31, 32, 37–39

Borocyon robustum Peterson, 1910.
Large daphoenine, n. sp., Hunt and Stepleton, 2004: 87, 89.

HOLOTYPE: CM 1918 (field no. 2905), right mandibular fragment with c, p2, an isolated m2 (not reported by Peterson), three complete and one partial caudal vertebrae, a right astragalus, navicular, ecto-, ento-, and mesocuneiforms, 11 phalanges, a trapezoid, sesamoid, five fragmentary metapodials [left proximal metatarsal 3, proximal and ?distal metacarpal 5, two metapodial diaphyses without proximal or distal ends, complete right metacarpal 1], distal tibia, shaft and distal end of fibula (fig. 3).

HOLOTYPE HORIZON AND LOCALITY: From the Runningwater Fm., Sioux Co., Nebraska. The original field label states: upper Loup Fork (Nebraska beds), 5 miles east of Agate, 3 miles south of the Niobrara River, Sioux Co., Nebraska. Collected by T.F. Olcott, 13 October 1905. Peterson (1910: 263) reported the horizon as "Upper Harrison beds" and the locality as "Whistle Creek, Sioux County, Nebraska".

DIAGNOSIS: Largest known daphoenine amphicyonid, and the largest species of *Borocyon*, with basilar skull length of 285–294 mm, differing from *B. niobrarensis* by larger average body size and dentition (c–m2 length, ~110–120 mm), consistent loss of M3, more elongate forelimbs, and greater modification of proximal tarsals (figs. 33, 34, astragalus-calcaneum) for fore–aft motion (see text for detailed discussion). Distinguished from *B. neomexicanus* by much larger body size, dentition (figs. 17, 18; tables 2, 3), and more elongate yet anatomically similar distal forelimbs.

PARATYPES: UNSM 25686 (field no. 2-6-8-35NWP), skull lacking basicranium, with right P3, M1–2, left P2–M2; UNSM 25685 (field no. 3-6-8-35NWP), right mandible, p2, p4–m3. The mandible was found in proximity to the skull; the skull and mandible probably represent a single individual.

Fig. 4. Cranium of *Borocyon robustum* (UNSM 26416), Hemingford Quarry 12D, Box Butte Co., Nebraska, upper Runningwater Fm., early Hemingfordian. **A**, Dorsal view showing broad forehead for expanded frontal sinuses; **B**, ventral view showing broad palate, P4–M2, and characteristic absence of M3 in *B. robustum*.

PARATYPE HORIZON AND LOCALITY: Runningwater Formation (upper part), Marsland Quarry (UNSM Loc. Bx-22), Box Butte Co., Nebraska.

REFERRED SPECIMENS: Runningwater Formation, northwestern Nebraska—

SKULLS, MANDIBLES, AND ISOLATED TEETH

Box Butte Co., Nebraska: (1) UNSM 25547 (field no. 2499-39), skull with right P2, P4–M2, left P4, Hemingford Quarry 7B; (2) UNSM 26416 (field no. 4553-41), skull

Fig. 5. Stereoimage of the diagnostic upper molars (M1–M2) and carnassial (P4) of *Borocyon robustum* (UNSM 25547), Hemingford Quarry 7B, upper Runningwater Fm., Box Butte Co., Nebraska. Note elongate P4, the notch (at arrow) in the anterolingual cingulum of M1, the "folded" M2 (see text), and absence of M3.

lacking posterior cranium, with right P4–M2, left P2, P4–M2, Hemingford Quarry 12D; (3) UNSM 25548 (field no. 2200-39), right mandible, c, p1–m3, Hemingford Quarry 7B; (4) UNSM 25549 (field no. 1000-39), right mandible, i2–i3, p1–m3, Hemingford Quarry 7B; (5) UNSM 25550 (field no. 2201-39), right mandible, p2–m3, Hemingford Quarry 7B; (6) UNSM 25551 (field no. 4946-40), right mandible, p4–m2, Hemingford Quarry 12D;

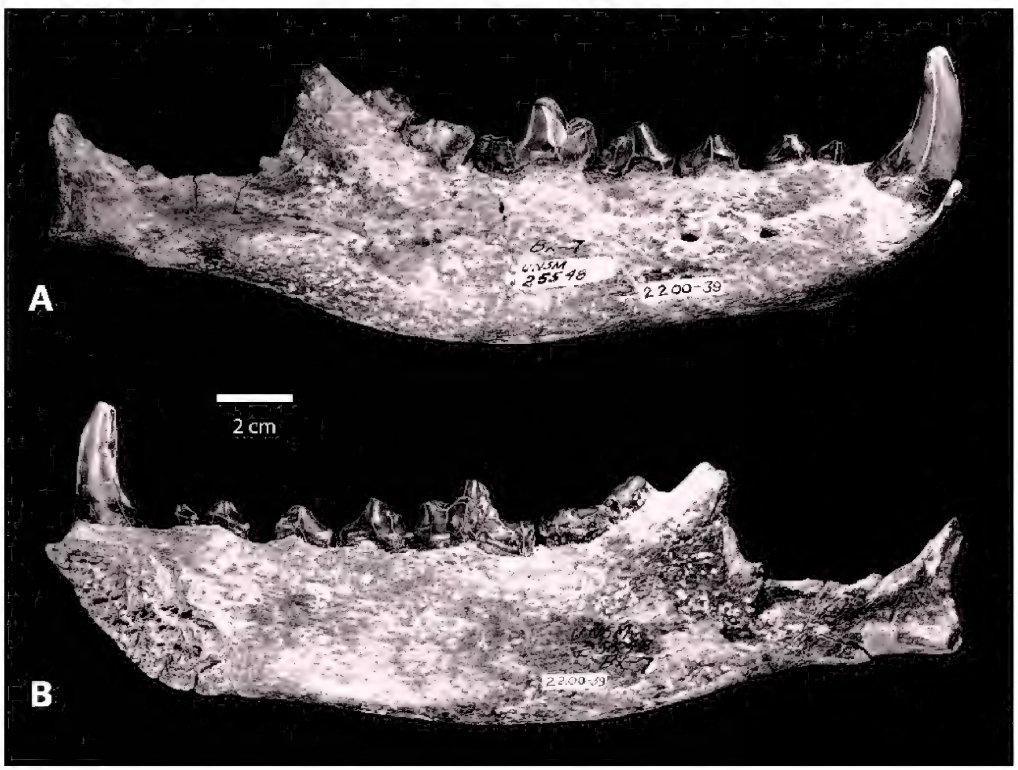

Fig. 6. Mandible of *Borocyon robustum* (UNSM 25548), Hemingford Quarry 7B, Box Butte Co., Nebraska, upper Runningwater Fm., early Hemingfordian. **A**, Lateral view, right c, p1–p4, m1–m3; **B**, medial view. Note m3 elevated on margin of ascending ramus.

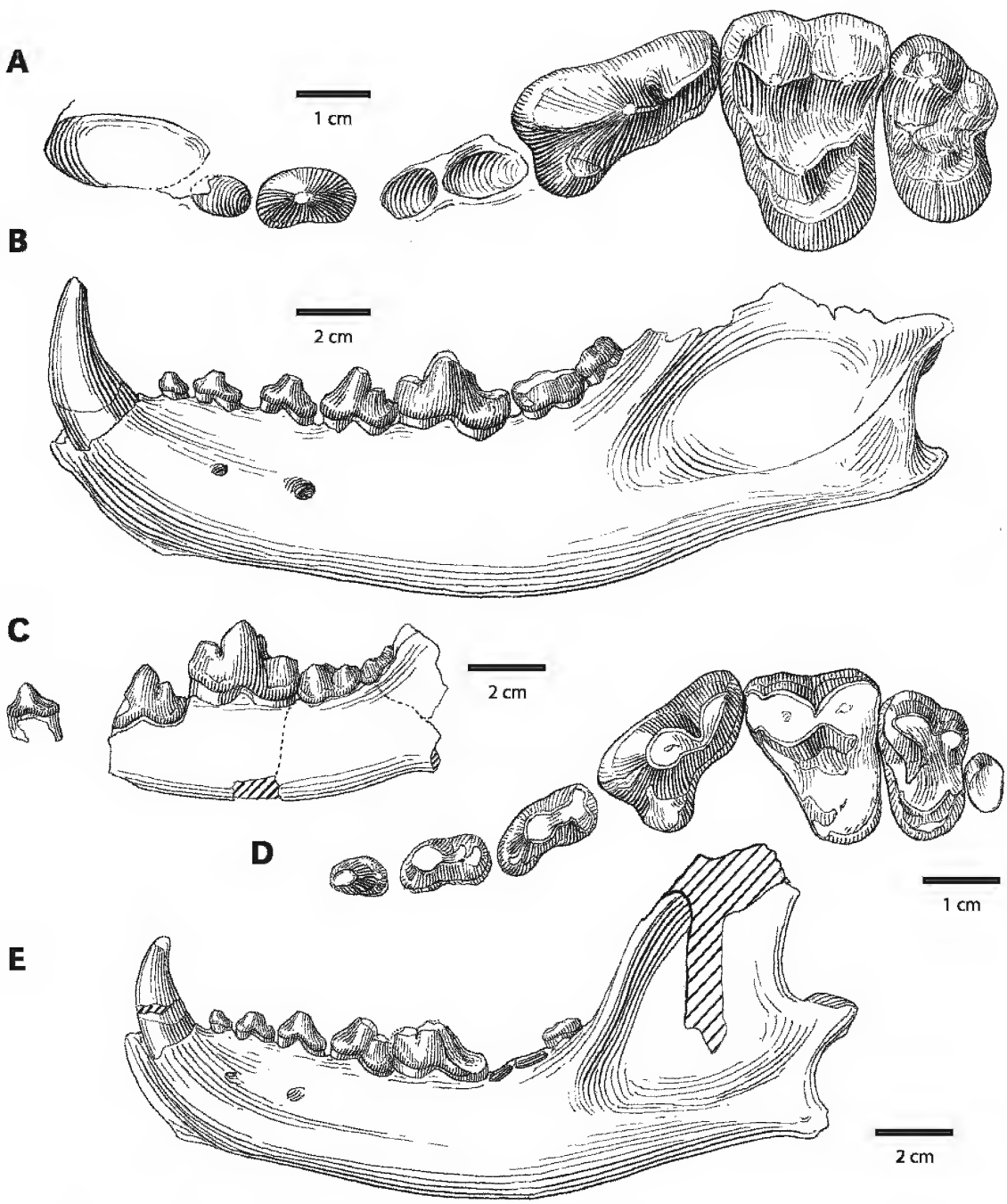

Fig. 7. Comparison of dentitions of *Borocyon robustum* (**A**, **B**) and *B. neomexicanus* (**C–E**), end member species of the *Borocyon* lineage. **A**, UNSM 25547, P2, P4–M2, alveoli for C, P1, P3; **B**, UNSM 25684, c, p1–p4, m1–m3; **C**, F:AM 49241, juvenile, p2, p4–m3; **D**, F:AM 49239, P1–P4, M1–M3; **E**, F:AM 49239, c, p1–p4, m1, m3, alveoli of m2.

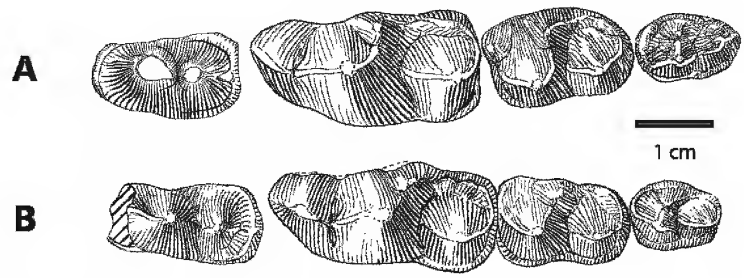

Fig. 8. Occlusal views of p4–m3 of the end-member species of the *Borocyon* lineage. **A**, *B. robustum*, UNSM 25552; **B**, *B. neomexicanus*, F:AM 49241. The squared posterior border of p4 is characteristic of species of the subgenera *Borocyon* and *Daphoenodon*.

(7) UNSM 25552 (field no. 73-9-8-37NP), juvenile right mandible, dp4, m1–m3 erupting, Hemingford Quarry 12D; (8) UNSM 25684 (field no. 181-7-8-37SP), left mandible, c, p1–m3, Hemingford Quarry 7A; (9) UNSM 25577 (field no. 4941-40, right mandibular fragment, p2–p4, Hemingford Quarry 12D; (10) UNSM 27002 (field no. 4675-40), left mandible, c, p2–m2, Hemingford Quarry 12D; (11) UNSM 26417 (field no. 5549-68), right mandible, i2–i3, c, p2–m3, Hemingford Quarry 21 (Hovorka's Quarry); (12) FA:M field no. H457-4060, left mandible, p4–m2, Hemingford Quarry 1 (Barbour-Hemingford Quarry); (13) UNSM 25576 (field no. 1701-39), mandibular fragment, p3 and partial p4, Hemingford Quarry 7B. **Dawes Co., Nebraska:** (14) F:AM 25408, left mandible, m1–m2, damaged p3–p4, Dunlap Camel Quarry. **Dawes Co., Nebraska:** (15) F:AM 25402, left P4; (16) F:AM 25403, left P4; (17) F:AM 25404, left M2; all from Dunlap Camel Quarry. **Box Butte Co., Nebraska:** (18) UNSM 25571 (field no. 2207-39), right m1, Hemingford Quarry 7B; (19) UNSM 26422 (field no. 19-29-7-35NWP), right m1, heavily worn, Hemingford Quarry 23 (Shimek's Quarry); (20) UNSM 26423 (field no. 1018-39), left p4, Hemingford Quarry 7B; (21) UNSM 26452 (field no. 2004-39), right P4; (22) UNSM 26427 (field no. 5-12-8-37SP), right M2, Hemingford Quarry 12A.

Postcranials—Forelimb

Box Butte Co., Nebraska: (1) UNSM 26419 (34-26-6-35NWP), diaphysis of right humerus, Hemingford Quarry 23 (Shimek's Quarry); (2) UNSM 26420 (field no. 4863-41), distal left humerus, Hemingford Quarry 12D; (3) UNSM 26421 (field nos. 1 to 3-17-7-37NP), distal left humerus, proximal radius, proximal ulna, Hemingford Quarry 12D; (4) UNSM 25554 (field no. 5500-38), distal left humerus, left proximal ulna, left radius, proximal left MC2 and left MC3, a distal metapodial, and numerous fragments, ~0.25 mi west of Hemingford Quarry 1; (5) UNSM 26424 (field no. 39-7-8-37SP), proximal right ulna, Hemingford Quarry 7B; (6) UNSM 25553 (field no. 179-7-8-37SP), left radius, Hemingford Quarry 7B?; (7) UNSM 25595 (field no. 73-4-8-37NP), right radius, Hemingford Quarry 12D; (8) UNSM 26425 (field no. 4025-40), right radius, Hemingford Quarry 7A; (9) UNSM 26426 (field no. 4612-41), right radius, Hemingford Quarry 12D; (10) UNSM 26428 (field no. 171-39), right scapholunar, Hemingford Quarry 12D; (11) UNSM 26429 (field no. 334-13-8-38NP), right scapholunar, Hemingford Quarry 12D; (12) UNSM 26430 (field no. 2636-40), right scapholunar, Hemingford Quarry 7B; (13) UNSM 26431 (field no. 12-24-6-35NWP), right scapholunar, Marsland Quarry (Bx-22).

Metacarpals (MC1 is not represented): (14) UNSM 25574 (field no. 24,281-39), left metacarpal 2, Hemingford Quarry 7B; (15) UNSM 26432 (field no. 4395-41), left MC2, Hemingford Quarry 12D; (16) UNSM 25564 (field no. 35-7-8-37SP), right metacarpal 3, Hemingford Quarry 7B; (17) UNSM 26433 (field no. 145-27-10-37), right metacarpal 3, Hemingford Quarry 12D; (18) UNSM 26434 (field no. 3-4-6-35NWP), right metacarpal 3, Marsland Quarry (Bx-22); (19) UNSM 25572 (field no. 347-39), left metacarpal 5, Hem-

ingford Quarry 12D. **Dawes Co., Nebraska:** (20) F:AM 68263, right metacarpal 4, Dunlap Camel Quarry.

Postcranials—Hindlimb

Box Butte Co., Nebraska: (1) UNSM 26435 (field no. 4-15-7-35NWP), left femur, Hemingford Quarry 23 (Shimek's Quarry); (2) UNSM 25558 (field no. 1639-39), right tibia, Hemingford Quarry 7B; (3) UNSM 44720 (field no. 53-13-8-38NP), left ectocuneiform, Hemingford Quarry 12D; (4) UNSM 26436 (field no. 1565-39), left astragalus, Hemingford Quarry 7B; (5) UNSM 25585 (field no. 73-39), left astragalus, Hemingford Quarry 12D; (6) UNSM 25562 (field no. 1898-39), right astragalus, right distal calcaneum, right cuboid, Hemingford Quarry 7B (see associated metatarsals); (7) UNSM 26437 (field no. 9-12-8-37SP), left astragalus, Hemingford Quarry 12A; (8) UNSM 25584 (field no. 73-39), left calcaneum, Hemingford Quarry 12D; (9) UNSM 26438 (field no. 4929-41), left calcaneum, Hemingford Quarry 12D; (10) UNSM 26439 (field no. 4929-41), right calcaneum, Hemingford Quarry 12D; (11) UNSM 25586 (field no. 13-11-7-35NWP), right calcaneum, Hemingford Quarry 23 (Shimek's Quarry); (12) UNSM 48478 (field no. 2588-40), left calcaneum, Hemingford Quarry 7B; (13) UNSM 26440 (field no. 389-39), right calcaneum, Hemingford Quarry 12D; (14) UNSM 26441 (field no. 7-6-8-37SP), left calcaneum, Hemingford Quarry 6; (15) UNSM 26442 (field no. 5-20-6-35NWP), right cuboid, Marsland Quarry (Bx-22); (16) UNSM 26497 (field no. 40-2-10-37NP), right cuboid, Hemingford Quarry 12D.

Metatarsals (MT1 is not represented): (17) UNSM 26443 (field no. 325-13-8-38NP), left MT2, Hemingford Quarry 12D; (18) UNSM 26444 (field no. 2-4-6-35NWP), right metatarsal 2, Marsland Quarry (Bx-22); (19) UNSM 26445 (field no. 5091-40), left metatarsal 3, Hemingford Quarry 12D; (20) UNSM 26446 (field no. 14-3-8-35NWP), right metatarsal 3, Marsland Quarry (Bx-22); (21) UNSM 25562 (field no. 1898-39), right metatarsal 3 and proximal metatarsal 4, Hemingford Quarry 7B; (22) UNSM 25563 (field no. 14-13-8-38NP), left metatarsal 4, Hemingford Quarry 12D; (23) UNSM 26447 (field no. 4611-40), right metatarsal 4, Hemingford Quarry 7B; (24) UNSM 26448 (211-13-8-38NP), right metatarsal 4, Hemingford Quarry 12D; (25) UNSM 26449 (field no. 4517-41), right metatarsal 5, Hemingford Quarry 12D; (26) UNSM 26450 (field no. 2-3-8-35NWP), right metatarsal 5, Marsland Quarry (Bx-22).

Dawes Co., Nebraska: All from Dunlap Camel Quarry: (27) F:AM 68265B (field no. H198-2392), right astragalus; (28) F:AM field no. H173-1509, left calcaneum; (29) F:AM field no. H275-2716, right metatarsal 4; (30) F:AM 68265A, metatarsal 5.

Referred Specimens: Bridgeport Quarries, Unnamed formation, western Nebraska—if a particular quarry is not indicated, then the general designation for all quarries applies:

Mandibles and Isolated Teeth

Morrill Co., Nebraska: (1) UNSM 25878 (field no. 20-7-32SPD), partial mandible with i2–i3, c, p1–p4; (2) UNSM 25852 (field no. 11537-40), mandible with damaged p4–m2, alveoli for p1–p3, m3; (3) UNSM 26070 (67-SPD-32), right P4; (4) UNSM 26071 (field no. SPD), left P4; (5) UNSM 25961 (field no. 13-20-10-32SPD), right P4; (6) UNSM 26451 (field no. ?), right P4; (7) UNSM 26017 (field no. 53-SPD-3), right M1; (8) UNSM 26015 (field no. 43-SPD-32), right M1; (9) UNSM 25928 (field no. 16-28-10-33NSM), right M1; (10) UNSM 26016 (field no. 8NSM), left M1; (11) UNSM 26072 (field no. SPD), left M1; (12) UNSM 26018 (field no. 81-SPD-32), left M2; (13) UNSM 26019 (field no. NSM), left M2; (14) UNSM 26009 (field no. 22-SPD-32), left p3; (15) UNSM 25924 (field no. 13-20-10-32SPD), left p4; (16) UNSM 26011 (field no. SPD), right p4; (17) UNSM 25923 (field no. 13-20-10-32SPD), right p4; (18) UNSM 26012 (field no. 15-SPD-32), left p4; (19) UNSM 25781 (field no. 6-SPD-32), right m1; (20) UNSM 25907 (field no. 16-28-10-33NSM), left m1; (21) UNSM 26080 (field no. SPD), right m1; (22) UNSM 26082 (field no. 2-SPD-32), right m1; (23) UNSM 26083 (field no. 8-SPD-32), right m1; (24) UNSM 26084 (field no. 26-SPD-32), left m1; (25) UNSM 26281 (field no. SPD-13-10-20-32), right m2; (26) UNSM 26282 (field no. SPD-13-10-20-32), left m2;

(27) UNSM 26283 (field no. ?9-8-32SPD), right m2; (28) UNSM 26284 (field no. ?9-9-32SPD), right m2; (29) UNSM 26287 (field no. ?9-8-32SPD), left m2 trigonid.

Postcranials—Forelimb

Morrill Co., Nebraska: (1) UNSM 26260 (12-17-10-33NSM), right humerus, Mo-114; (2) UNSM 26261 (14-28-10-33NSM), left humerus lacking proximal end; (3) UNSM 26262 (field no. SPD-B-7-20-32), left distal humerus; (4) UNSM 26263 (SPD-B-7-20-32), left distal humerus; (5) UNSM 26264 (field no. 14-28-10-33NSM), right distal humerus; (6) UNSM 26265 (field no. 11-17-10-33NSM), left distal humerus; (7) UNSM 26266 (field no. 11-17-10-33NSM), right distal humerus; (8) UNSM 26267 (field no. 11-17-10-33NSM), left distal humerus; (9) UNSM 26268 (field no. 14-28-10-33NSM), left distal humerus; (10) UNSM 26269 (field no. 10405-40), left distal humerus, Loc. A, Qu. 1; (11) UNSM 26270 (field no. SPD-4-10-20-32), right distal humerus; (12) UNSM 26218 (field no. 4-10-20-32-SPD), right distal humerus; (13) UNSM 26210 (field no. 17-27-9-33NSM), left distal humerus; (14) UNSM 26297 (field no. 14-17-10-33NSM), right radius, Mo-114; (15) UNSM 25877 (field no. 10694-40), left radius, Loc. A, Qu. 1; (16) UNSM 26453 (field no. 27-9-11-32NSM), left scapholunar; (17) UNSM 26454 (field no. 2-7-37-SPA), right scapholunar, Qu. 4; (18) UNSM 26455 (field no. 1-9-32SP), right scapholunar, Qu. 2; (19) UNSM 26456 (field no. 14106-40), left scapholunar, Qu. 1; (20) UNSM 26457 (field no. 1-9-32SP), left unciform, Qu. 2; (21) UNSM 26458 (field no. 1-9-32SP), left unciform, Qu. 2; (22) UNSM 26459 (field no. 11394-40), Qu. 1.

Metacarpals: (23) UNSM 26460 (field no. 10-10-32-SPD), left metacarpal 1; (24) UNSM 26461 (field no. SPD), right metacarpal 1; (25) UNSM 26462 (field no. NSM 26), left metacarpal 2; (26) UNSM 26463 (field no. 4-28-10-33NSM), left metacarpal 2; (27) UNSM 26464 (field no. 10-10-20-32-SPD), right metacarpal 2; (28) UNSM 26465 (field no. 29-17-10-33NSM), right metacarpal 2; (29) UNSM 26466 (field no. NSM 6), right metacarpal 2; (30) UNSM 26467 (field no. 10719-40), left metacarpal 3; (31) UNSM 26468 (field no. 5-27-9-33NSM), left metacarpal 3; (32) UNSM 26469 (field no. SPD), right metacarpal 3; (33) UNSM 26470 (field no. 10495-40), right metacarpal 3, Loc. A, Qu. 1; (34) UNSM 26471 (field no. 29-17-10-33NSM), right metacarpal 3; (35) UNSM 26472 (field no. 10-10-20-32-SPD), right metacarpal 3; (36) UNSM 26473 (field no. 10164-40), left metacarpal 4, Qu. 1; (37) UNSM 26474 (field no. 29-17-10-33NSM), right metacarpal 4; (38) UNSM 26475 (field no. 10-10-20-32-SPD), right metacarpal 4; (39) UNSM 26476 (field no. 10164-40), right metacarpal 4 (pathologic), Qu. 1; (40) UNSM 26477 (field no. 25-6-34SP), left metacarpal 5; (41) UNSM 26478 (field no. NSM 6), left metacarpal 5; (42) UNSM 26479 (field no. NSM 6), right metacarpal 5; (43) UNSM 26480 (field no. 10-10-20-32-SPD), right metacarpal 5.

Postcranials—Hindlimb

Morrill Co., Nebraska: (1) UNSM 26343 (field no. 10-4-10-33NSM), left femur; (2) UNSM 26360 (field no. 18-17-10-33NSM), right tibia, Qu. 2, Mo-114; (3) UNSM 26361 (field no. 8-7-8-34SP), right proximal tibia, Qu. 8; (4) UNSM 26481 (field no. 7514-83), left calcaneum; (5) UNSM 26482 (field no. 28-17-10-33NSM), right calcaneum; (6) UNSM 26483 (field no. 1-9-32-SP), right calcaneum, Qu. 2; (7) UNSM 26484 (field no. 1-9-32-SP), left calcaneum, Qu. 2; (8) UNSM 26485 (field no. 27-9-33NSM), right calcaneum, Qu. 2; (9) UNSM 26486 (field no. 27-9-33NSM), left calcaneum, Qu. 2; (10) UNSM 26496 (field no. ?), left calcaneum; (11) UNSM 26487 (field no. 1-9-32-SP), left astragalus, Qu. 2; (12) UNSM 26488 (field no. 10125-40), left astragalus, Qu. 1; (13) UNSM 26489 (field no. 27-9-33NSM), left astragalus, Qu. 2; (14) UNSM 26490 (field no. 27-9-33-NSM), left astragalus, Qu. 2; (15) UNSM 26491 (field no. 11-10-20-32-SPD), right astragalus; (16) UNSM 26492 (field no. 8-28-10-33NSM), right astragalus; (17) UNSM 26493 (field no. 1-17-7-35-SP), right astragalus, Qu. 5; (18) UNSM 26494 (field no. 11-10-20-32-SPD), right astragalus; (19) UNSM 26495 (field no. 6-27-9-33NSM), right astragalus; (20) UNSM 26498 (field no. 6-7-34SP), right cuboid, Qu. 1; (21)

UNSM 26499 (field no. 11156-40), left cuboid, Qu. 10; (22) UNSM 26405 (field no. 27-9-33NSM), left cuboid, Qu. 2; (23) UNSM 26406 (field no. 27-9-33NSM), right navicular, Qu. 2; (24) UNSM 26407 (field no. 11005-40), left navicular, Qu. 10; (25) UNSM 44703 (field no. SPD-12-10-20-32), right calcaneum; (26) UNSM 44704 (field no. SPD-12-10-20-32), right calcaneum; (27) UNSM 44706 (field no. SPD-12-10-20-32), right calcaneum; (28) UNSM 44707 (field no. SPD-12-10-20-32), right calcaneum; (29) UNSM 44708 (field no. SPD-12-10-20-32), left calcaneum.

METATARSALS: (30) UNSM 26408 (field no. SPD), right metatarsal 2; (31) UNSM 26409 (field no. NSM), left metatarsal 2; (32) UNSM 26410 (field no. 10164-40), left metatarsal 2, Qu. 1; (33) UNSM 26411 (field no. 29-17-10-33NSM), right metatarsal 3; (34) UNSM 26412 (field no. 10-10-20-32-SPD, right metatarsal 3; (35) UNSM 26413 (field no. 4-4-10-33NSM), left metatarsal 3; (36) UNSM 26414 (field no. 29-17-10-33NSM), right metatarsal 4; (37) UNSM 44700 (field no. 10-10-20-32-SPD), left metatarsal 5; (38) UNSM 44701 (field no. 10-10-20-32-SPD), right metatarsal 5.

REFERRED SPECIMENS: From sediments yielding an early Hemingfordian mammal fauna from the Rose Creek Member, John Day Formation, north-central Oregon— **Grant Co., Oregon:** (1) UCMP 76875, left p2–m2 (UCMP locality V76124); (2) UNSM 8061-93, right upper canine, right m2, left I3, right and left I2 (UCMP locality V76124), possibly from the same individual as UCMP 76875; (3) UNSM 7088-94, lingual fragment of M1 (UNSM locality Rose Creek North), tentatively referred; (4) UCMP 76864, right astragalus (UCMP locality V76124).

REFERRED SPECIMENS: From sediments yielding an early Hemingfordian mammal fauna, Zia Sand Fm., Chamisa Mesa Member— **Sandoval Co., New Mexico:** (1) F:AM 68254 (field no. Jemez 31-504), left metacarpals 4 and 5, Blick Quarry.

Daphoenodon (*Borocyon*) cf. *B. robustum*
Peterson, 1910
Figure 9

REFERRED SPECIMENS: From sediments yielding an early Hemingfordian mammal fauna that filled a sinkhole or fissure in the channel of the Suwanee River, northern Florida— **Dixie–Levy Counties, Florida:** (1) UF 95092, KU 114592 (a cast: the specimen is retained by a private collector), palate with complete dentition, right and left I1–I3, C, P1–M2; (2) KU 114585, partial right P4; (3) KU 114584, partial left P4; (4) KU 114552, left m1; (5) KU 114492, left m1; (6) KU 114487, mandibular fragment with right m2–m3; (7) KU 114542, mandibular fragment with right p4; (8) KU 114543, mandibular fragment with right p3–p4, p2 broken; (9) KU 114479, 114532, 114536, 3 edentulous mandibles.

POSTCRANIALS: KU 113751, left humerus; KU 113765, 113756, 113769, 113750, 113768, 113753, 113774, 7 distal humeri; KU 113706, right radius; KU 113664, left proximal radius; KU 113784, left ulna; KU 113792, 113793, 113800, 113834, 116663, 5 proximal right ulnae; KU 113788, proximal left ulna; KU 113645, right femur; KU 113650, partial distal femur; KU 113736, right tibia; KU 113727, left distal tibia; KU 113722, left distal tibia; KU 113718, left astragalus; KU 113619, 113620, 2 left calcanea; KU 113608, 113609, 113610, 113613, 4 right calcanea.

Daphoenodon (*Borocyon*) *niobrarensis*
Loomis, 1936
Figures 10, 11, 20, 23

HOLOTYPE: ACM 3452 (field no. 34-52), left mandible with c, p2–m3, right mandible with c, p1–m3, and isolated right M1, associated with nearly complete forelimbs; holotype of *Daphoenodon niobrarensis* Loomis, 1936: 47, figs. 2, 4. There is no doubt as to the identification of the holotype mandibles and forelimbs, which Loomis published as ACM 34-52, although the field number 34-58 appears on many of the individual bones.

HOLOTYPE HORIZON AND LOCALITY: From the lower Runningwater Fm., Cherry Co., Nebraska. Loomis (1936) reported that the holotype was "Found in 1934 in middle Miocene beds equivalent to the upper Harrison formation, near mouth of Antelope Creek, 12 miles southeast of Gordon, Nebraska. Associated with *Aletomeryx* [ACM 1915]." In fact the holotype was found with a large sample of *Aletomeryx* and the camel

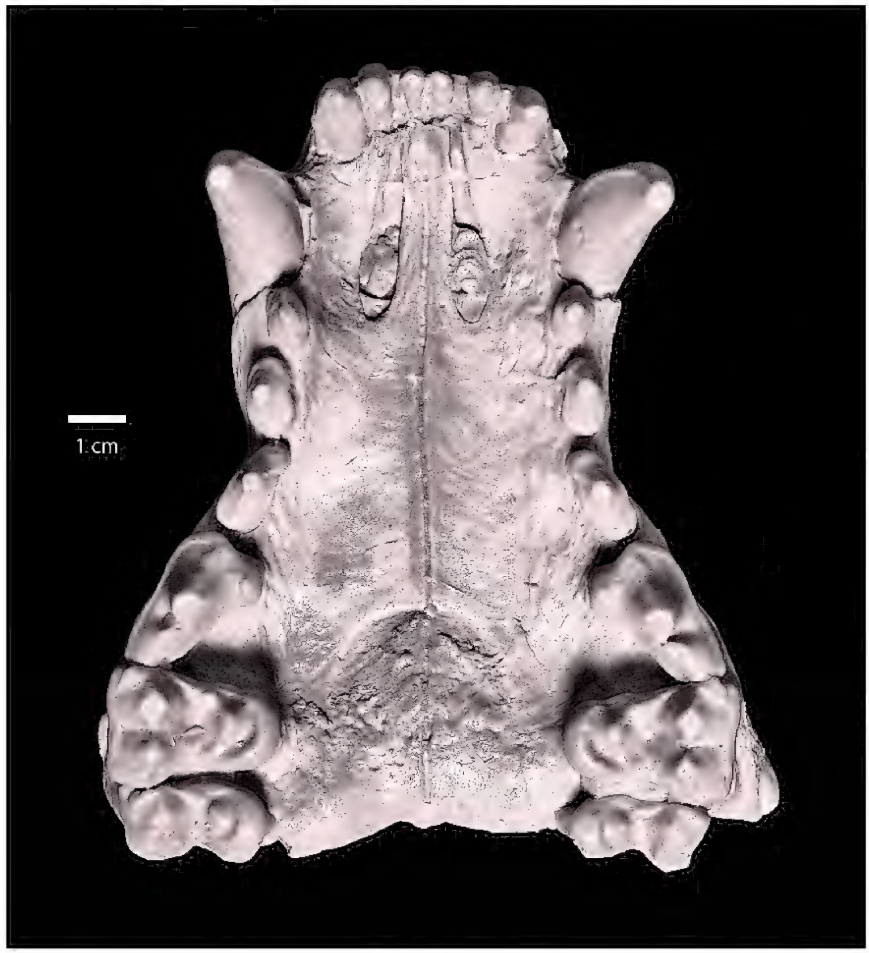

Fig. 9. Reconstructed palate of *Borocyon* cf. *B. robustum* (cast, KU 114592) from sinkhole or fissure, Suwanee River, north Florida. Complete dentition includes I1–I3, C, P1–P4, M1–M2. Note absence of M3.

Michenia [ACM 1844] in Aletomeryx Quarry, an early Miocene locality in the lower Runningwater Fm. worked by several museums during the 1930s.

DIAGNOSIS: *Borocyon* species of intermediate size, with basilar skull length of ~270 mm, and c–m2 length of ~103–115 mm, its skeletal and dental measurements (figs. 17, 18; tables 2, 3) generally falling between those of the large species *B. robustum* and small *B. neomexicanus*. Proximal tarsals (figs. 33, 34, astragalus, calcaneum) shorter and differently proportioned relative to those of *B. robustum*.

REFERRED SPECIMENS: Runningwater Formation, northwestern Nebraska— **Cherry Co., Nebraska:** (1) ACM 11796 (field no. 34-58), left metacarpals 3 and 4, Aletomeryx Quarry; (2) F:AM 68269, right metatarsal 4, cuboid, navicular, phalanx, Aletomeryx Quarry. **Dawes Co., Nebraska:** (1) UNSM 25683 (field no. 1-11-9-36NP), left mandible, p4–m2; (2) UNSM 25555 (field no. 1-13-8-36NP), left humerus; (3) UNSM 44702 (field no. 9-12-8-36NP), right metacarpals 2, 3, and 4, possibly the same individual as UNSM 25555 and 25683. All from Red Horse Quarry (UNSM Dw-103). **Sheridan Co., Nebraska:** (1) UNSM 26418 (no field no.), right m2, UNSM Loc. Sh-101B. **Sioux Co., Nebraska:** (1) F:AM 107601 (F:AM field nos. NEA 1–2, 8–130; UNSM field no.

Fig. 10. Holotype right mandible of *Borocyon niobrarensis* Loomis with c, p1–p4, and m1–m3 from Aletomeryx Quarry, lower Runningwater Fm., Cherry Co., Nebraska (ACM 3452).

RH104), right mandible with c, p1–m3, partial right scapula, left ulna, left scapholunar, left metacarpal 2, right innominate, right calcaneum, astragalus, and cuboid, proximal metatarsal 5, proximal phalanx, intermediate phalanx, partial proximal phalanx. F:AM 107601 is an associated partial skeleton from a massive pinkish silty sandstone in SW1/4, SW1/4, sec. 1, T29N, R55W, northeast of the post office of Agate, Nebraska. F:AM specimens were collected by Ron Brown in August 1970; UNSM material (metacarpal 2, ulna, calcaneum, partial scapula) was collected in July 1971 by R.M. Hunt, T. Hussain, and L. Hunt and donated to the American Museum. Associated with *Merycochoerus* cf. *M. magnus*. (2) UNSM 44827, nearly complete skull and mandibles but lacking much of the rostrum; teeth extremely worn; right P3–M2, left M1–M3, partial P4; damaged right p4–m3 and left m1–m3; from massive pale reddish brown sandstone, Skavdahl Ranch, NW1/4, NW1/4, sec. 29, T29N, R53W.

Referred Specimens: Late early Miocene beds east of the Laramie Mountains, southeastern Wyoming (Cassiliano, 1980: 30–39)— **Laramie Co., Wyoming:** (1) UW 10004, left mandible with p4–m2 (a right mandible was retained by the field collector and is now lost), left M3, left P3, left canine, left scapula, humerus, ulna, and radius, right humerus and ulna, two right radii, right magnum, both pisiforms, left metacarpals 4 and 5, right innominate, left femur, tibia, and fibula, right astragalus and calcaneum, left navicular, right metatarsal 2, left metatarsals 3 and 4, four proximal phalanges, axis, two cervical vertebrae, three thoracic vertebrae, two lumbar vertebrae, one caudal vertebra, partial ribs. From the "Middle Miocene Formation" of Cassiliano (1980) at Horse Creek Quarry.

Referred Specimen: Carpenter Ranch Formation, southeastern Wyoming (Hunt, 2005)— **Goshen Co., Wyoming:** (1) UNSM 44815, partial left mandible with m1–m3, partial p4, described in Hunt (2005: 32, fig. 22). From indurated sandstone caprock at Merycochoerus Butte.

Daphoenodon (*Borocyon*) *neomexicanus*, new species
Figures 7, 8, 12–16

Holotype: F:AM 49239, a skull with associated mandibles (figs. 7D, E, 12, 13).

Holotype Horizon and Locality: Piedra Parada Member, Zia Sand Formation, collected in 1947 by Ted Galusha and party at Standing Rock Quarry, Canyada Piedra Parada, 7 mi south and 1.5 mi west of San Ysidro, Sandoval Co., New Mexico, NW1/4, sec. 11, T14N, R1E.

Fig. 11. Associated holotype right forelimb of *Borocyon niobrarensis* Loomis (ACM 3452), Aletomeryx Quarry, Cherry Co., Nebraska.

DIAGNOSIS: Smallest species of *Borocyon*, with basilar skull length of ~245 mm, and c–m2 length of ~97–100 mm, averaging smaller than both *B. niobrarensis* and *B. robustum* in body size and dentition (figs. 17, 18; tables 2, 3), and in males, by a more developed bony exostosis on the distal radius. Differs from *Daphoenodon superbus* (basilar

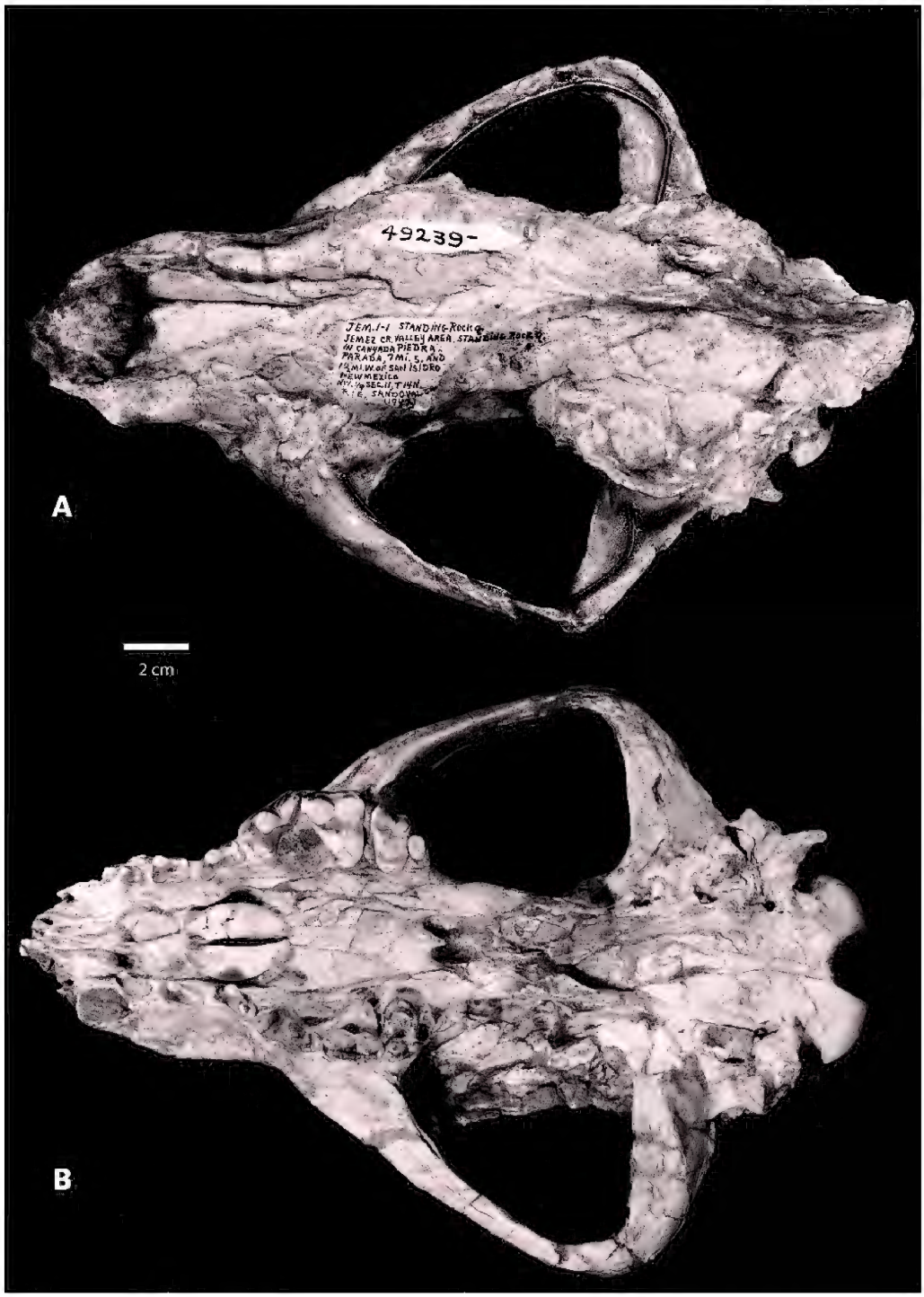

Fig. 12. Holotype cranium of *Borocyon neomexicanus* (F:AM 49239), Standing Rock Quarry, Zia Sand Fm., Sandoval Co., New Mexico. **A**, Dorsal view; **B**, ventral view. This is the only known cranium and is an old adult with worn teeth: P1–P4, M1–M3. Although reduced in size, an M3 persists in this species.

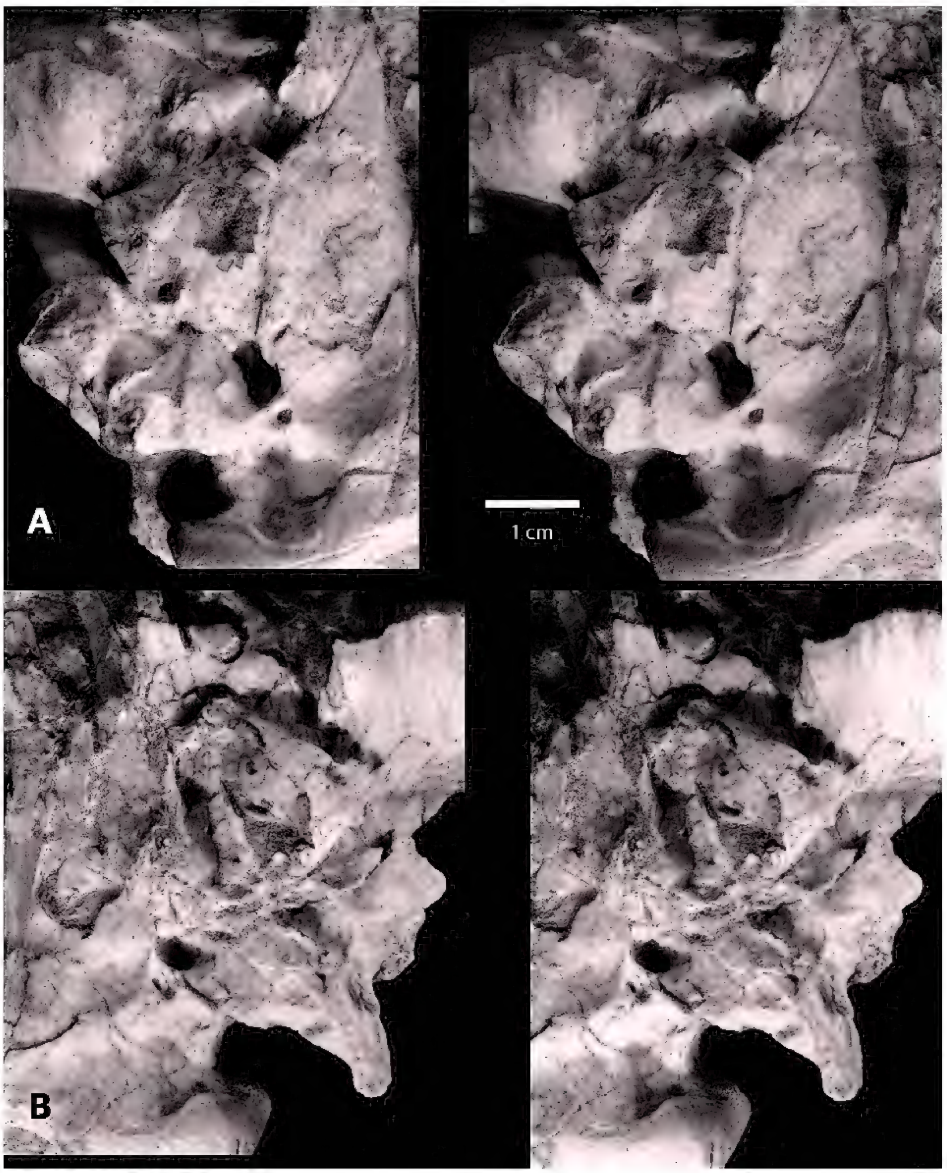

Fig. 13. Basicranium of *Borocyon neomexicanus* (F:AM 49239), Standing Rock Quarry, Zia Sand Fm., Sandoval Co., New Mexico. **A**, Right auditory region; **B**, left auditory region. Despite crushing, the auditory bulla and surrounding basicranium are anatomically similar to the bulla and basicranium of *Daphoenodon superbus*. The bulla of the Standing Rock amphicyonid is a thin-walled, flask-shaped, single chamber, as is the rudimentary auditory bulla of *D. superbus*.

skull length, 215–222 mm) by its greater size, longer forelimbs, larger m1 (fig. 18A), a "folded" M2, and proportionately longer m2 (fig. 18B).

REFERRED SPECIMENS: All referred material was collected at Standing Rock Quarry during the 1947 field excavation by the Frick Laboratory (American Museum): (1) F:AM 49240, left mandible, complete, with i2–i3, c, p1, p3–m1, alveoli for m2–m3; (2) F:AM 49240A, right mandible with c, p2–p4; (3) F:AM 49241, juvenile left mandibular fragment with p3–m3—this is probably the same individual as a basicranium (F:AM 68240)

Fig. 14. Elongate radii of (**A**) female and (**B**) male *Borocyon neomexicanus*, Standing Rock Quarry, Zia Sand Fm., Sandoval Co., New Mexico. Note large distal radial exostosis (arrow) of the male, a trait also present in *Daphoenus vetus* and *Daphoenodon superbus* but not developed in *B. robustum* despite a sample of eight radii from the Hemingford and Bridgeport Quarries. The single radius of *Borocyon* cf. *B. robustum* from Florida retains a small exostosis.

Fig. 15. Elongate metacarpals 4 and 5 of (**A**) *Borocyon neomexicanus* (F:AM 68242) from Standing Rock Quarry and (**B**) *B. robustum* (F:AM 68254) from Blick Quarry, Sandoval Co., New Mexico, demonstrating that the *Borocyon* lineage persisted in the southwestern United States from latest Arikareean into the early Hemingfordian. The only Hemingfordian record of *Borocyon* in the Southwest are these two metacarpals from Blick Quarry.

and an MT3 with unfused epiphysis (F:AM 68240A); (4) F:AM 68241, several ribs, podials, axis vertebra, both humeri and ulnae, right scapula, various vertebrae, a canine, metacarpals 1 and 2, and metatarsal 5; (5) F:AM 68242, left femur, articulated vertebrae, phalanges, carpals, both radii (without exostoses), partial articulated tarsus in matrix, metacarpals 4 and 5, and metatarsals 2, 3, and 4; (6) F:AM 68243, right femur, complete pelvis lacking anteriormost ilial blades, atlas vertebra; (7) F:AM 68244, partial fibula, phalanges, tarsals, articulated vertebrae, metacarpals 3 and 4, metatarsal 1; (8) various postcranial elements cataloged under field numbers as follows: Jemez 7-105, radius (with exostosis); Jemez 7-106, tibia; Jemez 6-86, femur; Jemez 5-77, distal femur; Jemez 5-72, distal humerus, proximal ulna; Jemez 5-73, distal humerus; Jemez 5-74, ulna; Jemez 5-77, atlas vertebra; Jemez 7-117, atlas and two articulated vertebrae.

DISCUSSION: The Standing Rock Quarry sample of *Borocyon* is made up of at least three disarticulated individuals including a juvenile (fig. 7C). In skull proportions, den-

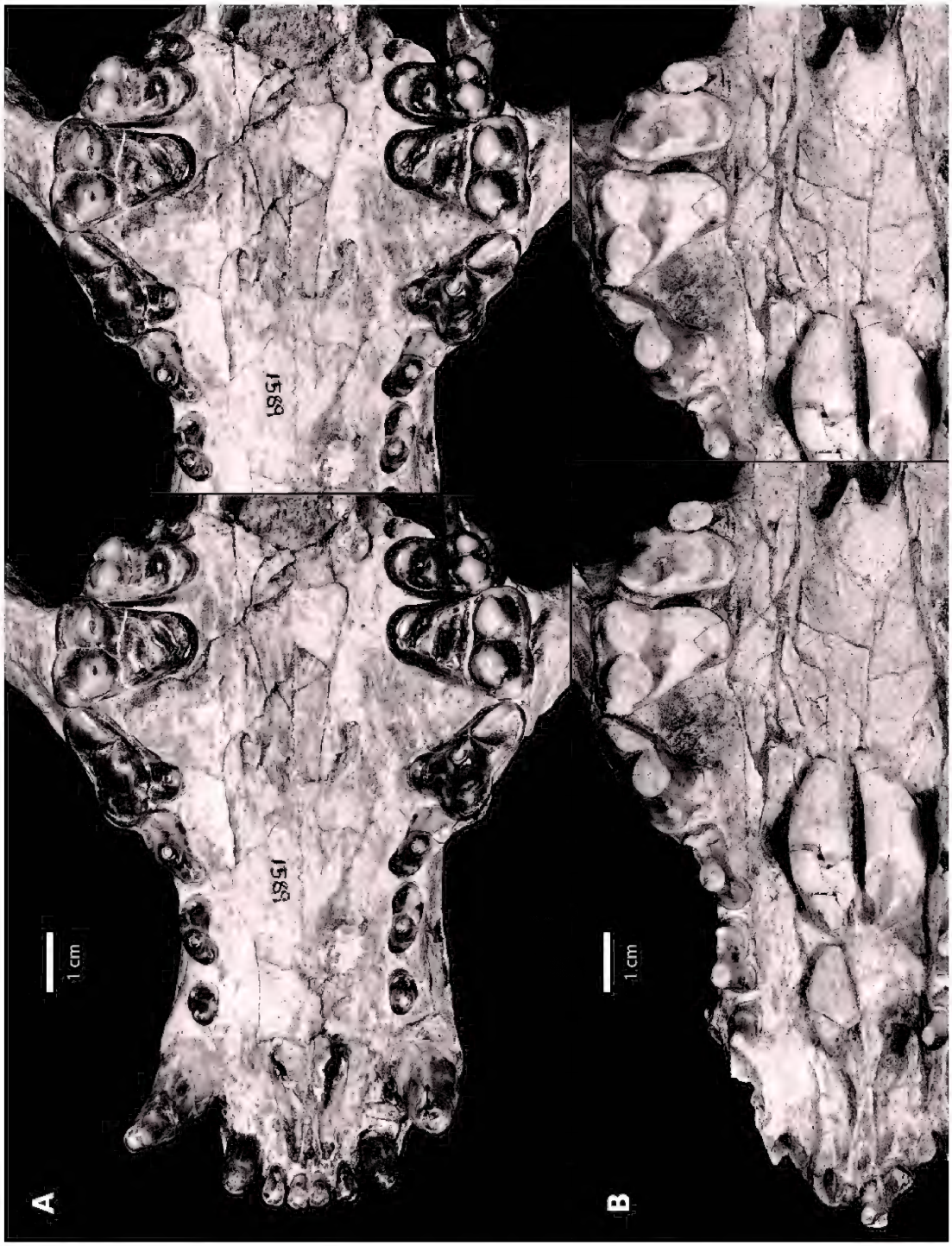

Fig. 16. Upper dentition and palate of *Daphoenodon superbus* (**A**) and *Borocyon neomexicanus* (**B**). Although the teeth of *B. neomexicanus* are worn, both species show similar unreduced premolar form, reduction of M3, and shearing P4. The New Mexican beardog has developed the "folded" M2, a synapomorphy of *Borocyon* species, not yet evident in *D. superbus*.

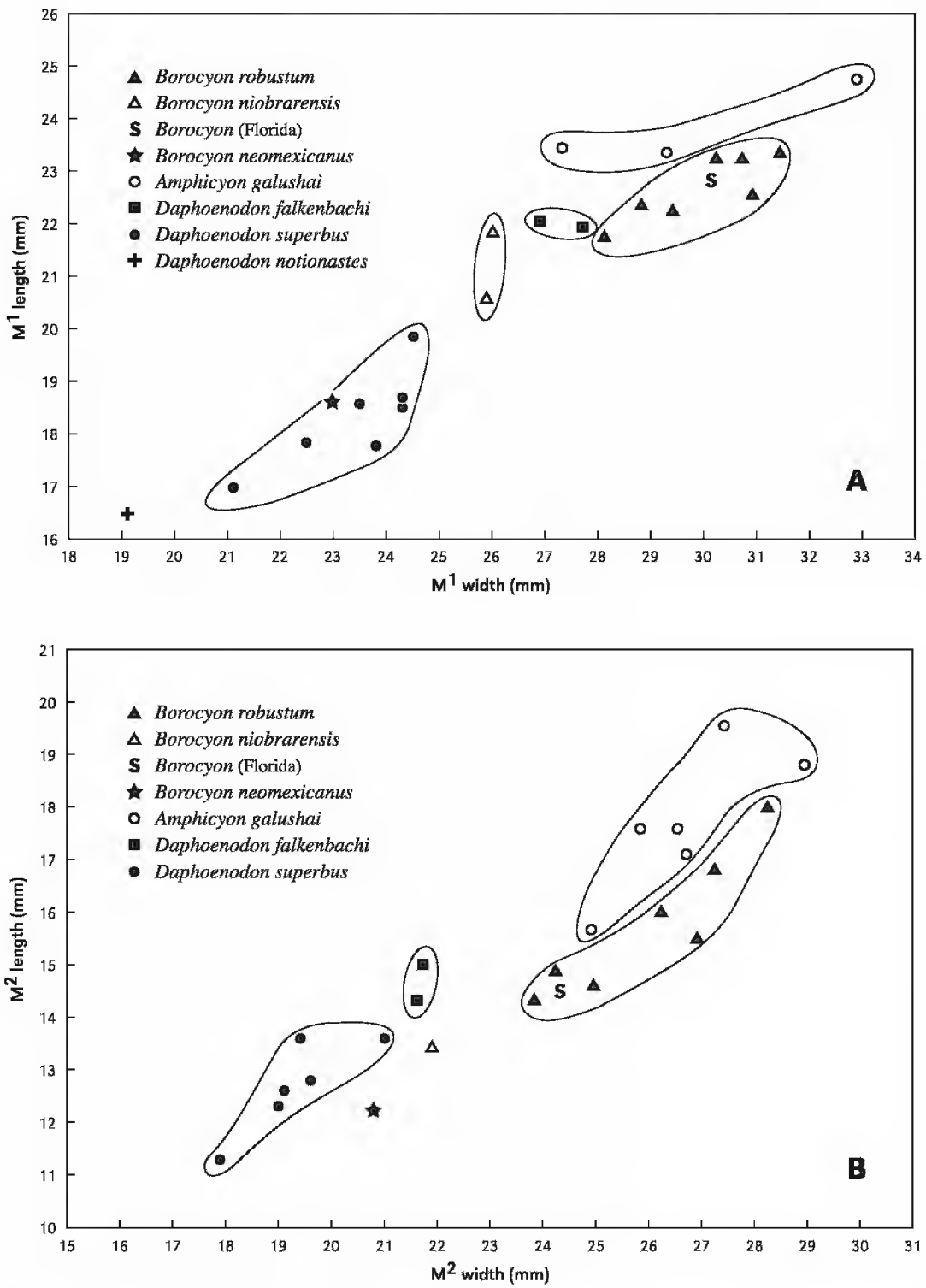

Fig. 17. Comparison of (**A**) M1 and (**B**) M2 dimensions of species of the daphoenine subgenera *Borocyon* and *Daphoenodon* and the amphicyonine *Amphicyon galushai* from the early Miocene of North America.

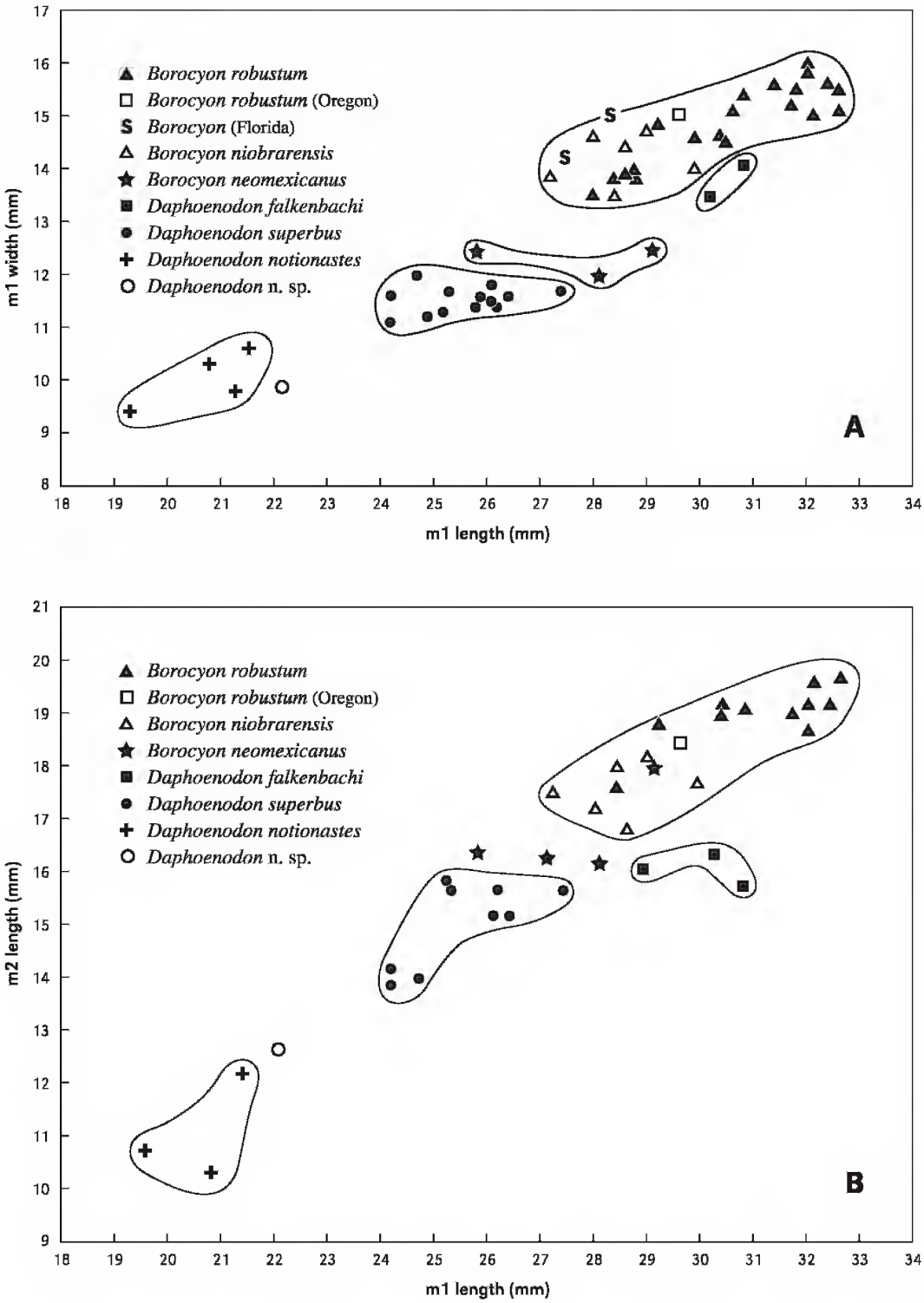

Fig. 18. Comparison of (**A**) m1 dimensions and (**B**) m1 length relative to m2 length for species of the daphoenine subgenera *Borocyon* and *Daphoenodon* from the early Miocene of North America.

tition, and the postcranial skeleton this species is very similar to both *Daphoenodon* (*D.*) *superbus* and the large species of *Daphoenodon* (*Borocyon*) and serves as a structural and temporal intermediate. The mammalian fauna found with *B. neomexicanus* indicates a latest Arikareean (Ar4) age, hence the New Mexican carnivore precedes the larger earliest Hemingfordian *Borocyon niobrarensis* from the Great Plains, and apparently postdates the sample of *D. superbus* from the carnivore dens at Agate National Monument on faunal grounds.

The hypodigm from Standing Rock Quarry includes partially articulated postcranial material requiring additional preparation and study. Only the diagnostic holotype skull and mandibles, an unworn juvenile dentition, and previously prepared limb and foot bones necessary to establish the species as the oldest member of the *Borocyon* lineage are included in this study.

Two metapodials found in Blick Quarry (fig. 15), situated a few miles north of Standing Rock Quarry, can be referred to *Borocyon robustum*, suggesting that the transition from the smaller Standing Rock carnivore to large *B. robustum* is possibly documented in northern New Mexico. The failure to find *B. neomexicanus* in Arikareean rocks of Nebraska and adjacent states in the central Great Plains despite extensive field collecting suggests its actual absence from the fauna of that region, indicating that *Borocyon* may have migrated north into the midcontinent from the southwestern United States in the earliest Hemingfordian.

CRANIODENTAL OSTEOLOGY

CRANIAL: *Borocyon robustum* is represented by three large, nearly intact crania (UNSM 25547, 25686, 26416) and *B. neomexicanus* by only one (F:AM 49239), crushed nearly flat. A skull assigned to *B. niobrarensis* (UNSM 44827, an aged individual), although without a rostrum and with extremely worn teeth, is intermediate in size. These species retain a similar skull form (see frontispiece), which derives from the short, broad skull of *Daphoenodon superbus* (CM 1589, 2774). The cranium, mandible and teeth are best represented for *B. robustum*; this species is therefore the principal subject of this section, with *B. niobrarensis* and *B. neomexicanus* supplementing the account where appropriate.

Skull lengths of *B. robustum* were determined from the three crania and the sample of mandibles of *B. robustum* from the Runningwater Formation. An undistorted mandible (UNSM 25684) was fitted to the paratype cranium (UNSM 25686) so that upper and lower teeth occluded properly, and then, estimating from that relationship, basilar skull lengths corresponding to the remaining mandibles were calculated. A strong correlation exists between mandibular length and skull length for living Carnivora (Christiansen and Adolfssen, 2005). Dimorphism, presumably sexual, is reflected in the range of values for mandibles, and this is supported by "male" and "female" examples from a single quarry (UNSM 25549, 25550, UNSM locality Bx-7). The calculated values for skull lengths (using basilar length) for *B. robustum*, derived from seven mandibles and the three known skulls, yield a range of 258–328 mm, a mean of 294.5 mm, with standard deviation of 20.8 and coefficient of variation of 7.0.

Basilar lengths of *Borocyon robustum* skulls (table 1) indicate the large size attained by these predators, and they show that the ~30–31 cm maximum value recorded for *Borocyon* is similar to this measurement for large New World early Miocene amphicyonine amphicyonids (*Amphicyon*, *Ysengrinia*), values similar to those for living large felids such as *Panthera leo* (~24–34 cm), *P. tigris* (~22–30 cm), and North American mainland *Ursus arctos*.

The skull of *Borocyon robustum* displays a rather short rostrum coupled to a long postorbital cranium (fig. 4, UNSM 26416; frontispiece, UNSM 25686), similar to the proportions of its contemporary *Amphicyon galushai* (Hunt, 2003). Among living carnivorans of similar size, the snout and orbital region of *B. robustum* are most like those of *Ursus arctos*, although the snout of the beardog appears somewhat shorter. It is not so swollen as in *Panthera leo* and *P. tigris* due to the absence in *Borocyon* of the particularly robust canines and incisors of these cats. *Borocyon* is also similar to *U. arctos* in the

TABLE 1
Basilar Skull Lengths of Early Miocene Daphoenine and Amphicyonine Amphicyonids Compared to Living *Panthera*

Taxon	Mus. no.[a]	Basilar Length (mm)
Ysengrinia americana	F:AM 54147	298
Adilophontes brachykolos	F:AM 27568, 54148, 54140*	243, 305, ~300
Amphicyon galushai	F:AM 25400	310
Daphoenodon superbus	CM 1589, 2774	215, 222
Daphoenodon falkenbachi	F:AM 54144	265
Borocyon neomexicanus	F:AM 49239	245
Borocyon niobrarensis	UNSM 44827*	~270
Borocyon robustum	UNSM 25547, 25686,* 26416*	294, ~304, ~287
Cynelos lemanensis	Université de Lyon*	220
Panthera leo	9 individuals	283 (240–344)[b]
Panthera tigris	18 individuals	260 (226–304)[b]

[a]Asterisk (*) indicates estimated.
[b]Mean (range).

diameter and lateral placement of the orbits, whereas in the large felids the orbit is relatively larger and more forwardly directed. The enlarged infraorbital foramina of the large cats for sensory fibers supplying the facial vibrissae are lacking in *Borocyon*, which has a small foramen comparable to that of *U. arctos*.

Borocyon robustum retained the broad forehead of *Daphoenodon superbus* for expanded frontal (paranasal) sinuses, with the cranium constricted behind the orbits to enclose a relatively small braincase surmounted by impressive sagittal and occipital crests (see frontispiece). The volume of the braincase is proportionately smaller in *B. robustum* relative to living lions, tigers, and *U. arctos* of similar size; hence, the sagittal crest for attachment of temporal muscles in *Borocyon* is more prominent. At the base of the braincase adjacent to the narrow occiput, the squamosal root of each zygoma departs the skull at essentially a right angle, and the zygomatic arches extend farthest from the braincase at this point. The breadth of the zygomata and height of the sagittal crest demonstrate that a massive jaw musculature filled the temporal fossae, this volume augmented by the relatively small size of the braincase. The width of the palate is considerable, attaining ~9 cm in some individuals, measured between the posterior limit of the P4 carnassial blades.

The basicranium (fig. 13) is preserved only in the holotype cranium of *B. neomexicanus* (F:AM 49239) and, although badly damaged, in the referred skull of *B. niobrarensis* (UNSM 44827). The auditory bulla and surrounding basicranial structure are essentially the same as previously described for the holotype cranium of *Daphoenodon superbus* (CM 1589, Hunt, 2002a, fig. 23; 2002b, fig. 18). This plesiomorphic bulla is distinguished by its simple, flask-shaped form, by thin medial and posterior bulla walls, and by lack of posterior expansion of the middle ear cavity; this bulla morphology is characteristic of both subgenera of *Daphoenodon*.

DENTAL: Dimensions of the upper and lower teeth of the species of *Borocyon* are here compared with those of other Late Arikareean–early Hemingfordian amphicyonids (tables 2, 3). From the small species *Borocyon neomexicanus* to large *B. robustum*, the teeth increase in size over time, in keeping with the increase in body size. However, the dentition is well represented only in *B. robustum*.

Skulls of *Borocyon robustum* are most easily distinguished from those of the large contemporary amphicyonine *Amphicyon* by the teeth. Nine mandibles and three skulls from the Hemingford Quarries in the upper Runningwater Formation of Nebraska comprise a population sample that best defines *Borocyon robustum*. The teeth of these

individuals show a remarkably uniform morphology, principally varying in size, which in North American amphicyonids is attributable to sexual dimorphism. The population from the Hemingford Quarries (primarily Quarries 7A–7B, 12D, 22, 23) includes the largest carnivores assigned to the genus. The population sample from the Bridgeport Quarries is made up of numerous isolated teeth that correspond in size to those from the Hemingford sites. Because the molars of *Borocyon robustum* are diagnostic, the Bridgeport sample can be confidently allocated to the species, based not only on teeth but also isolated limb and foot elements.

Skulls and mandibles of *Borocyon robustum* are identified by the following defining dental traits (figs. 4–8, 17, 18): (1) the premolars are not reduced as in *Amphicyon* but are well-developed grasping teeth; (2) M3 is lost, a characteristic known elsewhere in North American amphicyonids only in temnocyonines (M3 is reduced in size in *D. superbus* and *B. neomexicanus*; it is minute but still present in the only known skull of *B. niobrarensis*); (3) the shearing P4 is longer and narrower than that of contemporary *Amphicyon* and retains a more prominent protocone; (4) M1 in occlusal view is a large triangular tooth with tall paracone and metacone and a conspicuous notch (fig. 5) indenting the anterolingual cingulum; (5) M2 is particularly diagnostic in its "folded" shape in *B. robustum*, *B. niobrarensis*, and *B. neomexicanus*; that is, in posterior view the lingual half forms a prominent angle (105°–130°) relative to the labial half of the tooth. Dentally plesiomorphic daphoenines (*D. superbus*, *D. falkenbachi*, *D. skinneri*) have an M2 with a much flatter occlusal surface; (6) the posterior cingulum of p4 is "squared" (fig. 8A), not rounded as in *Amphicyon*—a few individuals show some rounding of this posterior margin, but p4 always remains more laterally compressed than in *Amphicyon*; (7) m1 is a massive, robust carnassial that retains a prominent metaconid and a relatively narrow talonid, not a broadened talonid as in *Amphicyon* (because the *B. robustum* M1 paracone is a tall cusp, it occludes far ventrad against the labial face of the m1 talonid, cutting a broad facet, which is particularly evident in the Hemingford Quarries population); (8) m2 is elongate with a broad occlusal surface for crushing against the lingual half of the "folded" M2—it is not as broad as m2 of *Amphicyon*; (9) m3 is present, placed high on the ascending ramus, and tilted forward in an attempt to occlude with M2, due to loss of M3 (only the m3 trigonid occludes with M2, creating a small wear facet on the posterior cingulum) .

Identification of *Borocyon* from a sinkhole or fissure in the Suwannee River, Florida, rests on a reconstructed palate with complete upper dentition (fig. 9), a few isolated teeth, edentulous mandibles, and numerous isolated, diagnostic limb and foot elements. Additional craniodental material of *Borocyon* from the site is in private collections and not available. Although the size of the teeth in the palate suggests a large *B. robustum* male (particularly the canines), the isolated m1s and m2–m3 indicate small individuals, presumably females the size of *B. niobrarensis*. The p4s fall in the size range of *B. robustum* yet are not as large as p4s in the largest of the Hemingford Quarry individuals. Three edentulous mandibles do not equal the depth and robust quality of the Hemingford Quarry specimens and are similar in size to *B. niobrarensis* mandibles. The Florida sample is provisionally referred here to *Borocyon* cf. *B. robustum*; postcranials indicate individuals of the population are somewhat smaller on average than the upper Runningwater hypodigm from the Hemingford Quarries—whether this is a smaller southern population coeval with *B. robustum* or possibly animals from a geologically older interval is uncertain. It is also possible that these individuals constitute a diachronous sample that accumulated over a significant interval in the sinkhole(s) in the Suwannee River.

Figures 17 and 18 present dental dimensions of *B. robustum* for m1–m2 and M1–M2 relative to other early Miocene daphoenines. The Hemingford Quarries and Bridgeport Quarries populations are plotted as *B. robustum*, and the few individuals from Oregon and Florida, although included in the *B. robustum* hypodigm, are separately indicated on the graphs. M1–M2 and m1–m2 are useful in distinguishing *B. robustum* from *B. niobrarensis*—the latter species is consis-

TABLE 2
Dental Measurements (in mm) of Lower Teeth of North American Early Miocene Amphicyonids

Mus. no.	p2	p3	p4	m1	m2	c–m2	p1–p4
Daphoenodon superbus							
CM 1589	10.3 × 5.2	12.8 × 5.8	16.2 × 7.9	24.2 × 11.6	13.9 × 9.8	92.0	47.7
CM 1589a	(12.7) × —	(12.7) × —	18.6 × 8.8	26.2 × 11.4	(15.7) × —	(87.5)	
CM 1589b	(12.8) × —						
CM 1589b		14.8 × 6.8					
CM 1589b					17.4 × 11.5		
CM 1589b					14.6 × 10.4		
CM 1589d				25.9 × 11.6			
CM 1896g	12.2 × 5.8						
CM 2774	11.3 × 5.5	13.6 × 6.1	17.2 × 8.6	24.2 × 11.1	14.2 × 9.8	92.5	51.0
CM 2217				26.1 × 11.5			
AMNH 81003	12.4 × 5.9	14.3 × 6.7	18.1 × 9.5	25.2 × 11.3	15.9 × 10.1	102.7	57.4
AMNH 81025	(12.9) × —	(14.4) × —	18.7 × 9.8	27.4 × 11.7	15.7 × —		
AMNH 81055a	11.0 × 5.6	13.3 × 6.1	17.1 × 8.3				
AMNH 81055b	11.7 × 5.6	14.2 × 6.5					
AMNH 81052				24.9 × 11.2			
C:P12033	11.1 × 5.5	12.4 × 5.9	16.5 × 7.8	26.1 × 11.8	(15.2) × —	(93.4)	49.2
F:AM 54460	12.2 × 6.1	13.5 × 7.4	18.7 × 9.1	24.7 × 12.0	14.0 × 10.6	94.6	53.3
UNSM 44683				25.8 × 11.4			
UNSM 44688	12.3 × 6.0		18.0 × 9.1	25.3 × 11.7	15.7 × 10.8	95.5	51.6
UNSM 700-82	12.6 × 5.6	13.6 × 6.4	19.3 × 8.9	26.4 × 11.6	15.2 × 10.1	104.9	(60)
Daphoenodon, n. sp.							
YPM-PU 11554	11.1 × 5.3	12.5 × 5.5	16.7 × 7.3	22.1 × 9.8	12.7 × 8.6	87.2	47.5
Daphoenodon notionastes							
UF 16965				21.6 × 10.6			
FGS V1213				21.2 × 9.7			
UF 449				19.3 × 9.4			
UF 16905					12.3 × 8.7		
UF 16968			15.6 × 6.8				
UF 16970			14.9 × 6.0				
LSUMG-V2256				20.8 × 10.3	10.3 × 7.7	76.8	43.0
UF 16997	(11.2 × 4.5)	(12.6 × 5)	(16.1 × 6.4)	(19.6 × 8.9)	(10.8 × 7.4)	(80.4)	(48.4)
UF 16910	(12.0 × 5.1)	(13.3 × 5.5)	(15.7 × 6.6)	(21.4 × 9.8)	(12.2 × 8.6)	(81.3)	(46.9)
Daphoenodon falkenbachi							
F:AM 54144	13.1 × 7.3	14.8 × 7.4	19.3 × 9.7	30.2 × 13.5	16.4 × 11.5	104.5	56.7
F:AM 54145/54150	(11.9) × —	(15.0) × —	(19.3) × —	28.9 × —	(16.1) × —	(98.0)	53.5
CM 3719			19.6 × 10.3	30.8 × 14.1	15.8 × 10.6	(99.0)	(51.0)
F:AM 54146			17.8 × 9.1	— × 12.0	16.3 × 11.1		
Daphoenodon skinneri							
F:AM 70801	11.3 × 6.2	13.2 × 7.0	16.8 × 9.1	26.0 × 12.2	14.0 × 10.4	93.5	53.2
Borocyon neomexicanus, n. sp.							
F:AM 49239	11.7 × —	13.2 × —	18.1 × —	25.8 × 12.4	(16.4) × —	(96)	51.6
F:AM 49240		13.9 × —	18.4 × —	28.1 × (12.0)	(16.2) × —	(99.8)	56.8
F:AM 49240a	11.4 × —	14.4 × —	18.3 × —	(27.1) × —	(16.3) × —	(97.0)	(53.7)
F:AM 49241			20.5 × —	29.1 × 12.5	18.0		
Borocyon niobrarensis							
UNSM 44827			(19.6 × 9.7)	(28.0 × 14.6)	(17.2 × 11.0)		
UNSM 44815			(19.2 × 11.2)	27.2 × 13.8	17.5 × 11.8		
ACM 3452	13.4 × 7.2	15.4 × 7.9	20.4 × 9.9	29.0 × 14.7	18.2 × 12.2	115.0	60.0

TABLE 2
(Continued)

Mus. no.	p2	p3	p4	m1	m2	c–m2	p1–p4
F:AM 107601	11.9 × 7.1	14.1 × 7.4	18.0 × 10.4	28.6 × 14.4	16.8 × 12.1	103.0	57.4
UW 10004	(12.5) × 6.2	13.8 × 7.2	17.9 × 9.5	28.4 × 13.5	18.0 × 10.9	104.0	56.6
UNSM 25683		(15.8) × —	19.4 × 9.1	29.9 × 14.0	17.7 × 13.0	(114)	(57.0)
UNSM 26418					17.9 × 12.0		
Borocyon robustum							
			Sioux County, Nebraska				
CM 1918	13.3 × 7.6				17.9 × —		
			Bridgeport Quarries, Morrill County, Nebraska				
UNSM 25878	13.6 × 7.7	18.2 × 8.5	22.7 × 11.7				
UNSM 26009		15.9 × 8.0					
UNSM 25924			21.0 × 10.9				
UNSM 26011			19.4 × 9.8				
UNSM 26012			19.5 × 10.5				
UNSM 25923			19.0 × 10.5				
UNSM 26080				28.0 × 13.5			
UNSM 26081				28.8 × 13.8			
UNSM 26082				29.9 × 14.6			
UNSM 26083				30.6 × 15.1			
UNSM 26084				31.4 × 15.6			
UNSM 26040				28.6 × 13.9			
UNSM 26042				28.7 × 13.9			
UNSM 25907				32.6 × 15.1			
UNSM 25781				(30.5 × 14.5)			
UNSM 26280					19.9 × 14.0		
UNSM 26281					19.2 × 13.0		
UNSM 26282					19.1 × 13.2		
UNSM 26283					17.0 × 10.6		
UNSM 26284					17.1 × 10.7		
UNSM 26287					— × 13.7		
UNSM 25852	(13.3) × —	(17.0) × —	(20.4) × —	(28.1 × 13.6)	(18.6) × —	110.0	59.3
			Hemingford Quarries, Box Butte and Dawes Counties, Nebraska				
Quarry 12D							
UNSM 25577	13.9 × 7.7	16.1 × 7.9	21.3 × 12.3				66.0
UNSM 25551		(17.0 × 9.0)	21.2 × 10.9	29.2 × 14.8	18.8 × 12.6		
UNSM 27002	14.7 × 7.0	16.8 × 8.4	20.4 × 11.6	30.8 × 15.4	19.1 × 12.8	113.5	59.4
Quarry 7A and 7B							
UNSM 25548	13.1 × 7.2	16.0 × 8.6	21.4 × 11.8	32.4 × 15.6	19.2 × —	120.2	65.9
UNSM 25549	(13.4) × —	15.8 × 8.6	21.1 × 10.6	32.0 × 15.8	18.7 × —	118.4	65.4
UNSM 25550		15.6 × 8.1	19.4 × 10.3	28.4 × 13.8	17.6 × 11.4	113.8	(59.0)
UNSM 25684	12.5 × 6.8	15.8 × 8.4	21.7 × 12.2	31.7 × 15.2	19.0 × 12.7	119.2	66.5
UNSM 25576		17.6 × 8.8	21.8 × —				
UNSM 26423			21.0 × 11.6				
UNSM 25571				31.8 × 15.5			
Quarry 1							
F:AM H457-4060			22.3 × 11.7	32.6 × 15.5	19.7 × 12.7		
Marsland Quarry							
UNSM 25685	12.0 × 6.7	(16.0) × —	20.8 × 10.4	30.4 × 14.6	19.2 × 13.1	119.3	62.9
Hovorka Quarry							
UNSM 26417	14.5 × 6.7	16.4 × 9.3	22.9 × 11.9	32.1 × 15.0	19.6 × 12.9	119.0	66.0
Dunlap Camel Quarry							
F:AM 25408	(13.0) × —	(15.5) × —	21.9 × 10.7	32.0 × 16.0	19.2 × 13.3	(117)	62.2

TABLE 2
(Continued)

Mus. no.	p2	p3	p4	m1	m2	c–m2	p1–p4
			Grant County, Oregon				
UCMP 76875			21.3 × 12.0	29.6 × 15.0	18.5 × 12.5		
Borocyon cf. *B. robustum*							
			Suwannee River, Florida				
KU 114543		14.6 × 7.5	19.2 × 10.5				
KU 114542			20.4 × 11.5				
KU 114492				27.5 × 14.3			
KU 114552				28.4 × 15.0			
KU 114487					16.0 × 11.0		
Adilophontes brachykolos							
F:AM 27568	14.6 × 7.0	16.1 × 7.8	(18.0 × 10.7)	(29.0 × 13.9)	16.4 × 11.0	106.5	58.3
F:AM 54148	13.7 × 7.1	16.0 × 8.2	20.7 × 10.8	28.5 × 14.1	16.5 × 13.3	111.6	58.4
F:AM 54141	13.1 × 6.7			(29.0 × 13.6)	16.5 × 12.1	(100)	

Measurements in parentheses are estimates.

tently smaller, plotting in the lower part of the range of the former. When teeth of *Borocyon neomexicanus* are available, they are smaller than those of both *B. robustum* and *B. niobrarensis*.

Dimensions and the form of M1 and M2 distinguish *Borocyon robustum* from its contemporary *Amphicyon galushai*. These molars are particularly reliable in identification of the two species. M1–M2 of *Borocyon* are mesiodistally shorter relative to the upper molars of *A. galushai*, and *Borocyon robustum* has lost M3 whereas *Amphicyon* retains that tooth (*B. niobrarensis* and *B. neomexicanus* have reduced M3s). The carnassials of *B. robustum* are more sectorial than those of *A. galushai* and the premolars better developed for grasping, together indicating a more carnivorous diet in *Borocyon*. Although *B. robustum* can often be identified solely by dental and cranial characters, the species is more confidently recognized using a combination of dental and postcranial traits. When craniodental traits of *Borocyon robustum* are combined with its postcranial skeletal features, the species is anatomically unique among Miocene amphicyonids of both the Old and New World.

POSTCRANIAL OSTEOLOGY

Although no complete associated skeleton of *Borocyon* is known, postcranial bones of *B. robustum* from the Hemingford Quarries, supplemented by isolated elements from the Bridgeport Quarries, provide a relatively comprehensive overview of the postcranial skeleton, particularly the limbs and feet. Additionally, the associated forelimb of the holotype of *Daphoenodon* (*Borocyon*) *niobrarensis* Loomis from the lower Runningwater Formation serves as a useful reference in reconstruction of the forequarters. This forelimb (ACM 3452), complete from the scapula to the ungual phalanges (fig. 11), indicates a slightly less evolved antebrachium and forepaw relative to *B. robustum*. With regard to *B. neomexicanus*, only limb proportions, the radius, and metapodials are considered here. Additional preparation of the material from Standing Rock Quarry is necessary to obtain a complete description of its postcranial skeleton.

An estimate of body size for *Borocyon robustum* is speculative, given the lack of associated material. However, mid-shaft diameters of femora have often been used as predictors of body mass (Gingerich, 1990; Anyonge, 1993; see also Christiansen, 1999). The length and midshaft diameters of a complete femur (UNSM 26435: length, 378 mm; A-P and M-L diameters, 30.4 and 33.1 mm, respectively) of the species, probably representing a large adult male, exceed average values for the femora of *Panthera leo* (~324, 26, 28 mm) and *P. tigris* (~352, 27,

28 mm) presented by Bertram and Biewener (1990), suggesting at least a similar body mass perhaps slightly exceeding the mean for these large felids. On average, *P. leo* males range from 150 to 250 kg, and males of the Indian and smaller Sumatran *P. tigris* range from 100 to 258 kg (Nowak, 1991). Based on dimensions of the femur, *B. robustum* surely reached 100 kg, and probably some males at ~150 kg.

Forelimb

The proportions of the forelimbs of the species of *Borocyon* were compared with those of living ursids, felids, and canids (fig. 19A; table 4; appendix 1). A proportional increase in length of the radius relative to the humerus is evident as one progresses from ursids and felids to canine canids. Most New World amphicyonids for which an associated forelimb is known have a short lower forelimb, unlike living canids. *Borocyon*, on the other hand, has an elongated forelimb similar to proportions found in the wolf and cheetah (fig. 19A). An elongated forelimb (figs. 14, 15) is already present in the earliest known species of *Borocyon*, *B. neomexicanus*, and the lengthened forelimb is a principal synapomorphy of the species of the subgenus.

Scapula-Humerus

Poor representation of the scapula in *Borocyon* is likely due to targeted scavenging of the muscle mass concentrated at the shoulder—this bone survives for *B. niobrarensis* (fig. 20) and *B. neomexicanus* but not for *B. robustum*. Scapula and humerus are preserved in the associated forelimb of the holotype of *Borocyon niobrarensis* (ACM 3452), with the scapula nearly complete except for a small portion of the vertebral border (fig. 20A). The shape of this scapula is a composite of features of living ursids and large felids, and this shape was already characteristic of *Daphoenodon superbus* and *Borocyon neomexicanus*. No clavicle was present (it was already lost in *D. superbus*); the large acromnion process is configured as in *Ursus americanus* (breakage precludes determination of a metacromnion).

The cranial border of the scapula and the relative volumes of the supraspinatus and infraspinatus fossae are nearly identical to those of *Panthera leo* and *P. tigris*; in fact the overall form of the scapula is quite close to those of the large living felids. The principal osteological distinction of the *Borocyon* scapula from the scapulae of these cats is a broad teres process appended to the posterior axillary border, a process also found in living ursids (fig. 20). In the bears the teres process takes the form of a projecting bony plate whose lateral concave surface, termed the postscapular fossa, houses the subscapularis minor muscle. The postscapular fossa continues as a deep channel or groove (subscapular fossa of Davis, 1964) along the ventral axillary border, which houses the belly of the subscapularis minor muscle.

According to Davis (1949), fibers of the subscapularis minor of *Ursus americanus* maintain a separate identity from those of the subscapularis, both muscles inserting close together on the medial side of the humeral head, where they would effect medial rotation of the humerus. *Canis* and living felids lack the teres process and the subscapularis minor is not distinct from the subscapularis itself. In *Ursus americanus* the teres major muscle has been displaced to the medial side of the scapula by the subscapularis minor, where it arises from the surface of that muscle and from the thin adjacent edge of the scapula (Davis, 1949). The form of the teres process of *Borocyon niobrarensis* and the postscapular fossa on its lateral face are developed as in living ursids and in amphicyonids where the scapula is known, and certain procyonids have a scapular anatomy presaging the ursid condition.

In order to confirm the anatomy of the postscapular fossa and subscapularis minor, R.M. Joeckel and I dissected the shoulder of the Malayan Sun Bear (*Helarctos malayanus*). The subscapularis minor, here a fusiform muscle belly that occupies the postscapular fossa and its continuation forward into the subscapular fossa or groove, is a ventral derivative of the subscapularis muscle. Fibers of subscapularis minor run subparallel to the bony margins of the groove. The belly of this muscle lies loosely in the postscapular fossa and along the axis

TABLE 3
Dental Measurements (in mm) of Upper Teeth of North American Early Miocene Amphicyonids

	P2	P3	P4	M1	M2	C–M2	P1–P4
Daphoenodon superbus							
CM 1589	11.5 × 5.3	13.1 × 7.1	22.3 × 13.7	18.6 × 23.5	12.6 × 19.1	84.6	55.1
CM 1589a	12.3 × 5.7	14.1 × 7.2	25.1 × 15.0	18.7 × 24.3	13.6 × 19.4	83.1	56.8[c]
CM 1589b		16.3 × 8.7	23.8 × 14.6		12.8 × 19.6[b]		
CM 1589b					13.6 × 21.0		
CM 2774	11.1 × 5.2	(12.5)[a] × 6.4	22.8 × 13.9	17.8 × 23.8	12.3 × 19.0	80.6	52.4
AMNH 81055	11.7 × 5.0		22.3 × —	17.9 × 22.5	11.3 × 17.9		
AMNH 81046				19.9 × 24.5			
AMNH 81048				18.6 × 24.3			
AMNH 81050				17.0 × 21.1			
AMNH 83484			23.2 × 13.8				
Daphoenodon notionastes							
UF 449				16.5 × 19.1			
UF 16906			20.3 × 11.7				
Daphoenodon skinneri							
F:AM 70801	12.0 × 6.1	13.8 × 7.5	24.0 × 14.0	17.9 × 22.9	11.4 × 18.5	83.9	62.4
Daphoenodon falkenbachi							
F:AM 54144	13.7 × 7.5	15.8 × 8.9	27.1 × 18.8	22.1 × 26.9	15.0 × 21.7	96.1	67.6
UNSM 99420	13.0 × 6.5	16.1 × 8.0	26.4 × 16.2	22.0 × 27.7	14.3 × 21.6	101.2	70.5
Borocyon neomexicanus, n. sp.							
F:AM 49239	12.6 × 5.9	14.9 × 7.5	23.3 × 13.5	18.8 × 23.2	12.2 × 20.8	88.2	60.4
Borocyon niobrarensis							
UNSM 44827		15.2 × 7.5	24.9 × 15.6	20.6 × 25.9	13.4 × 21.9		
ACM 3452				21.9 × 26.0			
Borocyon robustum							
Bridgeport Quarries, Morrill County, Nebraska							
UNSM 2-25-6-35SP		15.6 × 8.3					
UNSM 26070			23.4 × 15.0				
UNSM 25961			24.7 × 15.3				
UNSM 26071			25.6 × 16.6				
UNSM —			25.3 × 15.1				
UNSM 26017				22.3 × 29.4			
UNSM 26015				22.4 × 28.8			
UNSM 25928				21.8 × 28.1			
UNSM 26016				22.6 × 30.9			
UNSM 26018					14.9 × 24.2		
UNSM 26019					15.5 × 26.9		
Hemingford Quarries, Box Butte and Dawes Counties, Nebraska							
UNSM 26416	13.2 × 7.7		28.7 × 17.9	23.3 × 30.7	16.0 × 26.2	106.2	74.6
F:AM 25402			27.8 × 17.7				
F:AM 25403			27.1 × 17.1				
F:AM 25404					14.3 × 23.8		
UNSM 26427					18.0 × 28.2		
UNSM 25547	12.9 × 7.7		29.2 × 17.2	23.4 × 31.4	16.8 × 27.2	~108	~75
UNSM 25686	12.9 × 7.1	17.7 × 9.7	27.5 × 17.5	23.3 × 30.2	14.6 × 24.9	108.5	74.9
Borocyon cf. *B. robustum*							
Suwannee River, Dixie–Levy Counties, Florida							
KU 114592	13.7 × 7.6	17.2 × 8.1	28.0 × 16.8	22.9 × 30.1	14.5 × 24.3	103.7	72.5

TABLE 3
(Continued)

	P2	P3	P4	M1	M2	C–M2	P1–P4
Adilophontes brachykolos							
F:AM 27568	13.9 × 7.0	16.5 × 7.9	26.0 × 15.2	21.3 × 24.0	13.0 × 20.0	93.3	66.4
F:AM 54148	13.6 × 7.5	19.5 × 9.4	27.4 × 17.6	22.0 × 27.7	15.1 × 23.0	108.1	75.3
F:AM 54140	13.2 × 7.0	17.2 × 8.4	27.5 × 17.9	21.1 × 27.7	13.7 × 22.1	103.8	74.5

[a]Estimated measurement.
[b]These three teeth may not belong to one individual but are sampled from a single population.
[c]Juvenile individual.

of the groove and is separated from the bone by a thin fascial sheet; fibers do not attach strongly to the bone of the fossa or groove. As the subscapularis minor is followed craniad to the forward edge of the groove, its fibers merge with fibers at the ventral margin of subscapularis. Of interest is that subscapularis minor does not twist around the ventral border of the scapula as described for *Ursus* by Davis (1949), but rather joins the large subscapularis and loses its identity before reaching the medial face of the scapular blade. The subscapularis, considered a major internal rotator of the arm, had 6–7 major pinnate bellies that join to form a thick, tendinous aponeurosis covering the medial head of the humerus. The ventral edge of this muscle extends 1–2 cm ventral to the scapular border as a fleshy muscle mass, which sends a slip caudad into the postscapular fossa. In *Helarctos* the subscapularis minor cannot function differently than the main body of the subscapularis. Consequently, the distinctive anatomy associated with the teres process of ursids and amphicyonids probably derives from an ancestral pattern retained in these lineages but does not necessarily confer the functional significance attributed to this anatomy by Davis (1949) in which these muscles formed part of a muscular package of the shoulder that was thought to favor climbing behavior. Considering the total limb anatomy of *Borocyon*, a climbing facility is extremely unlikely, whereas an ability to retract the limb in digging might seem a better possibility.

Whether the anatomy of the shoulder in *Borocyon* relative to that of large living felids is of significance is questionable, given that the role of the subscapularis minor and its postscapular process in *Helarctos* and that of the subscapularis in felids probably differs little in terms of the efficient function of the shoulder joint. This view also finds support from electromyographic investigations of muscle actions involving the shoulder joint.

The head of the humerus in *B. niobrarensis* (ACM 3452) and in the Suwanee River *Borocyon* (KU 113751) displays well-defined scars for the insertion of rotator cuff muscles (supraspinatus, infraspinatus, subscapularis) that stabilize the shoulder and aid in extension of the forelimb; their placement is the same as these scars in much smaller *D. superbus* (CM 1589) and similar to the wolf, particularly the flat insertion scar for infraspinatus situated far forward beneath the greater tuberosity. In felids and ursids the infraspinatus scar is more posteriorly situated. Not only do rotator cuff muscles stabilize the shoulder joint, but their simultaneous contractions participate in maintaining the balanced anatomical alignment of the parasagittal digitigrade limb: electromyographic studies of the rotator cuff muscles of domestic dogs and cats (Tokuriki, 1973a, b; English, 1978; Goslow et al., 1981) show that they act in concert not only during the stance phase when the forefoot contacts the ground but also during extension of the shoulder joint at limb protraction. These cuff muscles appear to act together to control movements of the shoulder joint brought about by loading on substrate contact as well as accurately positioning the forelimb during protraction prior to placement of the forepaw on the ground. A controlled rotation and translation of the shoulder apparatus during

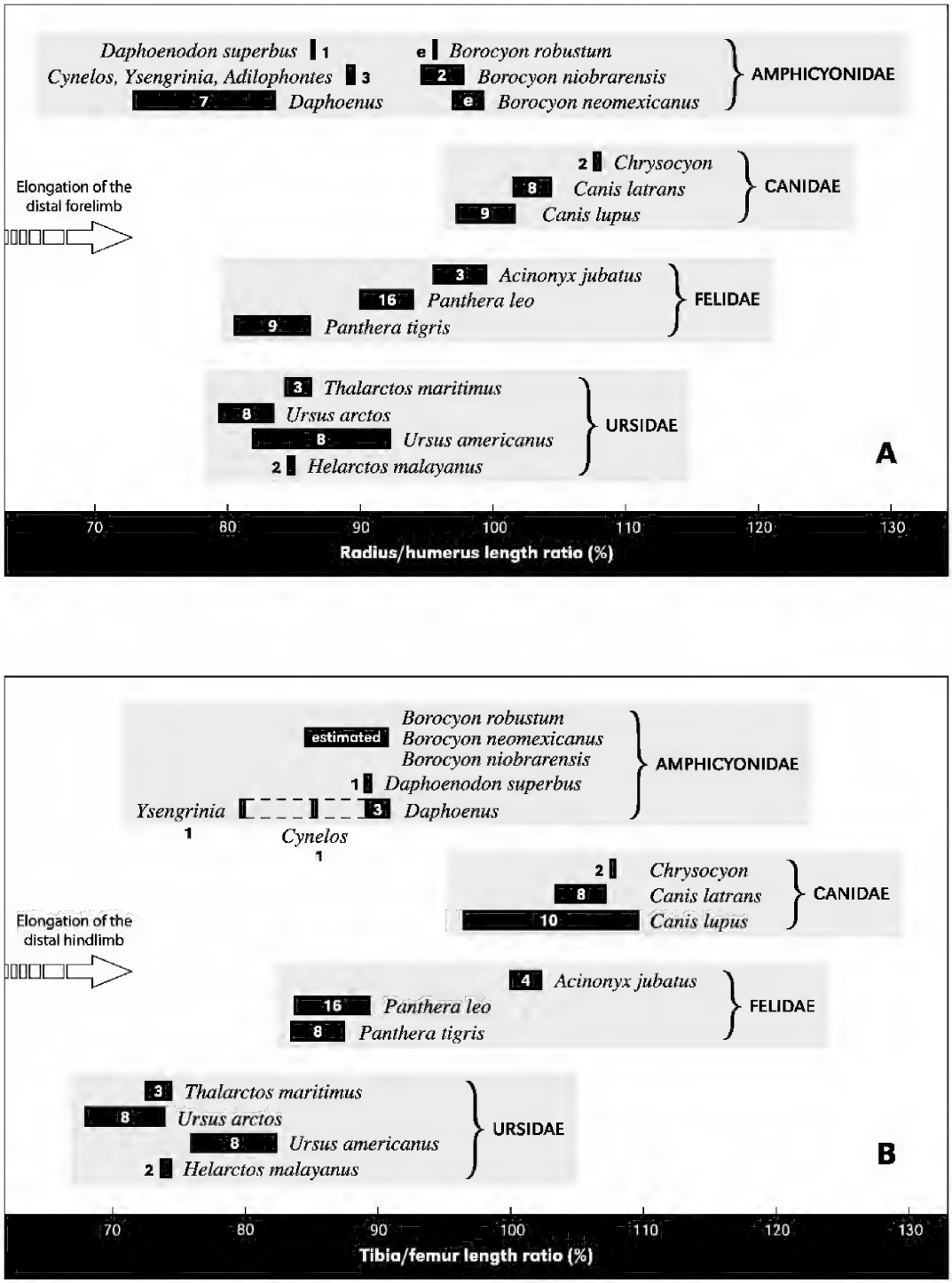

Fig. 19. Ratio (in %) of length of (**A**) radius/humerus and (**B**) tibia/femur for species of *Borocyon* relative to living canids, felids, and ursids and some additional amphicyonids. Species farthest to right show greatest elongation of the distal fore- or hindlimb segments. Numbers within or adjacent to black bars indicate sample size.

TABLE 4
Length Ratios Demonstrating Fore- and Hindlimb Proportions of Daphoenine and Amphicyonine Amphicyonids, Living Ursids, Felids, and Canids

	Radius/Humerus	Tibia/Femur
AMPHICYONIDAE		
Daphoenus vetus	73.0–83.8 (7)[c]	89.0–90.8 (3)
Daphoenodon superbus	86.7 (1)	89.1 (1)
Borocyon neomexicanus	97.0–99.6[d]	~90.8[d]
Borocyon niobrarensis	94.7–98.1 (2)	85.0 (1)
Borocyon robustum	95.8[d]	84.5–88.2[d]
Adilophontes brachykolos	89.6 (1)	—
Ysengrinia americana	~89.3[d]	79.8 (1)
Cynelos lemanensis[a]	89.5 (1)	85.1 (1)
URSIDAE		
Ursus americanus	82.0–92.4 (8)	75.9–82.4 (8)
Ursus arctos[b]	79.4–81.7 (3)	68.2–71.9 (3)
Ursus arctos (Kodiak)[b]	79.0–83.3 (5)	67.9–73.9 (5)
Thalarctos maritimus	84.4–86.3 (3)	72.5–74.4 (3)
Helarctos malayanus	84.4–85.0 (2)	73.7–74.2 (2)
FELIDAE		
Panthera tigris	80.7–86.4 (9)	83.4–87.6 (8)
Panthera leo	90.0–94.0 (16)	83.7–89.3 (16)
Felis concolor	82.2–83.9 (3)	91.7–94.8 (3)
Neofelis nebulosa	79.7–82.7 (3)	93.7–96.3 (3)
Acinonyx jubatus	95.8–99.6 (3)	100.0–102.3 (4)
CANIDAE		
Canis lupus[b]	97.2–101.9 (9)	96.5–109.8 (10)
Canis latrans	101.7–104.4 (8)	103.4–107.1 (8)
Chrysocyon brachyurus[b]	108.1 (2)	107.8 (2)

[a]Data from Ginsburg (1977).
[b]Some data from Davis (1964).
[c]Sample sizes are included in parentheses.
[d]Estimated from unassociated limb bones of several individuals (appendix 1).

the gait of carnivores is known to contribute to stride length. English (1978), based on electomyographic studies, thought that "the patterns of activity of the muscles of the shoulder girdle during stepping in most [living] carnivores ... may be qualitatively similar."

The scapular spine for deltoid musculature and the prominent deltopectoral crest of the humerus extending distad for two-thirds the length of the diaphysis suggest developed deltoid, cephalohumeralis, pectoral, and brachialis muscles supporting the forequarters and fixing the shoulder, with cephalohumeralis acting in forelimb protraction, much as in large living ursids (Davis, 1964); the deltopectoral crest does not extend as far distad in large felids such as *Panthera leo* but is a common trait of amphicyonids and ursids regardless of locomotor style. It seems probable that the deltopectoral crest of the humerus and the scapula's teres process with its postscapular fossa represent skeletal traits of *Borocyon* rooted more in phylogenetic considerations than in adaptive differences bearing on forelimb function.

Although we lack a complete humerus of the large *B. robustum* from the Hemingford Quarries, distal ends from these quarries and complete humeri and distal ends of *B. robustum* from the Bridgeport Quarries show a narrow distal humerus (fig. 21), differing from all New World amphicyonines. However, the distal humerus in *Daphoenodon superbus* is broader, essentially the same form as in amphicyonines, and in fact this type of

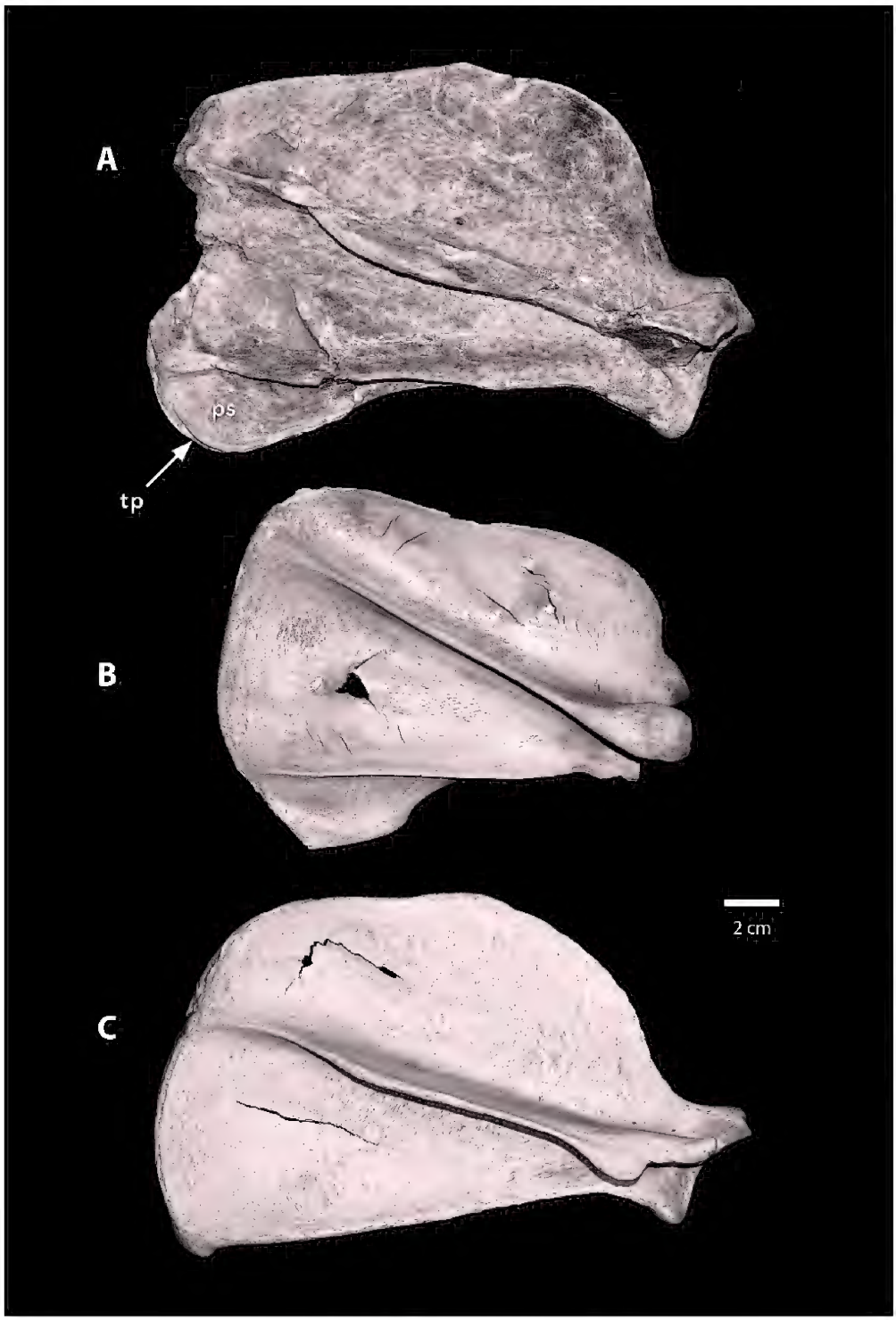

Fig. 20. Comparison of the scapulae of (**A**) *Borocyon niobrarensis* (ACM 3452); (**B**) *Ursus americanus* (ZM 1870); (**C**) *Panthera tigris* (ZM 14602): ps, postscapular fossa; tp, teres process.

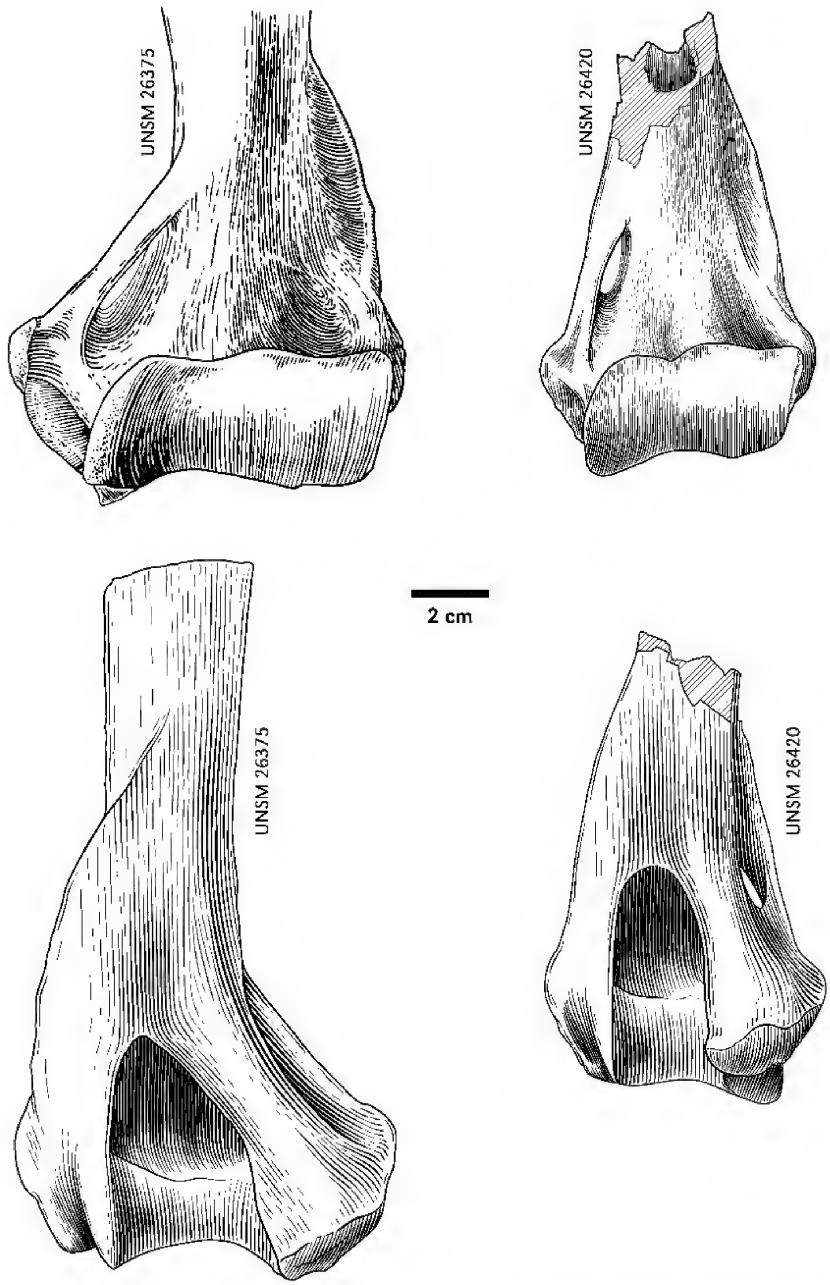

Fig. 21. Comparison of the distal humerus of *Borocyon robustum* (right, UNSM 26420) and *Amphicyon galushai* (left, UNSM 26375). The narrow distal humerus and symmetric olecranon fossa of *B. robustum* parallel the form of the distal humerus of the wolf and cheetah, indicating parasagittal orientation of the forelimb with minimal elbow eversion.

humerus is the plesiomorphic amphicyonid state. The mediolateral breadth of the distal humerus of *D. superbus* is due to a developed medial epicondyle for attachment of the flexor muscle group; also, in posterior view, the outline of the olecranon fossa is asymmetric because of the ulnar articulation, involving a slight outward angulation of the elbow joint. This type of distal humerus is also found in felids and ursine ursids. In

running carnivorans such as the wolf, the distal humerus is much narrower, and the medial epicondyle reduced, thereby altering the shape of the olecranon fossa to create a symmetrical (equilateral) triangular cavity. In these straight-legged cursors, the olecranon process of the ulna penetrates deeply into the olecranon fossa of the humerus, in some creating a perforate fossa accompanying the fully extended ulna.

A transformation in the shape of the distal humerus from the state seen in *D. superbus* to a state closely approaching the wolf occurs in the *Borocyon* lineage. The distal humerus of the *B. niobrarensis* holotype (ACM 3452, Loomis, 1936: fig. 4), a probable male, shows a modest reduction of the medial epicondyle and a somewhat asymmetric olecranon fossa. Humeri of *B. robustum* from the Bridgeport Quarries (UNSM 26210, 26260), from the Hemingford Quarries (UNSM 26420, Bx-12), and from the Suwanee River (KU 113751) show an even more reduced medial epicondyle and symmetrical olecranon fossa as in wolves. Jenkins (1973) observed that flexor muscles arising from an extended medial epicondyle exert a torque at the elbow joint not adequately compensated by the extensors. One of the options employed by cursorial carnivores to resist this torque involves diminished flexor musculature and reduction of the medial epicondyle. The narrow distal humerus of *B. robustum* is considerably modified from the plesiomorphic state evident in *D. superbus* and contemporary amphicyonines, such as *Amphicyon galushai*, and indicates a decreased torque and less eversion at the elbow and a more straight-legged stance with parasagittal alignment of the forelimb.

Radius-Ulna

The association of radius-ulna with humerus and scapula in the holotype of *Borocyon niobrarensis* (ACM 3452) establishes the proportions of the forelimb in this species relative to large living carnivorans (fig. 19A). A similar amount of limb elongation is estimated for *B. robustum* and *B. neomexicanus*, approaching that seen in the wolf and cheetah. There is some anatomical similarity to the forelimb of *Panthera leo*, particularly in the shoulder, yet significant differences exist in the antebrachium and forepaw of *Borocyon*. ACM 3452 is the most robust individual of *B. niobrarensis*, considered a male, yet the radius and ulna of the holotype (Loomis, 1936: fig. 4) are more slender and slightly more elongate than those elements of the lion. An associated radius and ulna in another *B. niobrarensis* individual (UW 10004), here interpreted as a female, are even more slender and gracile than in the male holotype.

The eight radii of *B. robustum* from the Hemingford Quarries are all longer than radii of *B. niobrarensis* (appendix 1), demonstrating that the lengthened distal forelimb has accompanied an increase in body size within the lineage. Although more robust than the radii of cheetah and wolf, the similarity in form of the *B. robustum* radius to the radii of these carnivores is striking (fig. 22). A complete ulna of *B. robustum* has not been recovered, but in *B. niobrarensis* the distal ulna (fig. 23) with its prominent rounded styloid process for articulation with the carpal cuneiform contrasts with the reduced and flattened process of the wolf and cheetah, suggesting a more mobile ulnar-cuneiform articulation at this joint. However, the distal ulnar process articulating with the radius is reduced, presaging the diminished state seen in the cheetah and wolf.

The radius of the wolf and cheetah differ from radii of large felids and ursine ursids in that the shaft is straighter, anteroposteriorly thin and bladelike, with reduction of both the styloid process and the width of the distal end of the bone. The distal ulna becomes more closely applied to the radius as mobility of the distal radioulnar joint is diminished. Furthermore, when manually articulated, the radius and scapholunar are more congruent in the wolf and cheetah than in large felids and ursids, creating a closely registered joint. *Borocyon robustum* and *B. niobrarensis* do not achieve this exacting fit of the wolf and cheetah but make a close approach. The radius of *B. robustum* in particular approximates the form of the cheetah radius (fig. 22). The shaft is elongate, anteroposteriorly thin and bladelike, with reduction in the width of the distal end as in the cheetah, although not to the extent seen in the wolf.

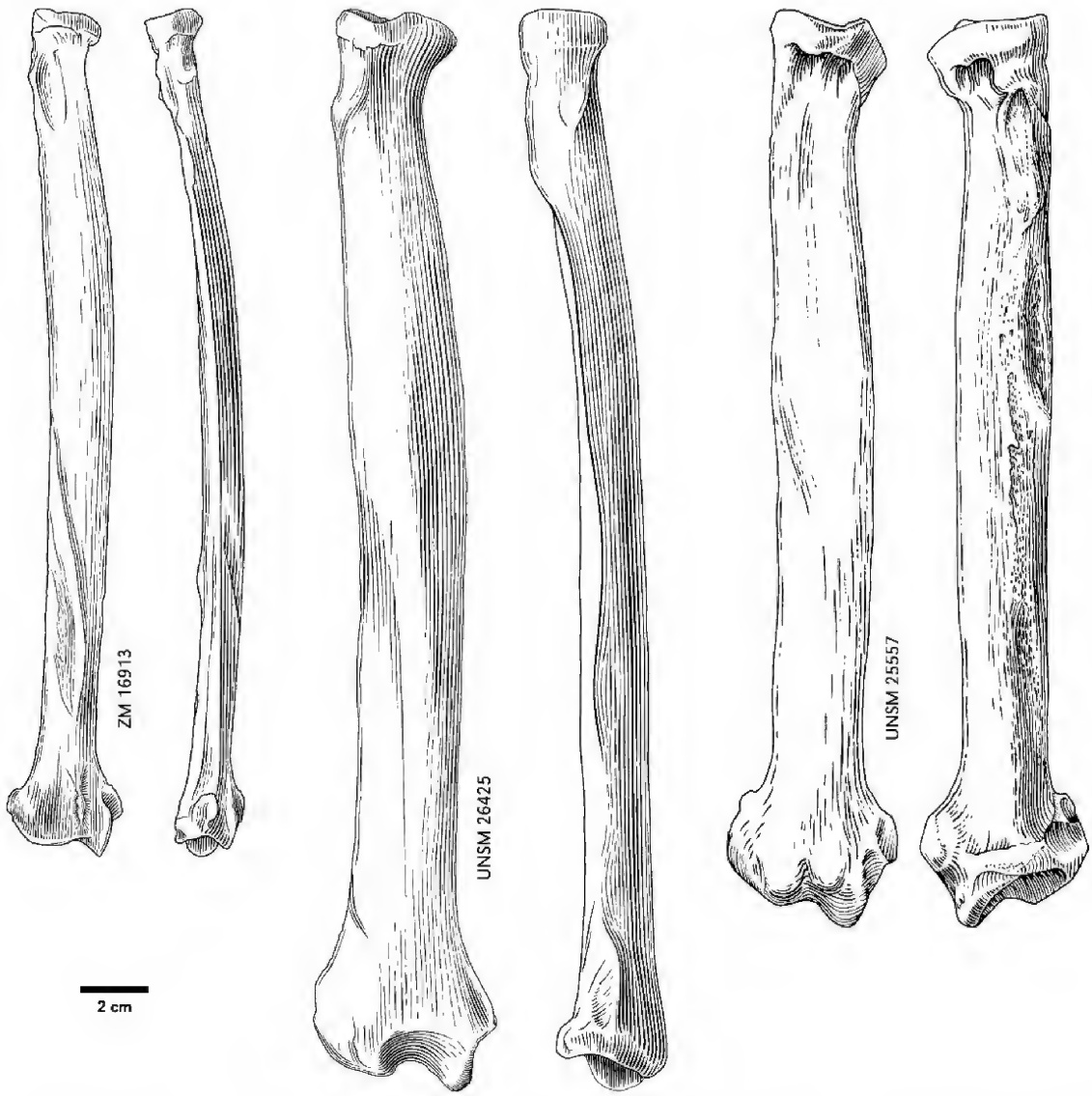

Fig. 22. Elongate radii of *Borocyon robustum* and the cheetah *Acinonyx jubatus* compared to the short, robust radius of *Amphicyon galushai*. A slender, elongate radius with flattened blade-like shaft and transversely narrow proximal and distal ends characterizes both *B. robustum* and the cheetah. Left, *Acinonyx*; center, *B. robustum*; right, *A. galushai*.

The size of the radial head is reduced relative to the breadth of the diaphysis, as in wolf and cheetah, but it is clear that the ovate shape of the radial head and the extent of its articular surface with the ulna show that less than 90° of supination was possible.

An associated radius and proximal ulna (UNSM 25554) and two additional radii (UNSM 25553, 44721) of *B. robustum*, in which the articular circumference of the radial head is well preserved, permit an estimate of the probable amount of rotation of the radial head in the trochlear notch of the ulna. The proximal articular surface of the radius is ovoid, similar in form to that of the lion, but not as concave. In *B. robustum* this is due to the flatter, less rounded capitulum of the distal humerus, which is also seen in the living bears where the proximal articular surface of the radius is

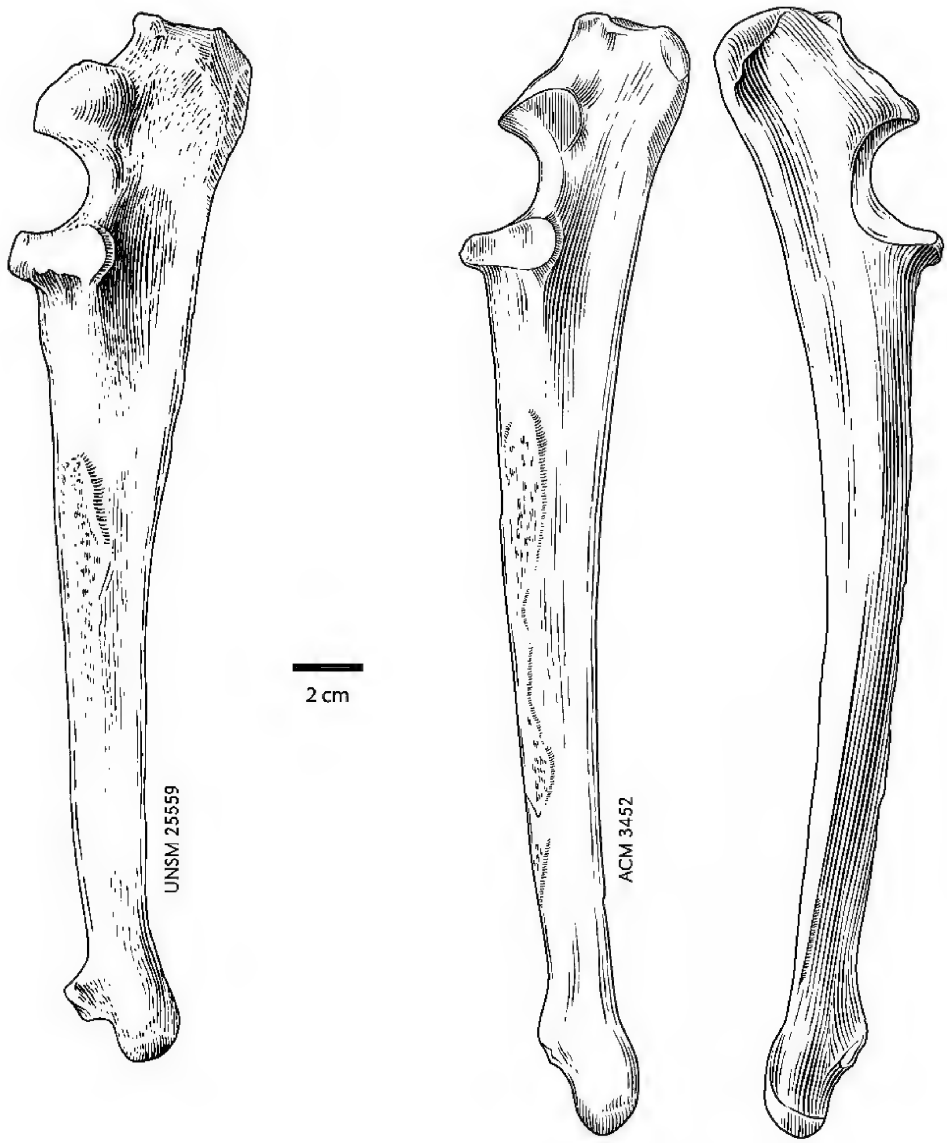

Fig. 23. Comparison of the ulnae of *Amphicyon galushai* (left) and *Borocyon niobrarensis* (center and right), showing the more elongate, slender, curved ulna of the latter species. No complete ulna of *B. robustum* is known; however, eight radii of this species demonstrate the existence of an even more slender, elongate ulna.

nearly flat; in the cheetah there is a much more concave, circular radial head. The anteromedial lip of the radial head in *Borocyon*, the wolf, and in large living felids and ursids is slightly elevated as a small process (the capitular eminence of Davis, 1964: 97) that allows better registration between the radius and capitulum of the distal humerus during flexion at the elbow. Davis considered the capitular eminence a bony stop that limited the rotary movements of the radius; it is quite reduced in the cheetah.

The radius is bound to the ulna at the elbow by the annular ligament that anchors the head in the radial notch. The radial notch of both *B. robustum* and *B. niobrarensis* is shallow, similar to that of the wolf, more so

than the slightly deeper notch in large living felids. The amount of potential rotation of the radial head in the notch during pronation and supination is indicated by a semicircular transverse facet situated on the articular circumference of the radial head. In *Canis lupus* this facet is both sharply demarcated and quite limited in its transverse extent, which greatly impedes pronation-supination in the wolf. In *B. robustum* the border of the facet is not as sharply indicated nor is the facet as transversely limited as in the canid, however manipulation of the associated radius and ulna of the beardog shows that the extent to which the radius can rotate in the radial notch exceeds that seen in the wolf but appears somewhat limited relative to *Panthera leo*. When this is considered together with the rather flat capitulum of the distal humerus, the less concave radial head, and the shallow radial notch, these features suggest a slightly more restricted capability for pronation-supination of the radius in the beardog.

Canis lupus and *Borocyon robustum* display similar placement of the scar for the interosseous ligament binding radius and ulna. The scar for the ligament and interosseous membrane extends from immediately below the bicipital tuberosity of the radius for two-thirds of the length of the radial diaphysis along its ulnar margin. The ligament is confined to the proximal diaphysis directly beneath the bicipital tuberosity. Dimensions and location of the narrow interosseous scar of the beardog are most similar to those of the wolf and cheetah: scar width relative to length of the radius calculates to 2.8 to 3.5% for wolf and cheetah and 3.0% for *B. robustum* (N=7); it is much broader in the large living felids. The ligament in these carnivores restrains the rotation of the radius about the ulna during pronation–supination, and the location of the narrow interosseous scar on the ulnar margin of radii of *B. robustum* and the bladelike form of the elongate radius shows that the ligament must have functioned much as in the wolf and cheetah. In a recent analysis of the cheetah antebrachium, Ohale and Groenewald (2003) describe the interosseous ligament as effectively limiting pronation and supination of the radius in this running carnivore.

Carpals

Close examination of the carnivoran carpus demonstrates that the principal movement in the wrist occurs at the articulation of the proximal carpals with radius-ulna (proximal carpal joint) with only subordinate adjustment at the mid-carpal joint. As Yaldon (1970) has shown for the larger running carnivorans, the carpus is chiefly a flexion hinge, with very limited ulnar and radial deviation restricted to the proximal carpal joint. When the forefoot strikes the ground, the carpus goes into full extension and is locked by virtue of carpal stop facets and binding ligaments and remains thus through limb retraction. Then, as protraction begins, carpal flexion is initiated and attains its climax during the protraction phase of the gait. The extent that the manus can be flexed varies in the different carnivoran families and is minimal at the mid-carpal joint. In felids (*Felis*, *Acinonyx*), canids (*Canis*, *Vulpes*), and a hyaenid (*Crocuta*) studied by Yalden (1970), flexion at the mid-carpal joint was always much less (~40°) than at the proximal carpal joint (90°–120°).

In the living carnivorans studied by Yalden (1970), extension of the wrist at the proximal carpal joint is arrested by binding ligaments that necessarily act to prevent extreme hyperextension at the moment when the forefoot contacts the ground, bears weight, and propels the animal forward. Hyperextension of the wrist in Carnivora occurs only in the proximal carpal joint (bones of the mid-carpal joint are locked) and does not exceed ~40 degrees in canids and felids, with ~55 degrees reported in *Ursus* (Yalden, 1970). Yalden thought that the ligaments binding the proximal carpal joint were likely stretched in extension, which seems a probable consequence of forefoot impact with the substrate. Stretching of these ligaments must play a major role in preventing hyperextension of the wrist at the proximal carpal joint in *Borocyon*, acting as a shock absorber just as in living large Carnivora.

The carpals are preserved in the associated *B. niobrarensis* forefoot (fig. 11) and in a composite foot of *B. robustum* (figs. 24, 25). The most evident innovation appearing in the

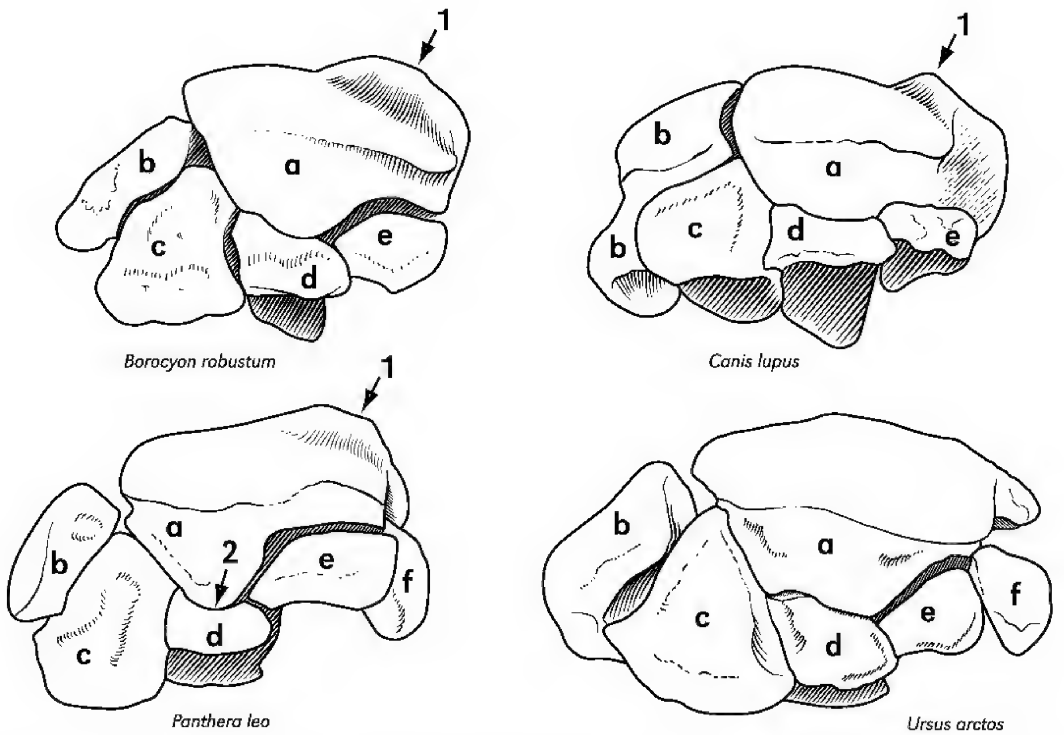

Fig. 24. Comparison of the carpus (anterior view) of *Borocyon robustum* and those of *Panthera leo*, *Canis lupus*, and *Ursus arctos*. See text for discussion. **1**, Elevated bony ridge on scapholunar forcing ulnar deviation of the forepaw during flexion of the wrist; **2**, scapholunar process inserted in concavity of magnum preventing hyperextension within the carpus (this stop mechanism is maximally developed in the cheetah). Abbreviations: a, scapholunar; b, carpal cuneiform; c, unciform; d, magnum; e, trapezoid; f, trapezium.

carpus is an increase in the size and proximodistal height of the scapholunar from *Daphoenodon superbus* through *B. niobrarensis* to *B. robustum*. In *B. robustum* it is particularly massive and robust, with its increased height accompanying elongation of the radius and reflecting the mass of the forequarters of this large carnivore. In living Carnivora the convex articular surface of the scapholunar conforms to the concave distal radius, permitting flexion and extension at the proximal carpal joint of the wrist.

Extension/flexion of the *Borocyon* manus at the proximal carpal joint is governed by these transversely aligned articular surfaces of scapholunar and radius that restrict the joint to fore–aft motion around a transverse axis of rotation. Based on the dimensions and extent of the proximal articular surface of the scapholunar, this surface in *B. robustum* appears somewhat flatter and less convex than those of large felids of similar body size such as *Panthera leo* and *P. tigris*, and displays a convexity more like that of the wolf and cheetah. Moreover, when the width of this articular surface in *B. robustum* is compared to that of, for example, *Panthera leo*, the scapholunar in the beardog is mediolaterally shorter, more abbreviate, corresponding to the more narrow, distal radius of the wolf, which lacks the distal breadth evident in the lion.

Flexion involves a relatively unimpeded transverse folding movement at the proximal carpal joint of the wrist until, as Yalden (1970) describes, the distal radius comes into contact with a volar process on the scapholunar that forces some amount of ulnar deviation of the paw as flexion continues. In all living carnivorans, on the radial side of the scapholunar at the posteromedial corner, there is a knoblike volar process (fig. 25, vp),

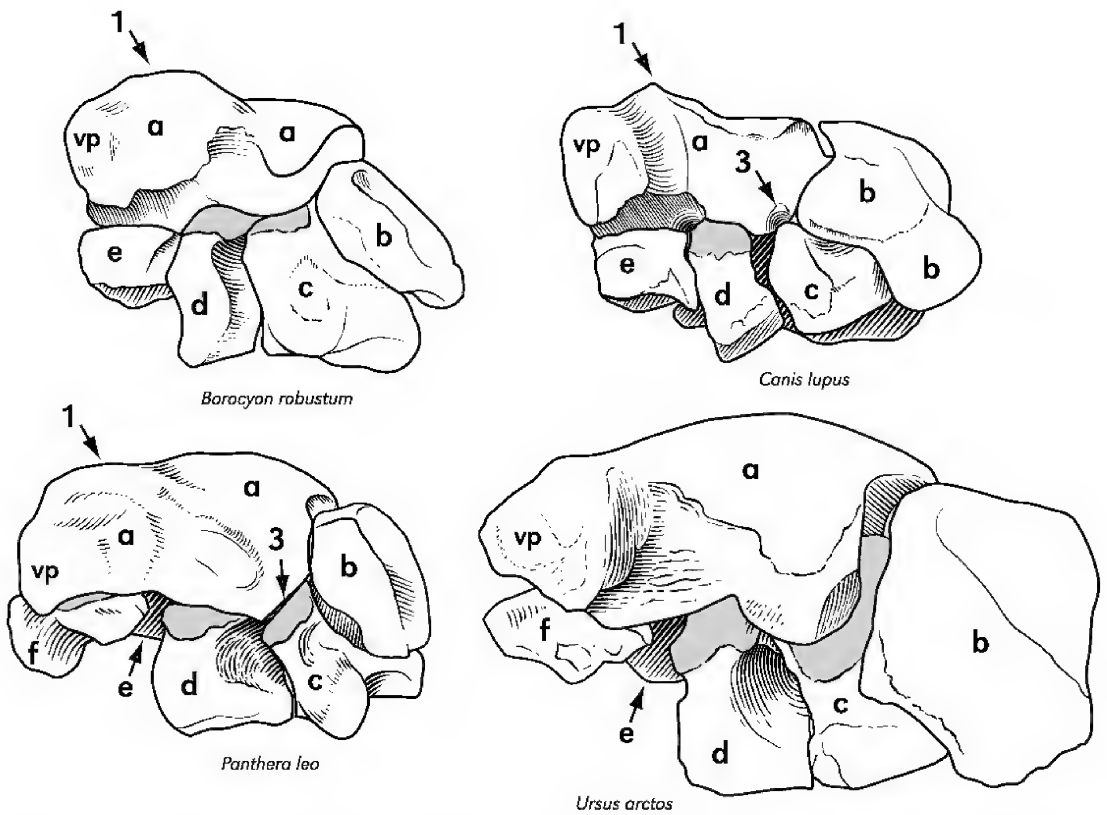

Fig. 25. Comparison of the carpus (plantar view) of *Borocyon robustum* and those of *Panthera leo*, *Canis lupus*, and *Ursus arctos*. See text for discussion. Gray tone indicates extent of articular surfaces for scapholunar on magnum and unciform; in ursid and *B. robustum* the scapholunar moves largely unimpeded over these surfaces during intracarpal flexion but in lion and wolf there is a bony stop (**3**) between unciform and scapholunar that arrests this movement (this stop is even more developed in the cheetah). Abbreviations as in figure 24: vp, volar process.

the scapholunar tubercle of Yalden (1970). In living canids, hyaenids, and felids, a bony ridge develops at the junction of this process with the body of the scapholunar. This ridge, acting as a bony stop (figs. 24, 25, #1), redirects the forward movement of the scapholunar on the radius during flexion. As the manus flexes during protraction of the forelimb, the ridge comes into contact with the posteromedial border of the distal radius, diverting the manus. The positive arcuate form of the bony ridge fits a complementary negative concavity on the radius, forcing the scapholunar (hence the paw) to move in ulnar deviation. This action has been noted previously in living carnivorans by both Taylor (1974) and Yalden (1970).

In the cursorial wolf, cheetah, and hyaenids (*Crocuta crocuta*, *Hyaena brunnea*), the bony ridge is particularly well developed. This ridge on the scapholunar is absent in living ursids and most other living arctoid carnivorans (a small ridge occurs in *Procyon lotor*), where, if ulnar deviation occurs to any extent, it is due to contact of the distal radius with the base of the volar process itself. Yalden (1970) viewed some form of ulnar deviation as common to all Carnivora, helping to prevent the protracting manus from contacting the contralateral forelimb as the limb swings forward.

In the species of *Borocyon* where the carpus is known, the scapholunar with its bony stop is developed similarly to the wolf and cheetah (figs. 24, 25, #1). In *Borocyon niobrarensis* the scapholunar ridge is not quite as pronounced as in some individuals of *B. robustum* where the ridge is indeed

prominent and the volar process itself is more massive.

Grooves on the distal surface of the scapholunar for the magnum and unciform control movement at the mid-carpal joint and are aligned essentially fore–aft in living Carnivora. The magnum serves as the principal guide for flexion of the distal on the proximal carpal row (fig. 25, d). It can move only a limited distance fore–aft in its scapholunar groove, perhaps ~20° at most, determined by the alignment of its proximal ridge. The groove for the magnum in the scapholunar is deep and similarly configured in felids (including the cheetah) and ursids, but is shallower and nearly in the same plane as the adjacent groove for the unciform in canids and *Borocyon*. The magnum of large felids and ursids is posteriorly broad (fig. 25), but in *Borocyon robustum*, despite the overall geometric similarity of magnum, unciform, and trapezoid to *Ursus arctos* (fig. 24, anterior view), the magnum has become narrow and mediolaterally compressed as in the wolf, suggesting an incipient adaptation for more restricted fore–aft motion.

Adjacent to the magnum, the unciform of *Borocyon* also participates in flexion of the wrist at the mid-carpal joint. This flexion is significantly inhibited in the wolf by stop facets developed between scapholunar, carpal cuneiform, and unciform (fig. 25). First, the posterolateral corner of the scapholunar makes a particularly broad contact with the carpal cuneiform. But of most significance in the wolf, the unciform has added a posterior process that locks against the posterior margin of the scapholunar immediately medial to the facet between scapholunar and carpal cuneiform (*C. lupus*, fig. 25, #3). A similar ridgelike unciform process that inhibits flexion occurs in large felids, but in them the process contacts more of the posterolateral corner of the scapholunar (*P. leo*, fig. 25, #3) than it does in the canid. The ridgelike unciform process of felids attains its maximum development as a bony stop in the cheetah where the top of the ridge forms a concave facet into which the posterolateral corner of the scapholunar fits and locks.

In both ursine ursids and the species of *Borocyon* the unciform lacks a posterior process and so the amount of flexion involving the unciform is not as restricted as it is in the wolf, lion, and cheetah, where stop facets greatly inhibit flexion of the mid-carpal joint (Fig. 25). Despite the absence of these stop facets in *B. robustum*, the limited extent and more horizontal nature of the proximal articular surfaces of the unciform and especially the magnum suggest very restricted flexion at the mid-carpal joint.

Medial to the groove on the scapholunar for the magnum of *Borocyon* is a broad facet for the trapezoid. In *B. niobrarensis* the trapezoid is a blocky, wedge-shaped bone (length, 20.3 mm; greatest transverse width, 19.7 mm). Its medial planar facet for the trapezium is rectangular (length, 11.7 mm; height, 6.6 mm). Posterior to the trapezoid on the distal surface of the scapholunar is a slightly concave, subcircular facet (*B. robustum*: length, 6 mm; width, 7 mm; *B. niobrarensis*: length, 5 mm; width, 5 mm) for the reduced trapezium. The *Borocyon* trapezium is proportionately much smaller than the large element in ursids and even smaller than the much differently configured trapezium of large felids. The trapezium itself is known only in *B. niobrarensis* (ACM 3452, greatest length ~13 mm), where it is a triangular element situated directly behind the trapezoid. Its placement and size are much like that of the wolf. It articulates with the slender, reduced first metacarpal (~5 cm in length). The size of the trapezium, first metacarpal, and its phalanges suggest that the extensor, flexor, abductor, and adductor muscles of digit I were as modified as those in the canid, where the first digit was similarly reduced.

Yalden (1970) observed that when the mid-carpal joint in Carnivora is fully extended, all stop facets are brought into contact and the joint is locked in full extension. Furthermore, flexion of metacarpus on carpus heavily depends on the heads of paraxonic metacarpals 3–4 (with participation of metacarpal 5) fitting into the corresponding concave facets of magnum and unciform. These facets are aligned to allow only very limited flexion and extension. There appears to be almost no movement between the trapezoid and second metacarpal in many large felids (*Panthera leo*, *P. tigris*, *Acinonyx*), due to the nearly flat intervening joint surfaces and to a bony stop

formed between the head of the second metacarpal and a round pit on the posteromedial side of the magnum. The second metacarpal of these felids is held largely immobile, locked between magnum and trapezium. In *Borocyon robustum* and in the wolf the second metacarpal is somewhat more mobile since the trapezium is essentially nonfunctional, and the facet on the magnum for the metacarpal is present but is not developed as a locking device.

Large felids also employ a bony stop involving the magnum to arrest extension at the mid-carpal joint. In the lion, tiger, puma, and jaguar the descending process on the anterior face of the scapholunar fits into a facet on the upper surface of the magnum (fig. 24, #2) that locks the two bones and prevents hyperextension of the distal carpals on the scapholunar. In the cheetah the magnum facet has further evolved to form a deep pit for the tip of the scapholunar so that the locking mechanism is better developed than in any other felid. Yalden (1970) noted that when the forefoot strikes the ground in the cheetah, hyperextension is limited to the radioulnar-proximal carpal joint; any extension at the midcarpal joint is prevented by this locking mechanism. In *Borocyon* the contact between magnum and scapholunar is like that of many arctoid Carnivora and canids in which the apposed joint surfaces are firmly held by ligaments but are not as tightly locked as in felids.

Alignment of the distal carpal row with the scapholunar and carpal cuneiform in *Borocyon* is developed as in the caniform Carnivora and lacks the "stepped" placement of the unciform, magnum, and trapezoid of felids (including *Acinonyx*) resulting from the offset heads of their overlapped proximal metacarpals (fig. 24, *P. leo*). This stepped configuration is characteristic of all large living felids and reflects the intricate interlocked character of the distal carpals and proximal metacarpals, a unique attribute of the felid manus not present in arctoid Carnivora.

Metacarpals

The metacarpals of *Borocyon*, while similarly paraxonic and elongate, differ in lacking the overlapping, "interlocked" proximal ends of MC2 on MC3, and MC3 on MC4, evident in the lion and cheetah, and also characteristic of the tiger, jaguar, and puma. The proximal metacarpals of *Borocyon* articulate without overlap and in this respect are typical of arctoid Carnivora. In large felids the interlocked character of the metacarpals can involve the distal carpals, best exemplified by the insertion of the proximal second metacarpal between magnum and trapezium. Here a palmar process of the metacarpal fits into a pit in the medial face of the magnum, locking the metacarpal between that bone and the trapezium. This does not occur in arctoid Carnivora or in hyaenids.

The cheetah and canine canids show close appression of the proximal shafts of the metacarpals, whereas *Borocyon* and the lion do not. *Borocyon* displays a distal separation or splay of the metacarpals much like *Panthera leo* (fig. 11) but emphasizes the weight-bearing paraxonic metacarpals 3–4 with somewhat greater reduction of metacarpals 2 and 5. Large living felids other than the cheetah also show this distal separation of the metacarpals. The forepaws (figs. 11, 26) of *Borocyon niobrarensis* and *B. robustum* must have resembled the broad paws of large living felids, possibly used to deliver a blow to prey, manipulate objects including food to a limited extent, and even excavate a burrow, with these behaviors having been witnessed for *P. leo* by Schaller (1973).

Phalanges

Phalanges are associated with individuals of both *B. niobrarensis* and *B. robustum*. Proximal, intermediate, and ungual phalanges are present in the forefoot of the *B. niobrarensis* holotype (fig. 11). A proximal and an intermediate phalanx occur with the partial skeleton of F:AM 107601 and four proximal phalanges with UW 10004 (both *B. niobrarensis*). The *B. robustum* holotype (CM 1918) described by Peterson (1910) included five proximal and three intermediate phalanges but no unguals. Overall, the proportions of the phalanges are most comparable to those of ursids such as *Ursus arctos*, but the detailed anatomy of the metacarpal-phalangeal joints are more similar to those of large felids.

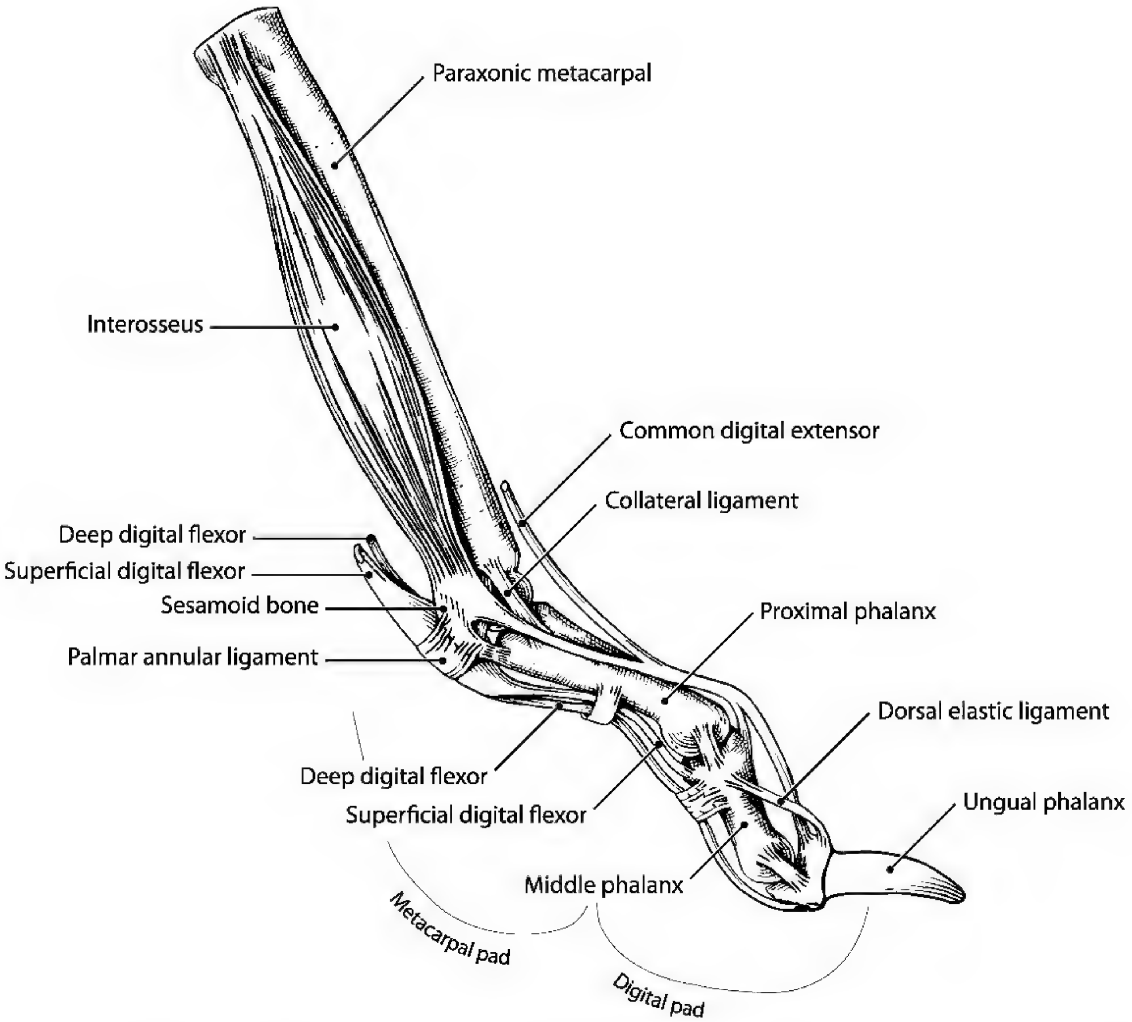

Fig. 26. Restoration of the *Borocyon robustum* forefoot illustrating the interosseous muscle supporting each paraxonic metacarpal-phalangeal joint, the short middle phalanges, elongate unguals, and presumed dense fibrous metacarpal and digital pads.

The holotype forefoot of *B. niobrarensis* (fig. 11) includes five proximal phalanges correctly assigned to the corresponding metacarpals by Loomis (1936), based on comparison with the articulated forefeet of *Daphoenodon superbus*. Two proximal phalanges are symmetrical (about their long axes) and elongate (lengths, ~31–32 mm) and therefore belong to the paraxonic metacarpals 3–4. The proximal phalanx of the third digit is slightly more robust than that of the fourth. Another symmetrical proximal phalanx (length, ~30.4 mm) fits metacarpal 2, and two smaller, asymmetric phalanges belong to metacarpals 1 and 5. Metacarpal 1 (41.8 mm) and its proximal phalanx (27.1 mm) are much reduced, although these bones are slender and gracile. Prominent bony keels on the distal metacarpals insert between and guide a pair of sesamoids for each digit. These keels compare with those of living large felids and are much more developed than the metapodial keels of ursine ursids.

Anatomically significant features of the proximal phalanges of digits 2–5 (fig. 26) include (1) a notch or groove in the base of the palmar surface for the metacarpal keel

and the combined tendons of the superficial and deep flexors of the digits, similar to those of large felids; (2) a pair of prominent bony tubercles on either side of this notch for attachment of the sesamoid and interosseous tendons—the interosseus muscles are flexors of the metacarpal-phalangeal joints but also contract to support these joints to prevent hyperextension when the carnivore places weight on the paw; (3) a concave base of the proximal phalanx congruent with the distal metacarpal so that the joint is firmly registered and further secured by sesamoid and collateral ligaments. Flexion is significantly limited by the height of the metapodial keels and adjoining sesamoid bones.

The intermediate (middle) phalanges are much shorter than the proximal ones and all have a strong proximal dorsal process for extensors of the digits (fig. 26). When the intermediate phalanx is plantar-flexed ~45°, the dorsal process fits a corresponding groove in the distal proximal phalanx. This restricts the joint to only flexion and extension, assisted by the biconcave base of the intermediate phalanx that, together with the dorsal process, prevents axial rotation of the digit. Some of these intermediate phalanges display slightly asymmetric shafts but the degree of asymmetry does not approach that seen in living felids where the trait is related to hyper-retractility of the claws (Gonyea and Ashworth, 1977; Wang, 1993). The distal articular surface of the intermediate phalanges extends onto the dorsal surface of the bone, demonstrating that the ungual phalanges could be slightly retracted. However, the ungual phalanges are not specialized for hyper-retractility and instead are slender, long, and nearly straight (not curved), as in living ursids.

Unguals are generally rare but six well-preserved unguals of the associated forefeet of *B. niobrarensis* (ACM 3452) range in length from 23.6 to 25.2 mm, averaging 24.2 mm (fig. 11); they appear quite elongate relative to the short intermediate phalanges. The foreclaws of large ursids are longer than the hindclaws, and this was possibly true of *Borocyon* (no unguals of the hindfoot can be certainly identified). These unguals show slight development of a bony hood and the presence of a dorsal process for attachment of the tendon of the common digital extensor.

The angulation of the phalangeal joints indicates the presence of thick fibroelastic metacarpal and digital pads cushioning impact with the ground during footfall (fig. 26). Undoubtedly, thick connective tissue pads supported and cushioned both the fore- and hindfeet, extending from the distal metapodials forward beneath the digits (Alexander et al., 1986).

Rather short intermediate phalanges emerge as a distinctive trait of *Borocyon robustum* and *B. niobrarensis*, confirmed in the former by associated phalanges in the holotype hindfoot (CM 1918) and in the latter species by associated forefeet in its holotype (ACM 3452). These short phalanges were unexpected since they are atypical of living large Carnivora: in the wolf the intermediate phalanges of the paraxonic digits 3–4 range from ~67% to 71% of the length of the proximal phalanges, and the intermediate phalanges of the side toes (digits 2 and 5) fall at ~58%–63%. In *B. niobrarensis* (ACM 3452), where associated digits are available, the intermediate phalanges of digits 3–4 (N = 4) all fall from ~59% to 67% and the side toes (digits 2 and 5, N = 3) at ~55%–58%. These values for *B. robustum* are ~61% for a paraxonic digit and ~58% for a side toe.

In contrast, ursids (*Ursus arctos*, *U. americanus*) fall at ~74%–77% for the principal weight-bearing digits. The lion and puma show similar values of ~71%–77% for paraxonic digits 3–4, and the cheetah has values somewhat lower at ~65%–66%. Despite these proportional differences, the shape of the phalanges of *Borocyon* are most like the phalanges of large bears such as *Ursus arctos*, presumably because of the shared arctoid ancestry of ursids and amphicyonids, whereas the more derived anatomy of the metacarpal-phalangeal joints parallels that of large felids like the lion. This joint anatomy is an adaptation to a more digitigrade stance.

Hindlimb

Proportions of the *Borocyon* hindlimb do not correspond to those of living canids or the cheetah, falling closer to the lion

(fig. 19B) and differing surprisingly little from plesiomorphic amphicyonids such as *Daphoenodon superbus* and *Daphoenus*. Caution is necessary here in that no associated hindlimb of *Borocyon robustum* is known (there is a possible association of femur and tibia in a small *B. niobrarensis* female, UW 10004), and so the estimate of hindlimb proportions is taken from unassociated femora and tibiae. This estimate, however, cannot be far from the mark.

Innominate

The innominate is known only in *B. niobrarensis* (F:AM 107601) where its form differs to some extent from that of large living felids and ursids. The acetabulum is deep, as in the large cats, but the ilium and ischium are proportionately slightly shorter. A broader ilium than seen in these felids (but much like wolves) suggests that gluteal muscles for retracting the femur were well developed for propulsive thrust. Extension and medial rotation of the femur at the hip joint performed by the gluteal group is balanced by the caudal hip muscles (gemelli, obturators, quadratus femoris) that laterally rotate the femur, resulting in the parasagittal path of the hindlimb. Extent and position of the articular surface of the head of the femur within the acetabulum are as in the large living felids, wolves, and cheetah (roof of the acetabulum a horizontal surface of similar depth and area with the same anterior and posterior ventral extension).

Pronounced eversion of the ischium and ischial tuberosity in living carnivorans corresponds to a parasagittal orientation of the hindlimb whereby the action of the hamstrings is brought into a fore–aft alignment. The cheetah and wolf show an extreme degree of ischial eversion among living Carnivora. *Borocyon* displays a degree of ischial eversion corresponding to the large felids and does not approach canine canids or the cheetah. When the innominates of *B. niobrarensis* and a Sumatran tiger of the same body size are compared, the ischium is of similar form and length and the tuberosity of the same size and degree of eversion, but the ilium is somewhat shorter and broader in the beardog.

Femur

Borocyon robustum is represented by two complete femora (UNSM 26435, KU 113645). UNSM 26435 is from a very large animal (length, ~38 cm), probably male, and was found at Shimek's Quarry, one of the upper Runningwater localities. This large femur is most similar to those of living lion and tiger but with some important distinctions. There is a close correspondence in orientation of the proximal femoral head, neck, and trochanters, the margins and shape of the femoral hemisphere, the location of the fovea capitis femoris (fig. 27) for the femoral ligament, and the form of the diaphysis. The form and amount of separation of the distal condyles are as in these large living felids; the condyles are not placed as close together as in the wolf. Femora of *Ursus arctos* and *Thalarctos maritimus* differ from those of *B. robustum* in that the femur of these ursids is more strongly abducted; the femoral neck and head are proximally elevated and the diaphysis rotated outward—this is the abducted ursid femur of Jenkins and Camazine (1977).

The anatomy of the femur provides useful information on hindlimb stance and excursion, particularly the orientation of the femoral head relative to the diaphysis; the configuration of the margin of the articular surface of the head relative to the diaphysis and acetabular rim; and the location of the fovea capitis femoris for the femoral ligament (Jenkins and Camazine, 1977). Jenkins and Camazine (1977) showed that the excursion of the femur of a domestic cat during walking describes a more adducted path than in a small canid (*Vulpes fulva*) and raccoon (*Procyon lotor*). When stationary, the femur of the fox was abducted ~10°, and the cat aligned in a parasagittal plane, whereas that of the ambulatory raccoon was abducted 25°–35°. Jenkins and Camazine (1977) observed a relationship between the alignment of the anterior margin of the articular surface of the femoral head and the amount of femoral abduction in these carnivores. In the domestic cat and foxes studied by them, the more parasagittal stance correlated with the alignment of the anterior margin of the articular surface of the femoral head. In these small carnivores, the anterior margin

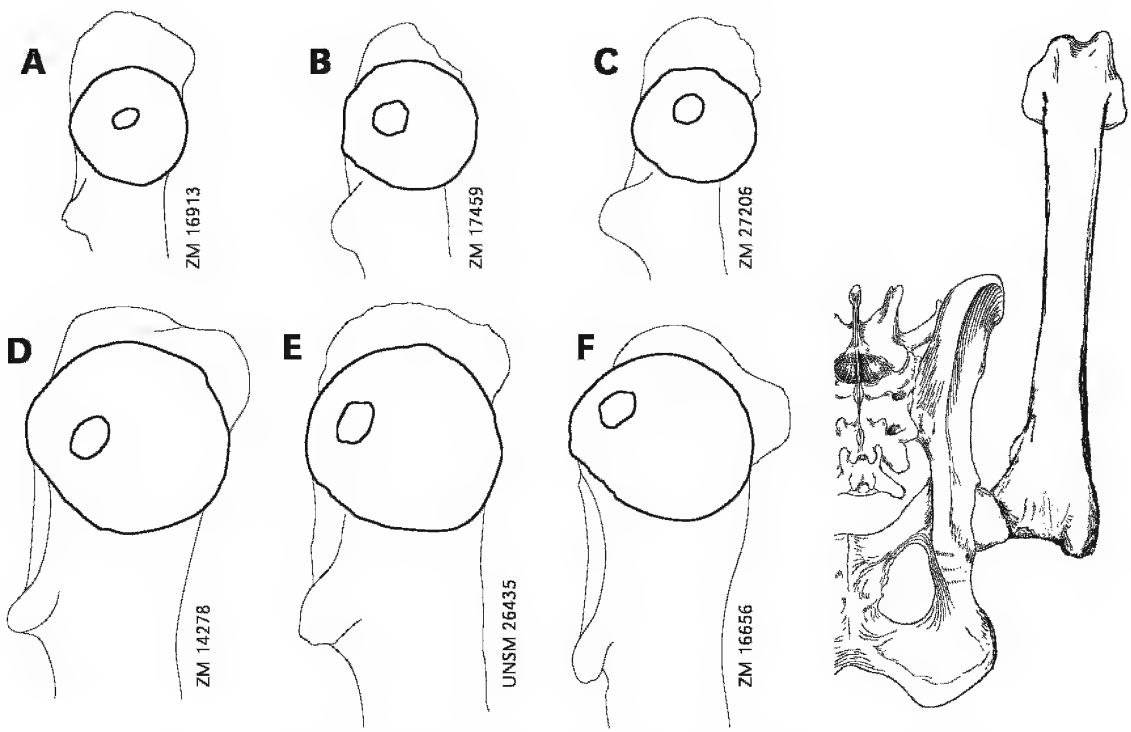

Fig. 27. Placement of the fovea capitis femoris for the femoral ligament in *Borocyon robustum* and some living carnivorans. In cheetah, puma, and wolf the fovea is more centrally situated on the femoral head, whereas in the lion, tiger, and *B. robustum* it is more posteriorly placed, indicating a somewhat more abducted femur in these large felids and *Borocyon*. Diagram of articulated femur and pelvis shows femoral head of *B. robustum* fully adducted; the femur is more abducted in normal stance. **A**, *Acinonyx jubatus*; **B**, *Canis lupus*; **C**, *Felis concolor*; **D**, *Panthera leo*; **E**, *Borocyon robustum*; **F**, *Panthera tigris*.

formed a more acute angle with the diaphysis than in ambulatory carnivores with more abducted femora where the angle is greater. The anterior margin of the articular surface in *Borocyon robustum* (UNSM 26435) forms an angle with the diaphysis slightly greater than in the domestic cat but more acute than in the ambulatory raccoon and ursids. In addition, the femoral head of *B. robustum* is aligned nearly at a right angle with the diaphysis, suggesting only a limited amount of femoral abduction. The orientation of the articular margin of the femoral head corresponds most closely to carnivores with more parasagitally aligned femora. *Procyon lotor* and living ursine bears have strongly abducted femora where the amount of abduction is greater than in any other family under discussion here, including amphicyonids.

In large living canids such as *Canis lupus* and *Canis latrans*, orientation of the femur is determined by the upward-angled femoral head (Jenkins and Camazine, 1977: fig. 8F), which is absent in felids and amphicyonids, in which the head is aligned nearly at a right angle to the diaphysis. The femoral anatomy of the wolf and coyote indicate not only greater femoral abduction than in the domestic cat and foxes but also in comparison to large felids (*P. leo*, *P. tigris*). The anterior, dorsal, and posterior margins of the femoral head are quite similar in *B. robustum* (UNSM 26435) and in the lion and tiger, yet in *B. robustum* the anterior margin is aligned at a somewhat more acute angle to the diaphysis than seen in the large cats. Also, *B. robustum* is characterized by a transversely broad proximal femur, in that the distance between greater trochanter and head is more extended, thicker, and straighter than in living felids. This condition would seem to favor a more parasagittal stance and is approached by some lions.

Whereas the amount of femoral abduction might be best measured in living or recently deceased animals, here, using only associated innominates and femora from osteological collections, a proxy measure was taken: the angle between a parasagittal plane aligned parallel to the dorsal acetabular rim and the long axis of the femoral diaphysis, when the femur is oriented at 45° below the horizontal. In this position the margin of the femoral head is made congruent with the dorsal acetabular rim. This is not a position that would be normally adopted in the living animal, but it allows a comparable measurement in large living felids, cheetah, wolf, and *B. niobrarensis* (no pelvis of *B. robustum* has been found). The abducted angle in the cheetah is ~29°, the tiger 34°–40°, the wolf ~47°–52°, and in *B. niobrarensis* somewhere in the range of ~28°–37° (although the femur [KU 113645] and innominate [F:AM 107601] of *B. niobrarensis* are not from a single individual, the measurement was considered acceptable because the femoral head was congruent within the acetabulum).

The placement of the fovea capitis femoris on the femoral head lies in a position nearly identical to that of the lion and tiger (fig. 27) so that, together with alignment of the proximal femur relative to the diaphysis as well as the orientation of the articular margin of the femoral head, a slightly abducted yet essentially parasagittal orientation of the hindlimb seems probable.

Certain additional observations derive from this comparison: the congruence of the margins of acetabulum and femoral head in *Borocyon niobrarensis* is most similar to that of cheetah and Sumatran tiger among skeletons at my disposal. As the femur starts to retract at the beginning of the propulsive phase, the anterior margin of the head is largely congruent with the dorsal rim of the acetabulum, but as retraction proceeds, a strip of the articular surface of the head remains outside the dorsal rim as a more parasagittal femoral alignment is adopted. When the femur of *Borocyon* is fully retracted (end of propulsive phase), the posterior acetabulum overlaps an area on the femoral head that lies beyond the articular surface, which approximates the limit of femoral retraction as described in the domestic cat and fox by Jenkins and Camazine (1977).

In all of these carnivorans, only in extreme abduction of the fully retracted femur could the articular margin of the femoral head ever be congruent with the posterior dorsal rim of the acetabulum; this is a position unlikely to occur in normal locomotion. Consequently, a portion of the femoral head's articular surface is commonly exposed during the terminal phase of femoral retraction in many living Carnivora, especially in those animals (e.g., procyonids, mustelids) where the dorsal rim of the acetabulum has not been extended laterad over the femoral head.

Tibia

B. robustum is represented by three tibiae (fig. 28), one (UNSM 25558) from UNSM locality Bx-7; a second (UNSM 44719) from Hovorka Quarry (Bx-21), both probably males; and a third (UNSM 26260) from the Bridgeport Quarries. The Runningwater tibiae are of similar size, whereas the Bridgeport tibia is more gracile and may belong to a female. A smaller tibia of *B. niobrarensis* is known from Horse Creek Quarry (UW 10004). In all of these individuals, the prominent tibial tuberosity and cnemial crest indicate a pronounced ability to extend the knee on the thigh; they form an anteriorly extended ridge on whose lateral side is the deep concavity for the anterior tibial muscle. In daphoenines the tendon of this muscle would extend across the dorsal surface of the tarsus to attach to a ridge on the medial base of metatarsal 2 and a rugose area on the base of metatarsal 1 and adjoining entocuneiform. It dorsiflexes the tarsus on the tibia. The tendency of the anterior tibial muscle to not only flex the tarsus, but to rotate the paw laterally, is balanced by the peroneal muscles that also flex the tarsus but rotate the paw medially. The peroneal muscles, the cranial tibial, and long digital extensor are all innervated by the peroneal nerve and perform an integrated action in dorsiflexion and rotational balancing of the hindpaw. Inversion and eversion of the hindfoot of *B. robustum* is only possible because of the ball-and-socket articulations of astragalus with navicular, and calcaneum with cuboid, which allow axial rotation within

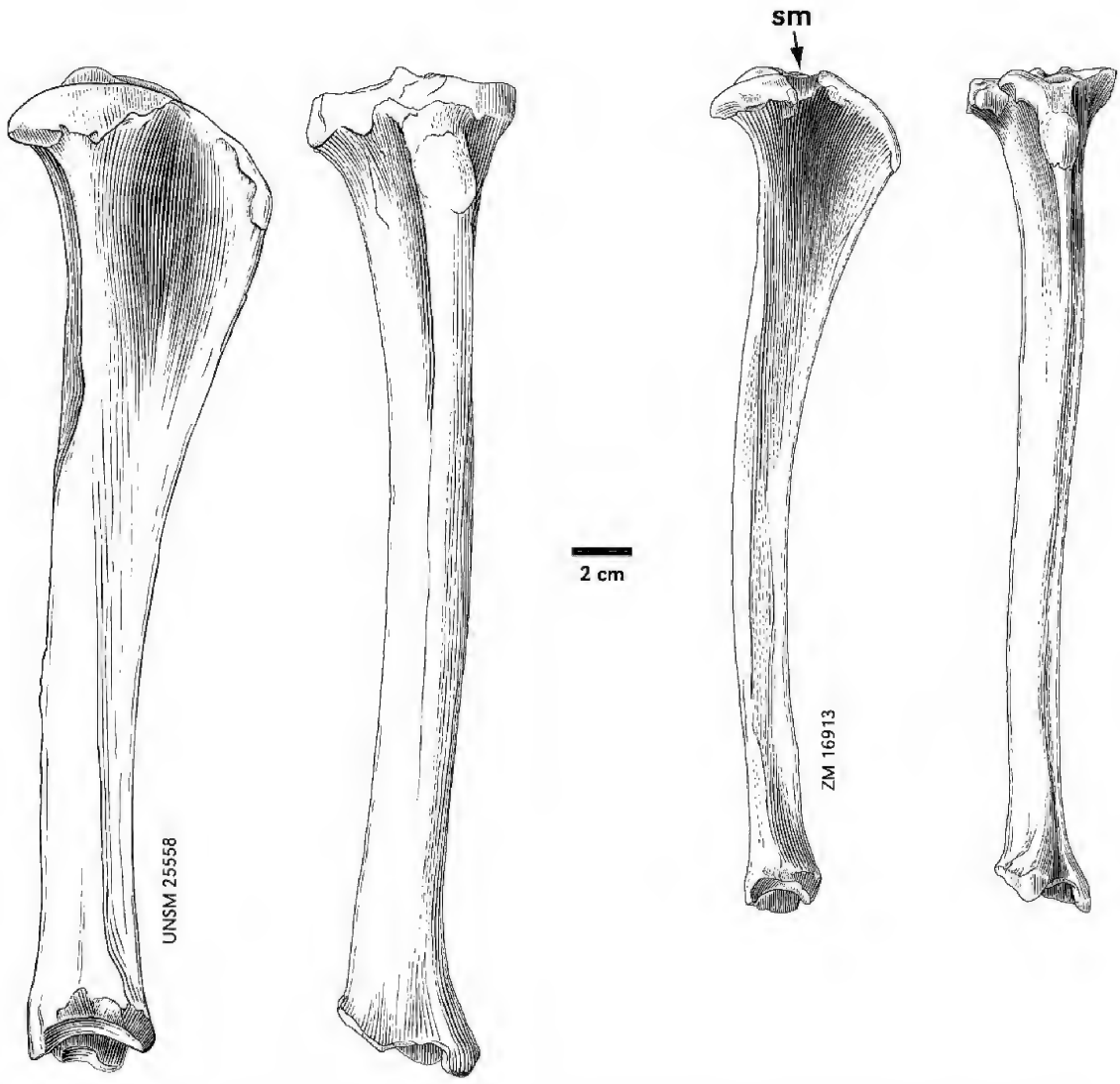

Fig. 28. Tibia of *Borocyon robustum* (UNSM 25558) compared with the tibia of the cheetah *Acinonyx jubatus* (ZM 16913) showing a similarity in form. The sulcus muscularis (sm), a groove for the long digital extensor muscle of cheetah and wolf is absent in *B. robustum*, but the extended cnemial crest and developed tibial tuberosity are shared traits.

the tarsus. The tibial-astragalar and tarsal-metatarsal joints do not permit axial rotation. Therefore, the ability of the *Borocyon* hindfoot to adjust to an uneven substrate was regulated by the coordinated action of the anterior tibial and peroneal muscle complex at the mid-tarsal joint.

Digitigrady in living carnivorans has been discussed relative to the pattern of muscle scars on the posterior surface of the tibia (Ginsburg, 1961; Wang, 1993). Proximally, four deep muscles are involved: flexor hallucis longus (FHL) laterally, popliteus muscle medially, and between them the tibialis posterior (TP) and flexor digitorum longus (FDL). In the wolf and domestic dog (Evans, 1993: 375), the TP and FDL are reduced and their registration on the tibia is restricted to a very narrow elliptical area, a thin lenticular scar trending downward along the upper third of the diaphysis toward the medial side of the bone (fig. 29). In contrast,

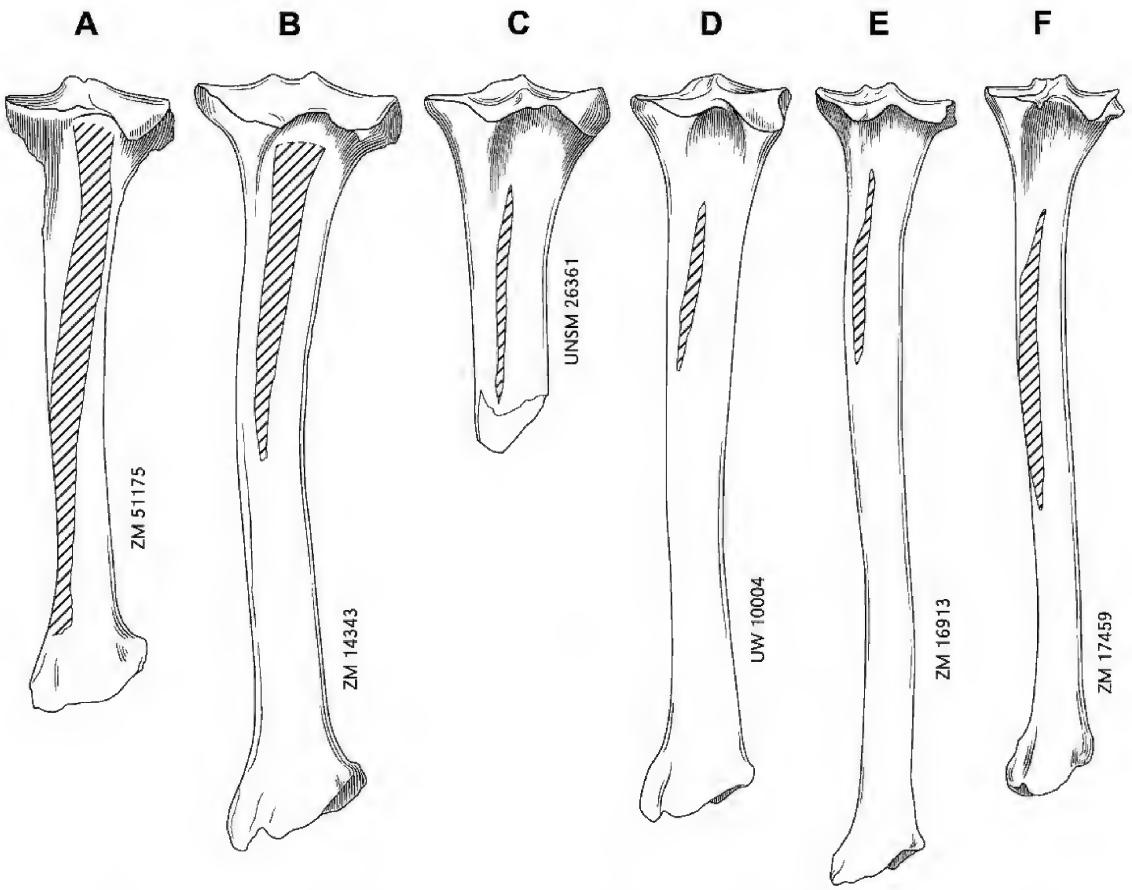

Fig. 29. Muscle scar pattern (cross-hatched area) of the posterior tibial (TP) and long digital flexor (FDL) muscles on the posterior surface of the right tibia in *B. robustum* and *B. niobrarensis* relative to the scar patterns in large living Carnivora. **a**, *Ursus americanus*; **b**, *Panthera tigris*; **c**, *Borocyon robustum*; **d**, *Borocyon niobrarensis*; **e**, *Acinonyx jubatus*; **f**, *Canis lupus*.

living ursids such as *Ursus arctos* and *Ailuropoda melanoleuca* display a well-developed area of attachment for these muscles that forms a broad, prominent scar running down nearly the entire length of the posterior tibia (Davis, 1964: 116). Moreover, the popliteus is restricted to the proximal tibial diaphysis in canines but extends down nearly two-thirds of the shaft in living ursids.

A prominent broad scar for TP-FDL is also characteristic of most digitigrade felids. This scar is centered on the posterior surface of the upper diaphysis and, although reduced in area relative to that of living ursids, it is broader than in the wolf. However, the cheetah is an exception among the large cats and retains a very narrow scar pattern most like the wolf.

Although these contrasting scar patterns have been linked to either a digitigrade or plantigrade stance, it is likely that the reduced area for tibialis posterior and the long digital flexor in the wolf and cheetah is related to the reduction in size and functional importance of the tibialis posterior. The short flexor muscles of the crus end in long tendons, and short-fibered muscles ending in long tendons indicate considerable elastic extension in the tendons (Alexander, 1988: 21), suggesting that reduction in the posterior tibial muscle and the long tendons of the other flexors are adaptations to efficient flexion-extension of the tarsus and digits, contributing to a fore–aft path of the hindlimb. The posterior tibial muscle inverts (outwardly rotates) the foot, an action less

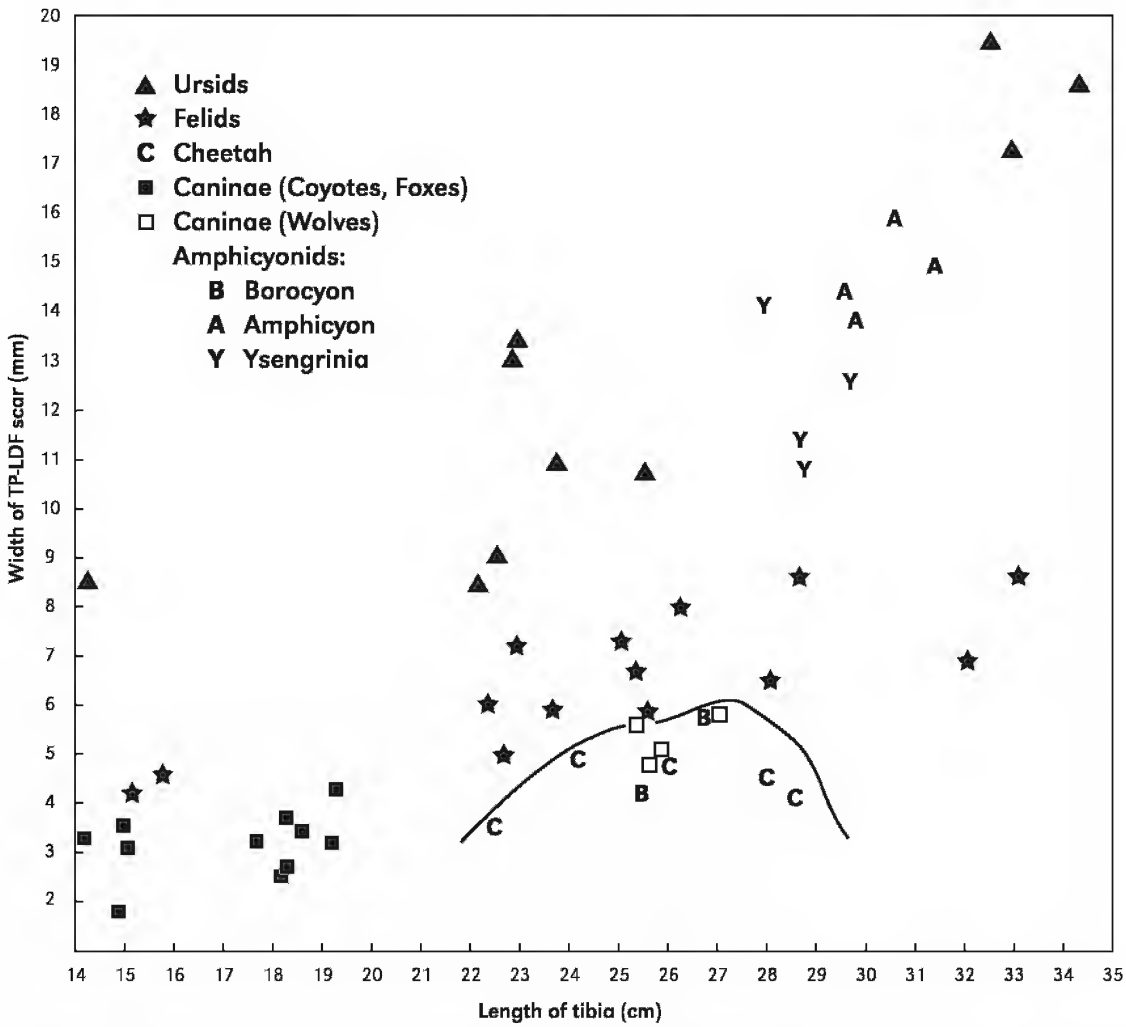

Fig. 30. Bivariate diagram of width of the posterior tibial–long digital flexor scar plotted against tibial length in representative living ursids, felids, canids, and in early Miocene amphicyonids. The cheetah, wolf, and *Borocyon* plot together beneath the enclosing curvilinear. Note the correspondence between the large ambulatory amphicyonines (*Amphicyon, Ysengrinia*) and ursine ursids.

necessary in digitigrade carnivores adopting a more fore–aft motion of the hindfoot. Also, the tendon of FDL joins that of FHL to form a conjoined tendon, becoming the deep digital flexor (flexor digitorum profundus) of the digits, and because FHL becomes the principal phalangeal flexor, FDL is less necessary to that role. The lenticular scar for tibialis posterior decreases in width and in area from that in *Daphoenodon superbus* (CM 1589) through *B. niobrarensis* (UW 10004) to *B. robustum* (UNSM 26361): in *D. superbus* like that of living wolves, and in *B. robustum* and *B. niobrarensis* nearly identical to the pattern seen in *Acinonyx jubatus* (ZM 16913). When tibial length is plotted against the width of the TP-FDL scar for a variety of living large carnivorans, *Borocyon* groups with the wolf and cheetah (fig. 30).

The tibiae of cheetah and wolf share a trait found in no other living carnivoran examined in this study. The proximal tendon of the long digital extensor, originating on the lateral condyle of the femur, travels downward to occupy a marked groove (sulcus muscularis, fig. 28, ZM 16913, *Acinonyx*)

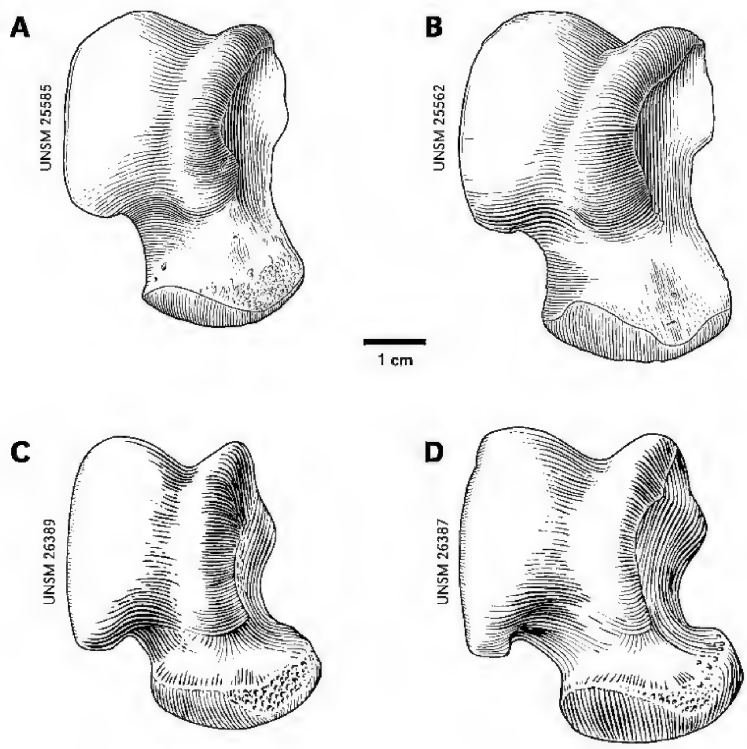

Fig. 31. Comparison of the astragalus of *Borocyon robustum* (**A**, **B**) and *Amphicyon galushai* (**C**, **D**). Dimorphic astragali within each species are thought to represent large males (B, D) and smaller females (A, C).

immediately anterior to the lateral condyle of the tibia. The tendon continues distad to a muscular belly, then transforms to a distal tendon to extend the digits and participate in flexing the tarsus. The sulcus muscularis is absent in living arctoid Carnivora, in amphicyonids (with the exception of some temnocyonines), and in hyaenids, and it does not occur in the other living felids, where a more shallow embayment is present farther anterior on the tibial crest. In the only tibia of *B. robustum* (UNSM 26361) in which the proximal region is intact, the sulcus is absent.

Tarsals: Astragalus-Calcaneum

Among the tarsals, the astragalus and calcaneum of *Borocyon robustum* are particularly diagnostic (figs. 31, 32) and differ from those of large contemporary amphicyonines. The astragalus is proximodistally elongated, the trochlea is narrower, and the distal condyle (head) migrates beneath the trochlea rather than remaining in its more plesiomorphic medial location as seen in *Amphicyon* and *Daphoenodon superbus* (fig. 33). Additionally, the sustentacular facet for the calcaneum on the posterior face of the astragalus is restricted to a more proximal location and does not extend distad to the base of the condyle as in *Amphicyon* and other large amphicyonines.

The ectal facet of the astragalus in *B. robustum* is moderately concave, more so than in *Amphicyon* and other large amphicyonines, in order to receive the ectal prominence of the calcaneum. This ensures a close registration of astragalus and calcaneum that somewhat restricts motion between the two bones, much as in living *Panthera tigris* and *P. leo* where this same type of registration occurs. In canine canids such as *Canis lupus* and *C. latrans* the ectal prominence is strongly protuberant, forming a ridge deeply inserted into the posterior surface of the astragalus, creating a tight, immovable registration between the two bones. The interlocked astragalus and calcaneum in these canines represents an extreme

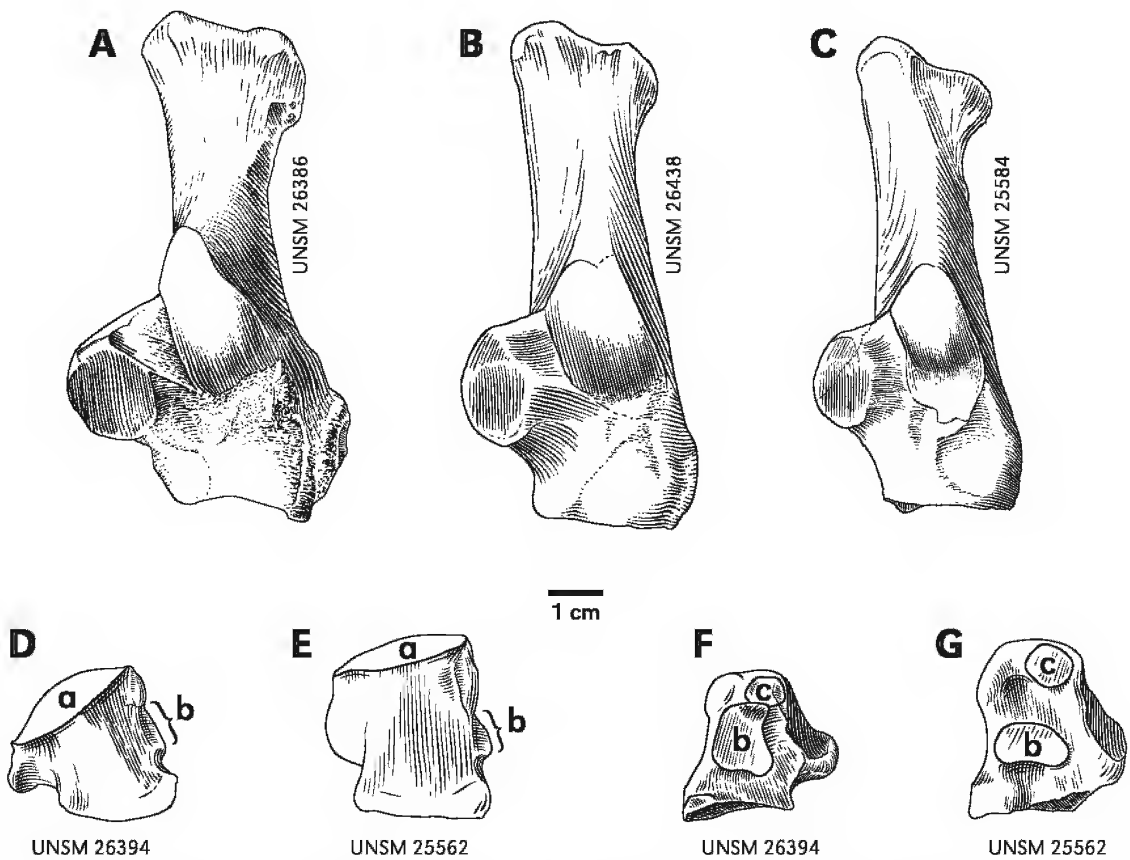

Fig. 32. Comparison of calcanea of *Amphicyon galushai* (**A**) and *Borocyon robustum* (**B**, male; **C**, female). Digitigrade calcanea of *B. robustum* are more slender and distally narrower than *Amphicyon* calcanea. Cuboids of *A. galushai* (**D, F**) and *B. robustum* (**E, G**), anterior and medial views: **a**, calcaneal articular surface; **b**, ectocuneiform and **c**, navicular facets.

expression of this trait in Carnivora. In the cheetah this locked relationship of astragalus and calcaneum is less developed than in the wolf and coyote but is more developed than in any other living large felid.

When compared to the *Amphicyon* calcaneum, the calcaneum of *B. robustum* is distally narrower with a smaller sustentaculum and less developed coracoid process. A distal extension of the calcaneum accompanies elongation of the astragalus. The length of the *Borocyon* calcaneum relative to its distal width differentiates it from distally broad, more robust calcanea of contemporary *Amphicyon* and other large amphicyonines (fig. 34), and the posterior surface of the sustentaculum is usually more deeply grooved by the flexor tendon of the digits.

The astragalus of *Borocyon robustum* is differently proportioned relative to *Amphicyon galushai* and two large contemporary amphicyonines from the Bridgeport Quarries and from Florida (fig. 33). These large amphicyonines, found together with *Borocyon*, all display a short astragalus with a wide trochlea and broad head relative to the elongate astragalus with narrow trochlea and head of *Borocyon robustum*. The astragali from the Rose Creek Member of the John Day Formation and from the Suwanee River locality are indistinguishable from those of *B. robustum* (fig. 33). The holotype of *B. niobrarensis* lacks an astragalus; however, two referred *B. niobrarensis* astragali and associated calcanea (UW 10004, F:AM 107601) are similar to *B. robustum* but are smaller and less elongate.

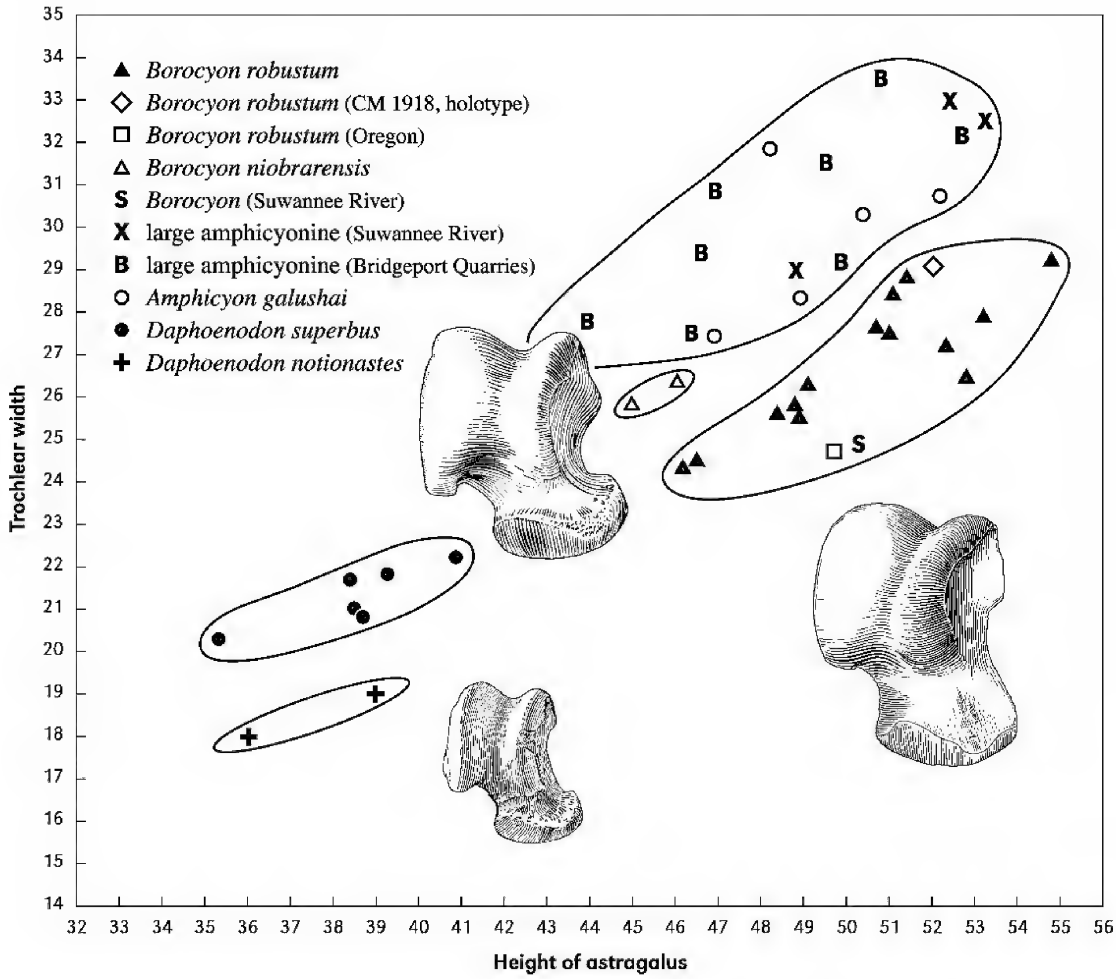

Fig. 33. Bivariate diagram of trochlear width of the astragalus plotted against height for species of *Borocyon*, large amphicyonines, and plesiomorphic species of *Daphoenodon*. A narrow trochlea sets *B. robustum* apart from large contemporary amphicyonines. Note that the holotype astragalus of *B. robustum* and the Oregon and Florida astragali fall within the *B. robustum* hypodigm.

The dimensions of the holotype astragalus (fig. 3, CM 1918) of *Borocyon robustum* plot with astragali of the upper Runningwater and Bridgeport samples (fig. 33) and hence support the inclusion of the *B. robustum* holotype with that hypodigm. The holotype astragalus is associated with a mandibular fragment, an isolated m2 (not reported by Peterson), and the navicular, ecto-, meso-, and entocuneiform (fig. 3).

There is a clear parallel between the astragalus-calcaneum of *Borocyon robustum* and those of large living felids. Distally extended, narrow calcanea of *P. leo* and *P. tigris* show proximal placement of the sustentaculum, a tall, narrow tuber calcis, and a tendency for flexor tendons to groove the posterior surface of the sustentaculum. These derived features, present in *Borocyon robustum*, are less developed in *B. niobrarensis*. Together they confirm an incipient specialization of the tarsus for digitigrady and more restricted fore–aft motion, a trend that independently reaches its culmination in canine canids. The tarsus, heavily bound by its investiture of ligaments, can only flex and extend at the tibia-astragalar and distal tarsal-metatarsal joints but retains limited axial rotation at the intratarsal joint between astragalus-navicular and calcaneum-cuboid. The similar form of

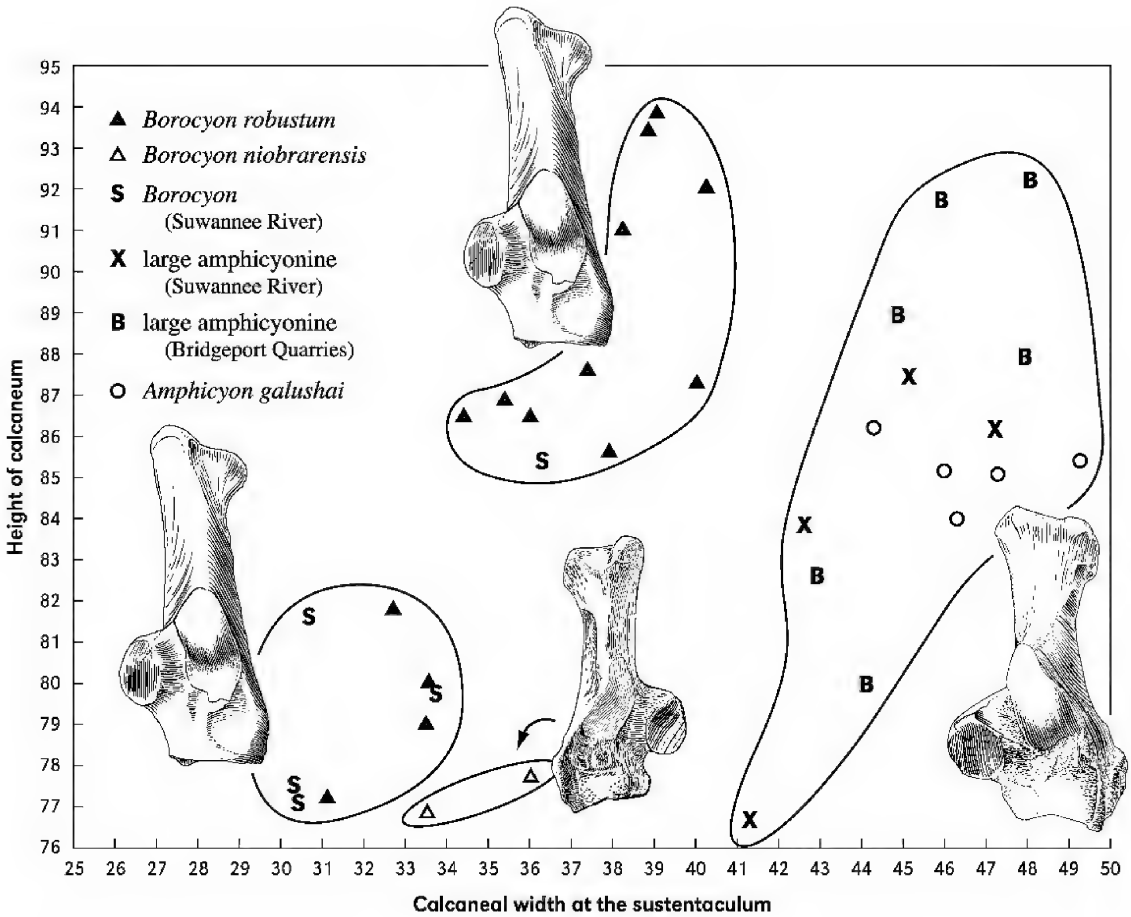
▲ Borocyon robustum
△ Borocyon niobrarensis
S Borocyon (Suwannee River)
X large amphicyonine (Suwannee River)
B large amphicyonine (Bridgeport Quarries)
O Amphicyon galushai
Height of calcaneum
Calcaneal width at the sustentaculum
95 94 93 92 91 90 89 88 87 86 85 84 83 82 81 80 79 78 77 76
25 26 27 28 29 30 31 32 33 34 35 36 37 38 39 40 41 42 43 44 45 46 47 48 49 50

Fig. 34. Bivariate diagram of calcaneal width at the sustentaculum plotted against height. The more slender, distally narrow *Borocyon* calcanea are readily distinguished from the more robust calcanea of large contemporary amphicyonines.

these tarsals in *B. robustum* to those of *P. leo* and *P. tigris* suggests a hindfoot capable of the same range of movements.

Tarsals: Cuboid and Cuneiforms

The cuboid is readily distinguished from the cuboids of living ursids and contemporary large amphicyonines. In *Borocyon robustum* and *B. niobrarensis* the cuboid is relatively tall. Its proximal surface that articulates with the distal calcaneum is nearly horizontal, and the anterior face of the bone is vertical, forming a right angle with the upper surface. Living ursids and contemporary large amphicyonines have a low cuboid in which the proximal surface is not horizontal but is inclined laterad, and the anterior face of the bone descends at a sloping angle. Because the amphicyonine and ursine cuboid is proximodistally short, the medial cuboid facets for the navicular are continuous (or nearly so) with the subjacent facet for the ectocuneiform. In *Borocyon*, the ectocuneiform facet is an isolated ellipse well distad (7–9 mm) of the navicular facets that are situated along the upper rim of the cuboid.

The tall *Borocyon robustum* cuboid is most closely paralleled by the elongate cuboids of the cheetah (ZM 16913, height, 21.6 mm) and wolf (ZM 15596, 19.1 mm), although the beardog cuboids are more robust. A Sumatran tiger cuboid (ZM 14602) is not as tall as in *Borocyon* nor is the anterior face quite as vertical. The *B. robustum* cuboid (UNSM

25562, locality Bx-7) is much larger and taller (32.8 mm) relative to that of *B. niobrarensis* (F:AM 107601, 26.8 mm) and a Sumatran tiger (ZM 14602, 23.6 mm). Cuboids of *Amphicyon galushai* (UNSM 26390, 26394) from UNSM locality Bx-12, an upper Runningwater site, measure only 28.3 and 27.6 mm.

The ectocuneiform is preserved in the *B. robustum* holotype in articulation with the meso- and entocuneiform and navicular (fig. 3), but its plantar half is missing. Nonetheless, an isolated ectocuneiform (UNSM 44720) of *B. robustum* from UNSM locality Bx-12 is complete and represents a larger animal than the holotype. Its upper surface is horizontal, more so than in the holotype. An elliptical cuboid facet (14.0 × 8.8 mm) situated nearly at the anterior margin of the upper rim of the bone is the only facet on the lateral face. There is a robust plantar condyle as in large felids (including the cheetah), which is absent in ursine ursids and much smaller in the wolf. On the medial face are an upper facet for the mesocuneiform and a lower facet for the elevated base of metatarsal 2. The mesocuneiform is a short, blocky element tapering backward to a point. It contacts medially the tall, bladelike entocuneiform, which is situated posteromedial to the mesocuneiform on the inner side of the tarsus. The concave distal end of this large entocuneiform (height, 23.5 mm; anteroposterior width, 18.1 mm) receives the base of a slender, short metatarsal 1. All cuneiforms and the cuboid have slightly concave ventral articulations with the corresponding metatarsals.

Alignments of facets joining the tarsal cuneiforms and cuboid are largely in the vertical plane, suggesting little movement between them when bound by investing ligaments. Intratarsal movement was chiefly limited to the articulations between astragalus and navicular on the one hand and cuboid and calcaneum on the other hand, which allowed the foot to adjust to an irregular substrate. These articulations indicate very little intratarsal flexion-extension.

The wolf tarsus (ZM 15596) shows some parallels with that of *Borocyon robustum*: (1) elongate calcaneum; (2) astragalar head situated more under trochlea; (3) astragalar trochlea narrow; (4) elongate cuboid with vertical anterior face and flat upper articular surface (cuboid facets, however, are typically canine and differ from those of *Borocyon*—there is an upper navicular facet, a middle circular navicular facet, and a lower elongate ectocuneiform facet); and (5) volar process of the ectocuneiform not as developed as in *Borocyon* but its relationship to a reduced meso- and entocuneiform similar. In the wolf, a thin, quadrate entocuneiform for attachment of a vestigial first metatarsal is much more reduced than in *Borocyon* (in the wolf the tiny entocuneiform is applied to a small convex facet on the posteromedial corner of the navicular). Only a small nubbin of bone represents the wolf's vestigial first metatarsal. The tarsus of *Canis lupus* shows a greater reduction of tarsal elements associated with the internal digits of the foot than does *Borocyon*.

The tarsus of living large felids shows many similarities with the *Borocyon* tarsus. This is evident in the form of calcaneum and astragalus, cuboid, navicular, and the geometry and placement of the tarsal cuneiforms. On the other hand, ursid tarsals differ markedly from the tarsals of *Borocyon*, more so than those of any other large living carnivorans. In *Ursus arctos* (ZM 17888) the meso- and entocuneiforms are not reduced and remain large blocky elements, and the three tarsal cuneiforms are all of the same height (thickness) and are aligned side-by-side; bears lack the offset mesocuneiform and reduced entocuneiform of living felids and canids. This contrasts with *Borocyon* in which the ectocuneiform is deep, mesocuneiform dorsoventrally compressed and elevated, and entocuneiform elongate and bladelike. The inner cuneiforms show less reduction in *Borocyon* relative to the cheetah and other large felids because the first digit of the hindfoot is not as reduced as in these cats and in canine canids, retaining an elongate, small metatarsal 1 with at least one phalanx remaining and probably two. In living felids the first metatarsal is a tiny vestigial spur of bone without associated phalanges. In living canids, the first metatarsal is a small, nearly spherical nubbin of bone attached by ligament to the distal terminus of the entocuneiform and the posterior surface of the second

metatarsal. Hence, the *Borocyon* tarsus differs from the tarsus of all living felids and canids in the retention of a less reduced first digit of the hindfoot, yet one entirely distinct from this robust digit in living bears.

Metatarsals

The metatarsals of *Borocyon* demonstrate a paraxonic, elongate hindfoot. Cheetah and wolves show close appression of the proximal shafts of the metatarsals, and the metatarsus of *Borocyon* parallels this, but to a lesser extent. The paraxonic metatarsals 3–4 are robust and straight, as in living canids, not curved as in many felids; they are flanked by shorter metatarsals 2 and 5 whose shafts display a flattened internal face, indicating that they were closely applied to the central paraxonic metatarsals. Some distal separation of the metatarsals occurs but this is much less, relative to the metacarpals. The distal metatarsal keels are pronounced as in felids. Large living felids other than the cheetah show a slight distal separation of the metatarsals, yet this appears even less evident in *Borocyon*.

Borocyon's metatarsals lack overlapping proximal ends as seen in the metacarpals of large living felids (MC2 on MC3, MC3 on MC4). Otherwise, the fit of the metatarsal articulations are anatomically similar. The proximal head of MT5 inserts into MT4, and the head of MT4 into MT3; the head of MT2 is raised above that of MT3 so that MT2 can articulate with the ectocuneiform. The relative lengths of MT3–MT4 to the shorter, flanking MT2 and MT5 are similar in the lion, tiger, and *Borocyon*. The fourth metatarsals of amphicyonids display a large, elongate ligament scar on the posterior diaphysis a little above mid-shaft. This scar appears to represent the insertion of a plantar tarsal ligament that reinforces and stabilizes the tarsal-metatarsal joint—this scar is particularly thick in *Borocyon robustum*, and more distally situated than in ursids, suggesting that the ligament may be important in maintaining a digitigrade stance. The paraxonic digitigrade hindfoot of *Borocyon* is doubtless adapted to fore–aft motion, contributing to the propulsive thrust provided by the hindlimb.

The principal weight-bearing metapodials of the paraxonic fore- and hindfeet of *Borocyon* are metacarpals 3–4 and metatarsals 3–4. These metapodials show an increase in absolute length from *B. neomexicanus* through *B. niobrarensis* to *B. robustum* (table 5), accompanying the overall size increase seen in these species. *Borocyon* metapodials also are dimorphic, which is interpreted as sexual and is documented at several localities (table 6).

Length measurements of the paraxonic metacarpals 3–4 and metatarsals 3–4 from living large felids, canids, and ursids, when compared with those for *Borocyon*, show that the metatarsals in many large cats (including the cheetah *Acinonyx*) are ~20%–40% longer than the metacarpals (fig. 35; appendices 2, 3). In *Panthera leo* and *P. tigris* this disparity between fore- and hindfoot is less (~11%–23%). But in wolves and coyotes, and in *Borocyon robustum* and *B. niobrarensis*, the paraxonic metapodials of the hindfoot are only ~8%–17% longer than those of the forefoot (fig. 35; appendix 4).

Axial Skeleton

There is no representation of the vertebral column, sternum, or ribs of *Borocyon robustum* except for three caudal vertebrae (fig. 3) belonging to the holotype described by Peterson (1910). He realized that these caudals indicated that a long tail was present as seen in *Daphoenodon superbus*. A partial vertebral column does accompany the Horse Creek skeleton (UW 10004) referred here to *Borocyon niobrarensis*. Its nine vertebrae (axis, two cervicals, three thoracics, two lumbars, and a caudal vertebra) are nearly identical in all respects to the column of *D. superbus* described by Peterson (1910). A capability to flex and extend the back is evidenced by inclination of the neural spines of the thoracic and lumbar vertebrae directed toward a centrally situated anticlinal vertebra.

Summary

The largest individuals of *Borocyon robustum*, all with markedly elongate limbs, occur in several of the Hemingford Quarries considered the youngest in the Runningwater

TABLE 5
Comparative Lengths (in mm) of the Paraxonic Metapodials of the Daphoenine Amphicyonids *Borocyon* and *Daphoenodon superbus*

Taxon	MC3[a]	MC4	MT3[b]	MT4
Daphoenodon superbus[c]	63.6 (3)[g]	60 (1)	72.4 (5)	75.6 (3)
Borocyon neomexicanus[d]	72.5 (1)	78.4 (2)	85.0 (1)	91.5 (1)
Borocyon niobrarensis[e]	84.6 (3)	85.6 (4)	92.3 (1)	97.0 (1)
Borocyon robustum[f]				
Runningwater Fm.	96.1 (3)	—	105.3 (3)	109.8 (5)
Bridgeport Quarries	95.0 (6)	99.4 (4)	103.9 (3)	108.0 (1)

Measurements are calculated from data in appendix 3.
[a]MC indicates metacarpal.
[b]MT indicates metatarsal.
[c]Measurements are from adults.
[d]Measurements are from several adult individuals from the same quarry.
[e]Measurements are from two adult individuals of the same approximate body size.
[f]Measurements are averages from multiple individuals.
[g]Sample sizes (N) are in parentheses. If more than one specimen, the value is the mean length.

Formation on biochronologic criteria. Sites in the lower Runningwater Formation yield on average smaller individuals referred to *B. niobrarensis*. When viewing limb elements of the largest individuals of *Borocyon robustum*, particularly the radius and paraxonic metacarpals, the size and elongation of the forelimb are striking.

To estimate the relative degree of limb elongation of the species of *Borocyon*, linear measurements of limb elements were compared with those of the plesiomorphic *Daphoenodon superbus* (fig. 36), based on Peterson's (1910) genoholotype (CM 1589). The slightly smaller size of *B. niobrarensis* relative to *B. robustum* is reflected in these percentages. Forelimb segment lengths for *B. niobrarensis* show increases of ~27%–46% over *D. superbus*. The increase in segment lengths for *B. robustum* is clearly more substantial, from as low as ~35% for the humerus to as much as 76% for the radius. The increase in length of the radius (hence the ulna), femur, and tibia of *B. robustum* relative to *D. superbus* is

TABLE 6
Sexual Dimorphism in the Daphoenine Amphicyonid *Borocyon* Indicated by Metapodials of the Fore- and Hindfeet

Taxon	MC3	MC4	MC5	Locality
Borocyon niobrarensis	ACM 3452m	ACM 3452m		Aletomeryx Quarry
	ACM 11796f	ACM 11796f		Aletomeryx Quarry
Borocyon cf. *B. robustum*	KU 118496m			Northern Florida
	KU 118484f			Northern Florida
Borocyon robustum		UNSM 26473m		Bridgeport Quarries
		UNSM 26475f		Bridgeport Quarries
Borocyon robustum			UNSM 26477m	Bridgeport Quarries
			UNSM 26478f	Bridgeport Quarries

Taxon	MT4	MT5	Locality
Borocyon cf. *B. robustum*		KU 118482m	Northern Florida
		KU 118484f	Northern Florida
Borocyon robustum	UNSM 26447m		UNSM Loc. Bx-12
	UNSM 25563f		UNSM Loc. Bx-12

MC indicates metacarpal; MT, metatarsal; m, male; f, female.

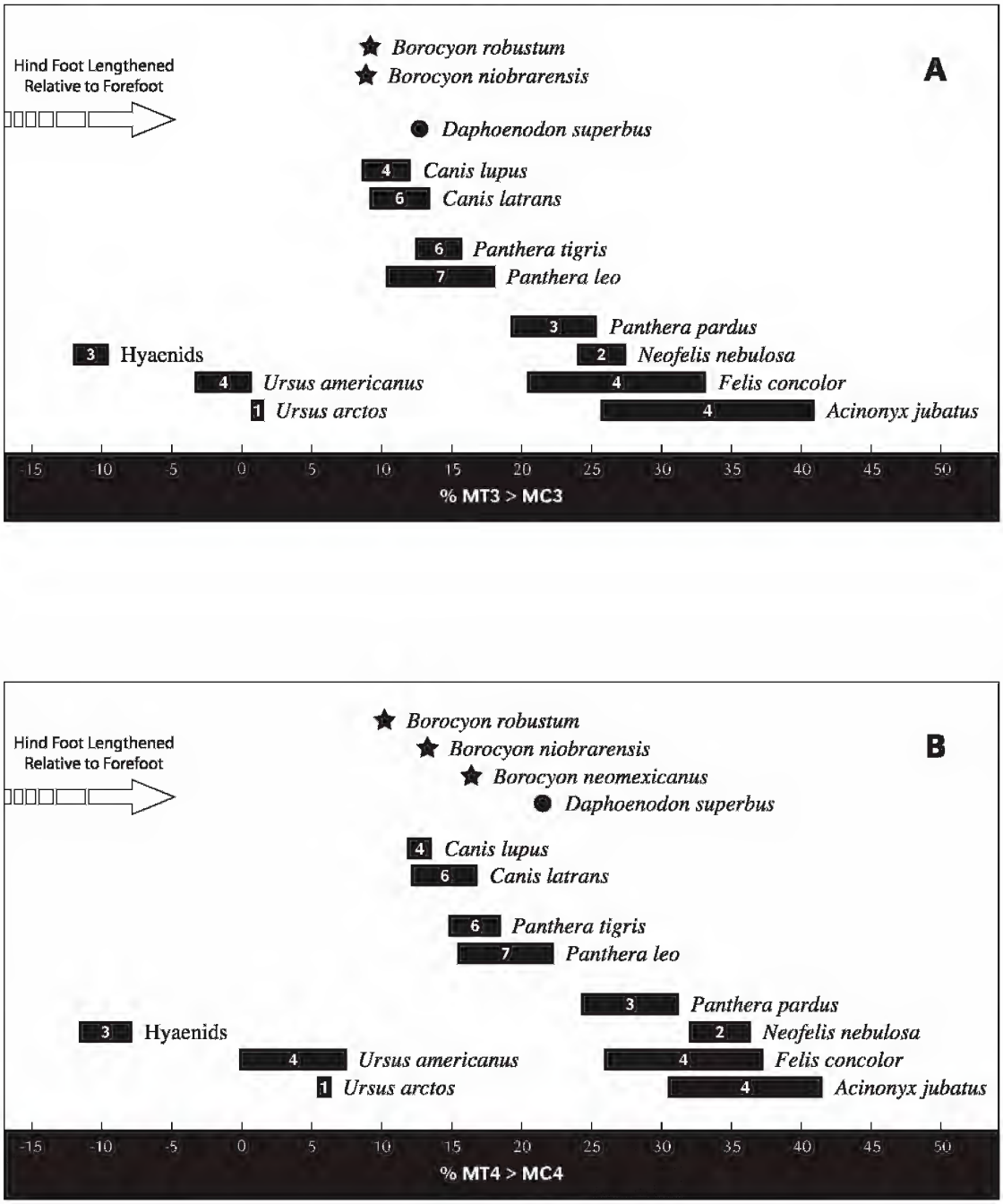

Fig. 35. Relative proportions (in %) of lengths of paraxonic (**A**) metatarsal 3 to metacarpal 3 and (**B**) metatarsal 4 to metacarpal 4 for species of *Borocyon and Daphoenodon superbus* compared with living canids, felids, ursids, and hyaenids. Species farthest to the right show the greatest disproportion between lengths of metacarpals and metatarsals, and therefore a hindfoot longer than the forefoot. Numbers within black bars indicate sample size.

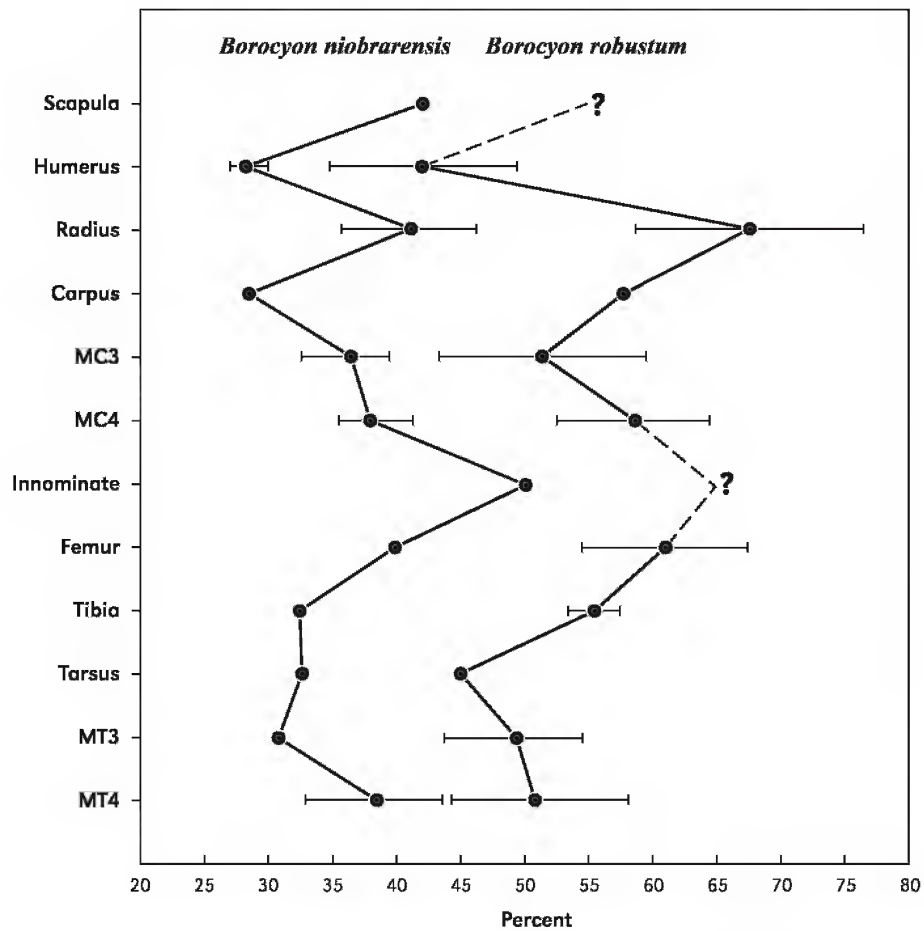

Fig. 36. Percentage increase in lengths of the bones of the fore- and hindlimb of *Borocyon niobrarensis* and *B. robustum* relative to the holotype skeleton of *Daphoenodon superbus* (CM 1589). Bars indicate the mean and range where more than one individual was available.

especially obvious. Fore- and hindlimb segment lengths of *B. robustum* exceed those of *B. niobrarensis* for all elements.

Despite the scarcity of associated limb material and small sample sizes, the available data suggest that the fore- and hindlimbs of *Borocyon robustum* are proportionately longer than those of *B. niobrarensis*. Although limb lengths of large male *B. niobrarensis* probably overlap those of small females of *B. robustum*, the proportions of these limbs differ, such that *B. robustum* limbs appear consistently more elongate.

Figure 37 illustrates a hypothetical restoration of a male *B. robustum* together with the holotype skeleton of *Daphoenodon superbus*. These two carnivores represent the two end-member states of this New World daphoenine amphicyonid lineage. *Daphoenodon* (*D.*) *superbus* demonstrates the plesiomorphic condition, probably retained in most or all species of *D.* (*Daphoenodon*), and *Borocyon robustum* represents the culmination of limb development in the subgeneric *Borocyon* lineage. Although the *D. superbus* holotype is a female, the males of its probable ancestor, *Daphoenodon notionastes* from the Arikareean of Florida, would have been similar in size and are known to exhibit the same absence of limb elongation. Hence, the two skeletons adequately illustrate the transformation in skeletal dimensions and limb proportion that occurred during evolution to larger body size in these daphoenines. Such a transition is unknown in Old World amphicyonid carnivores.

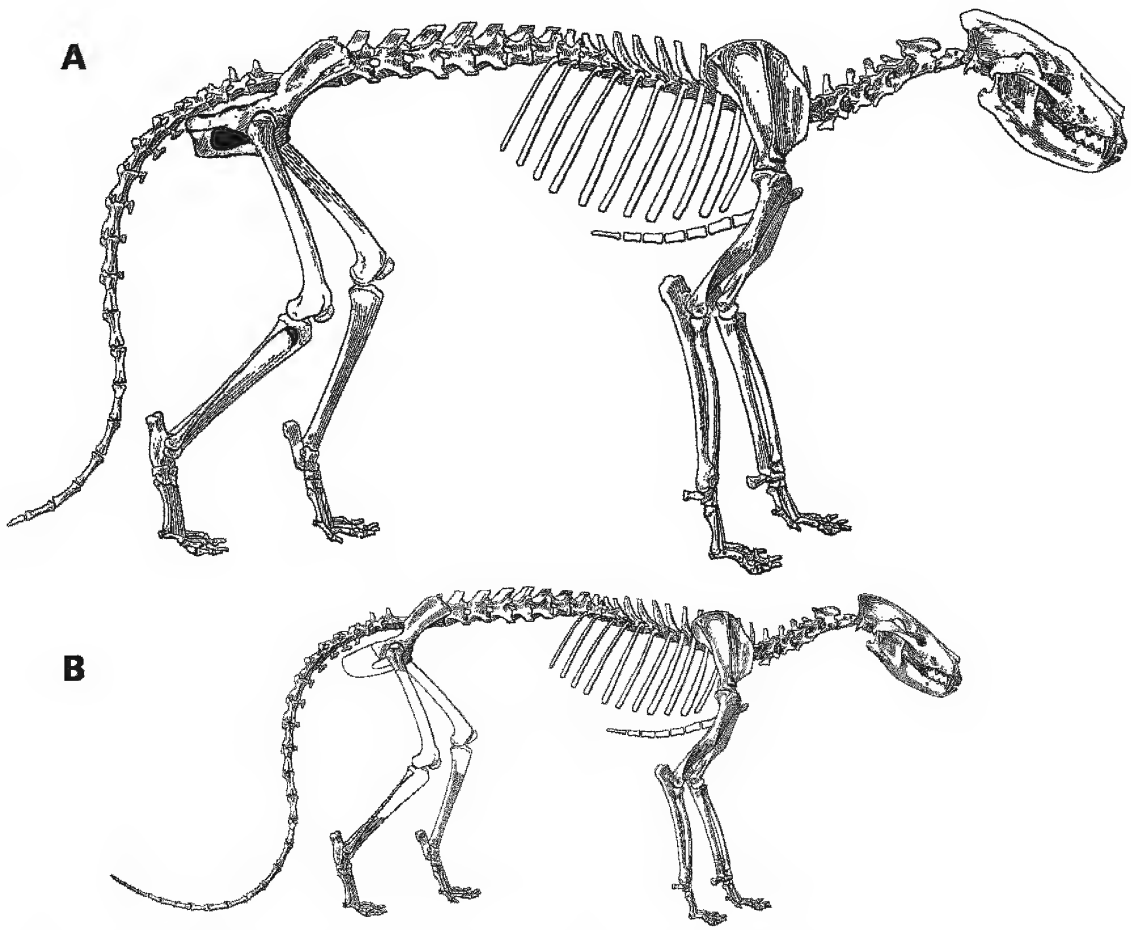

Fig. 37. Hypothetical restoration of the skeleton of *Borocyon robustum* (**A**) compared to the holotype skeleton of *Daphoenodon superbus* (**B**, from Peterson, 1910), representing the two end-member species of the *Borocyon* lineage during the early Miocene in North America. Fossils show that *Borocyon robustum*, the terminal species of the subgenus, was widely distributed from the Pacific Northwest to the Gulf Coast of Florida by the end of the early Hemingfordian.

The anatomy of the limbs demonstrates the following features of *Borocyon* bearing on stance and gait:

(1) correspondence in form of the scapula to that of the lion, but differing from all felids and similar to living ursids in the presence of a teres process and its associated musculature, and in possessing a broad distally extended deltopectoral crest of the humerus—the anatomy of scapula/humerus demonstrates effective stabilization of the shoulder joint and powerful extension/flexion of the upper arm contributing to stride length —there is no evidence of a clavicle;

(2) a more parasagittally aligned elbow than those seen in living ursids and in amphicyonine amphicyonids, indicated by transverse narrowing of the distal humerus involving suppression of the medial epicondylar area for the origin of flexor muscles and deepening and realignment of the olecranon fossa for extension of the ulna—the elbow in *Borocyon robustum* is only slightly everted and is parasagittally oriented as in living wolves;

(3) form and elongation of radius and ulna as in wolf and cheetah, thereby differing from all New World amphicyonines in which the antebrachium is not elongate; bladelike radius with transversely narrow proximal and distal ends and bound to ulna by a narrow interosseous ligament and membrane at mid-shaft that, together with the

form of the radial head and distal ulnar structure, indicates a more restricted capability for pronation-supination than found in the large living felids, but not as markedly developed as in the wolf; thus, a cuffing or swatting stroke of the paw could have been employed in bringing down prey;

(4) carpal bones sharing a similar form and placement with those of living ursids, but having adapted this arctoid carpal pattern for (a) a more fore-aft digitigrade motion of the forefoot; (b) reduction of lateral digits; (c) specialization of certain carpal elements (scapholunar, magnum)—however, *Borocyon* carpals lack specialized stop facets seen in the wolf and cheetah that arrest intracarpal hyperextension and flexion; principal flexion occurring at radioulnar-proximal carpal joint with minimal movement at intracarpal joints; hyperextension of the forefoot only possible between radius and scapholunar and this probably prevented by binding ligaments; prominent ridge on scapholunar forces ulnar deviation of the forepaw during protraction of the forelimb; trapezium much reduced, more so than in felids and much more than in living ursids, accompanying reduction of the first digit; species of *Borocyon* show an increase in scapholunar thickness through time, culminating in a robust scapholunar supporting the weight of the forequarters through the radius, much as in *Panthera leo* and *P. tigris*;

(5) paraxonic fore- and hindfeet with elongate, straight-shafted metapodials (MC3–MC4, MT3–MT4) accompany a digitigrade stance, with shorter second and fifth metapodials and reduction of the first digits of the fore- and hindfeet; in addition:

- (a) proximal ends of metapodials not overlapped (interlocked) as in living felids;
- (b) no close appression of proximal metacarpal shafts yet some appression of metatarsals as in cheetah and canine canids;
- (c) metacarpals splay much like those in the lion;
- (d) metapodials with sharp developed distal keels that align paired sesamoids and tendons to favor fore–aft motion of the digits;
- (e) paraxonic metacarpals (MC3–MC4) of *Borocyon robustum* approaching lengths of paraxonic metatarsals (MT3–MT4), a situation most like wolves but unlike the cheetah;

(6) proximal phalanges somewhat elongate and largest on the paraxonic metapodials 3–4; intermediate phalanges short (with developed dorsal extensor processes) and lacking the marked degree of asymmetry indicative of claw retractility in felids; ungual phalanges of the forefoot long, laterally compressed, and tapering, hence similar to those of living ursids, suggesting that digging was possible (lions dig warthogs from burrows despite their specialized phalangeal anatomy); articular alignment of phalanges indicates presence of cushioning fore- and hindfoot pads;

(7) hindlimb providing a strong forward propulsive thrust as in large living felids, in which the form of *Borocyon* innominate and femur best approximate the form of those bones in *Panthera leo* and *P. tigris* among large living carnivores; posterior placement of the fovea capitis femoris for the femoral ligament like that of large living felids, and lacking the more central location seen in living wolf and coyote or in small domestic cats with parasagittal hindlimbs—hence, slight abduction of the *Borocyon* femur and hindlimb as in lion and tiger; ischial tuberosity of the pelvis only moderately everted as seen in large living felids, without the extreme degree of ischial eversion of wolves and cheetahs; muscle scar pattern of the posterior tibia for flexor muscles of the hindfoot as in the wolf and cheetah, suggesting a proximal concentration of muscle with long distal tendons; tibia much more massive in the larger *Borocyon* species due to greater body size, and a tibial-astragalar joint indicating a hindfoot emphasizing flexion-extension;

(8) hindlimb proportions similar to those of *Panthera leo*, *P. tigris*, and New World amphicyonines and lacking the distal elongation of tibia-fibula seen in canine canids and the cheetah—*Borocyon* and these large cats also correspond in tarsal anatomy, especially in the form of astragalus and calcaneum, reflecting tarsal elongation and specialization for parasagittal motion of the ankle and hindfoot; tarsal elongation in the terminal species, *B. robustum*, is especially evident from the shape and marked elongation of the cuboid and adjacent tarsal elements; a limited ability for inversion-eversion of the hindfoot is retained at the astragalonavicular and calcaneocuboid joints;

(9) absence of a complete vertebral column prevents detailed analysis of the participation of the back as it contributes to stride length; however, correspondence of the few

known vertebrae of *Borocyon* to those of *Daphoenodon superbus* leaves little doubt as to the presence of a similar column in which an anticlinal vertebra serves as a fulcrum for extension and flexion of the spine during the running/bounding gaits, contributing to an increase in stride length—this inference receives support from the partial vertebral column of *B. niobrarensis* (UW 10004) from Horse Creek Quarry in Wyoming, which matches the column of *D. superbus*;

(10) absolute limb lengths increasing steadily from Oligocene *Daphoenus vetus* to early Miocene *Daphoenodon superbus*, continuing through *Borocyon neomexicanus*, *B. niobrarensis*, and ending with *B. robustum*, paralleling the increase in body size in the daphoenine lineage; however, a proportional increase in length of the distal forelimb also occurs in daphoenines, beginning with *Daphoenus vetus* (humeroradial ratio <84%), *Daphoenodon superbus* (86.7%), and concluding with the species of *Borocyon* (~95%–97%); *Borocyon robustum* displays the most evolved lower forelimb, relative to the propulsive felidlike hindlimb, of any New World daphoenine or amphicyonine beardog;

(11) dimorphism evident where sample size is adequate: examples include the mandible (with dentition), radius, astragalus, calcaneum, and metapodials; large males and smaller females of both *Borocyon robustum* and *B. niobrarensis* are inferred from the presence of dimorphic (robust and gracile) metapodials of both fore- and hindfeet coming from four different localities (table 6).

GAIT AND STANCE

The musculoskeletal structure of a quadrupedal carnivoran predator reflects the locomotor strategy used to obtain its prey. Anatomical innovations recorded in the skeleton as preserved in the fossil record can be described and measured by the investigator, whereas physiological and behavioral attributes that accompany skeletal adaptations usually cannot be identified in fossils. As a result, we lack important information such as estimates of metabolic efficiency and endurance bearing on the economy of pursuit. These require knowledge of oxygen uptake, muscle cross-sectional area and fiber orientation, energy economy of various gaits, as well as evidence of social behaviors such as group hunting. Despite such limitations the musculoskeletal configuration and proportions of the limbs and feet of fossil carnivorans provide insight into the locomotor adaptations aiding in prey capture. To overtake prey, a predator benefits from enhanced speed, acceleration, maneuverability, and endurance, and these attributes combine in differing proportions in the various species of living Carnivora, where they are reflected to a greater or lesser degree in the skeleton. Thus, in fossils the appendicular skeleton remains a useful albeit incomplete guide. Lengthening of the limbs and adoption of a more upright stance, accompanied by skeletal modifications promoting a more restricted fore–aft motion of the limb and foot, are obvious adaptations influencing the gait, stride, and energy budget of Cenozoic carnivorans.

The term "cursorial" has been commonly used to describe carnivorans seemingly adapted for sustained, often rapid, efficient locomotion. These "running" mammals display anatomical specializations of the skeleton that are thought to contribute significantly to this cursorial ability. Some recent investigators have regarded the use of the term as ill-defined and nonspecific as to the morphological and physiological attributes that are essential to the definition of a cursorial mammal (Stein and Casinos, 1997; Carrano, 1999).

It has been generally agreed that some discussions of cursoriality in mammals confuse speed and endurance, whereas these two aspects merit separate consideration. There is no a priori reason why a very fast mammal should also exhibit great physiological endurance and, similarly, the converse is true. Some ambush predators may be very fast yet cannot sustain this speed for any distance, whereas other mammals may travel great distances but at rather average rates of speed. Taylor (1989) identified three types of "cursors": (1) running carnivorans that possess both speed and endurance (e.g., gray wolf); (2) sprinting carnivorans that employ an initial rapid acceleration, capturing prey by their speed over a shorter distance; and (3) "trotting" carnivorans that engage in prolonged pursuit but at only moderate speeds.

Some suggested definitions of the term that have arisen as a result of recent biomechanical studies cannot be employed for fossil mammals because they emphasize physiological characteristics that are indeterminate for extinct species. As a result, paleontologists have tended to emphasize morphological features that distinguish rapid and metabolically efficient living mammals, most of large body size, usually >10 kg. Here I use the term cursorial to refer to carnivorans with morphological specialization of their postcranial skeleton favoring parasagittal alignment of the limbs and demonstrated ability for fore–aft movement of the limb segments and feet, indicating increased stride length and locomotor efficiency. There is the tacit assumption that physiological endurance and an economy of gait in some form are the likely accompaniments to this morphology.

The skeletal morphology of species of *Borocyon* is reasonably compared with the anatomical adaptations of living large carnivorans of similar body size, while conceding that physiological attributes, whether mundane or remarkable, must remain unknown. However, from this comparison comes the realization that *Borocyon* had evolved a skeletal morphology unique to large carnivorans of its time, prefiguring many parallel adaptations in large predatory Carnivora of the late Cenozoic and Recent. Moreover, in the terminal species, *B. robustum*, we find a mosaic of skeletal features not seen in combination in any large living carnivoran. The existence in the fossil record of carnivores with a blend of adaptive traits of the locomotor system not found in any living carnivoran was recognized by Van Valkenburgh (1987).

Lengthening the limbs, particularly the lower limb and foot, are essential to the endurance strategy by increasing stride length. Recent studies of mechanical design in mammals suggest advantages (mass-specific muscle forces are reduced by increasing their mechanical advantage) that often accompany lengthening of the limbs and attaining a more upright stance (Biewener, 1989a, 1989b, 1990). Energy is further conserved by concentrating muscle mass in the proximal limb segments, thereby reducing the limb's moment of inertia and the energetic cost of locomotion (Myers and Steudel, 1985). Thin distal tendons transmit the force of a much thicker, proximally placed muscle while effectively reducing the mass of the lower limb.

Table 4 (fig. 19A, B) presents fore- and hindlimb proportions for amphicyonids relative to those of living ursids, felids, and canids based on the length ratios of radius/humerus and tibia/femur. Ursids, regardless of size, consistently have a tibia <83% (many <75%) the length of the femur. Felids possess a tibial length >83% the length of the femur, hence always longer than ursids, and certain felids (the puma, clouded leopard, and cheetah) exceed 90%, with the cheetah >100%. Canids (Caninae) also have markedly elongated the tibia, having ratios >96% and often reaching 107% in several species. Against this background, the "short-limbed" amphicyonids have ratios generally falling between ~80% and 90%, with *Borocyon* estimated to fall within this range at ~85%–90%. Thus, hindlimb proportions of *Borocyon* are much like those of *Panthera leo* and *P. tigris* and do not show the extreme "cursorial" adaptations exhibited by the wolf and cheetah. The *B. robustum* hindlimb is capable of powerful forward thrust while nonetheless incorporating a number of skeletal features favoring fore–aft motion in all hindlimb segments.

In the forelimb, proportional relationships among these carnivoran families differ from those evident in the hindlimb (table 4, fig. 19A). Ursid ratios range from 79% to 86% in most bears, but the black bear data suggest a tendency to lengthen the lower forelimb (~82%–92%) in this species. Most amphicyonid ratios fall below 90%. However, among amphicyonids, the species of *Borocyon* are remarkable in the lengthening of the distal forelimb. Values of ~95%–100% exceed the ratios of almost all cats except for the cheetah, which has a ratio similar to *Borocyon*. Other than the cheetah, the only other large felid exhibiting distal forelimb elongation is the lion with ratios consistently >90%. Living canids exhibit pronounced elongation of the radius/ulna with ratios from 97% to 108%.

From these observations it is evident that the forelimb can lengthen independently

from the hindlimb, and within a family (such as felids), limb proportions of species may vary while reflecting a common anatomical pattern: (1) ursids usually do not elongate the lower limb bones in either fore- or hindlimb but maintain short lower limb segments; (2) living canids are in direct opposition to ursids in that they elongate both the lower fore- and hindlimb segments; (3) felids exhibit a variety of possible options in limb elongation—the lion and tiger show similar hindlimb ratios, whereas the cheetah clearly parallels canids in elongation of both fore- and hindlimb, and the lion (relative to the tiger) evolved a lengthened forelimb apparently as an adaptation for pursuit of prey on the open African plains.

Certain species of living carnivoran "cursors" that employ trotting gaits sustained for long intervals lengthen both hindlimb and forelimb, as exemplified by canine Canidae. Others such as the lion and cheetah that engage in rapid, often short, but what in some situations can evolve into a prolonged pursuit, elongate the lower forelimbs, but not to the degree seen in Caninae. And the lion, while exhibiting some lengthening of its forelimb (fig. 19A), still maintains a rather short hindlimb for powerful thrust as it explodes from ambush.

Borocyon is exceptional among amphicyonids and even large living felids in elongation of the lower forelimb (fig. 19A; table 4). Whereas the *Borocyon* hindlimb is similar in its proportions to that of *Panthera leo*, *P. tigris*, as well as some amphicyonids, forelimb proportions are comparable to the cheetah and wolf.

In addition to increasing stride length, economy of motion is also achieved by confining the limb to a fore–aft path. This is evident in modification of skeletal structure, particularly the shape of limb and foot bones and congruent joint surfaces. Living canine canids (*Canis lupus*, *C. latrans*) exemplify many skeletal traits seen in limbs modified for fore–aft movement: these include closely registered joint surfaces in the lower limb segments; by bringing the elbow inward to lie under the shoulder; by increasing extension of the lower forelimb on the humerus to produce a more erect stance; by reduction of the carpal extensors and flexors arising from the distal humerus; by close apposition of the radius and ulna so that pronation/supination is more limited; by tight appression of the metapodials; by development of pronounced keels on the distal metapodials to lock the proximal phalanges; by interlocking of astragalus and calcaneum; and by the deeply grooved astragalar trochlea inserted in the distal tibia-fibula, practically limiting tarsal motion to a single degree of rotational freedom about the tibia. These morphological specializations contribute to the seemingly effortless habitual trotting gait of a canine pack on the hunt.

The species of *Borocyon* lack many of these canine skeletal adaptations for fore–aft motion of the limbs but they have evolved enough in parallel to suggest a facultative ability for some form of limited pursuit. Of these, the most significant are: (1) inward reorientation of the elbow demonstrating a more parasagittal alignment of the forelimb, and an elbow joint restricted to parasagittal flexion/extension; (2) modified form of the distal humerus indicating an erect forelimb stance with proximal ulna deeply inserted in olecranon fossa of the humerus, and a diminished medial epicondyle of the humerus indicating reduced torque at the elbow joint; (3) lengthening of the radius-ulna, closely united by a narrow interosseous ligament and membrane, suggesting less capability for pronation/supination of the manus, and a slender bladelike radius with reduced proximal and distal ends, as seen in radii of the wolf and cheetah; (4) paraxonic digitigrade fore- and hindfeet with straight-shafted elongate metapodials; (5) pronounced distal keels on the metapodials; (6) various integrated adaptations of femur, tibia, and hindfoot that promote propusive thrust but that also reflect an incipient parasagittal alignment and limited fore–aft motion of the hindlimb; these adaptations include evidence of femoral adduiction, proximal shift and reduction of posterior tibial musculature, an altered form of proximal tarsals and metatarsals in keeping with an erect digitigrade stance, and lesser emphasis on eversion-inversion of the hindfoot.

These skeletal features indicate that *Borocyon robustum* was probably capable of an

economy of gait involving a lengthened digitigrade stride and parasagittal fore–aft limb and foot motion differing from that of all contemporary amphicyonine beardogs. A powerful propulsive thrust provided by the hindlimbs, together with the robust muscled shoulders and lengthened forelimbs, conveys an image of a large, formidable carnivoran capable of strong acceleration and an interval of prolonged pursuit, but without the extreme skeletal and perhaps physiological adaptations of large canine canids.

Whether *Borocyon* species were able to employ an extended trotting gait for long intervals over open terrain requires a currently unavailable knowledge of physiology and behavior. However, the fact that these species occupied semiarid, open plains in the North American midcontinent during the early Miocene seems to implicate that environment in selecting for such traits, at least locally. It is suggestive in this regard that *Borocyon* from the Suwanee River of the Florida Gulf Coast does exhibit somewhat shorter limbs than its Great Plains counterpart.

Once these large carnivores overtake their prey, adaptations for the kill come into play, involving anatomical specialization of the teeth, skull, jaws, and forelimbs. The killing strategy may require that the forelimbs adopt a compromised structure so that they function both in locomotion and in prey capture. This is evident in a large felid such as the lion in which the forelimbs are essential both in pursuit and in holding and dispatching the prey. However, in canine cursors the potential use of the forelimb in prey capture is sacrificed to the fore–aft gait, a compromise favoring endurance, and is accompanied in wolves and African hunting dogs by reliance on pack hunting. Sustained gaits of the canine type must be powered by aerobic locomotion, and since the metabolic rate of active striated muscle achieves maximum efficiency at a speed of contraction somewhat less than the speed of maximum power output (Alexander, 2003), a gait such as the sustained trot seems well adapted to endurance pursuit in these canine cursors. The limb morphology of *Borocyon robustum* occupies an "intermediate" position between limbs of a large predatory felid such as *Panthera leo* and those of fully specialized cursors, the wolf and cheetah. Such a large intermediate morph does not exist among the extant carnivoran fauna.

From this perspective, *Borocyon robustum* emerges as an exceptional predator, not only among amphicyonids but when compared to large carnivorans throughout the Cenozoic. When considering the totality of its skeletal adaptations, this beardog was likely capable of some facultative form of sustained pursuit. Because the species of *Borocyon* lack the retractile claws of large living felids (*Panthera leo*, *P. tigris*), grasping and holding the prey during the kill would not have been an option. The massive skull with canidlike dentition suggests that the jaws and teeth were employed much as in large wolves. Its skeleton, with parasagittally aligned limbs anatomically specialized for more restricted fore–aft locomotion, suggests that a wide-ranging trotting gait emphasizing endurance may have been part of the adaptive strategy of this carnivore.

Physiological unknowns limit the degree of confidence that can be placed on conclusions derived solely from skeletal morphology (McNab, 1990). For example, an estimate of a carnivore's metabolic rate can be based upon the difference in consumption of oxygen between its resting rate and the maximum rate that can be achieved; this is termed the metabolic scope (Schmidt-Nielsen, 1984). This ratio has been found to approximate a value of 10 for most mammals (Hemmingsen, 1960; Taylor et al., 1981; Schmidt-Nielson, 1984) and is independent of body size. From these investigations, it emerged that both domestic dogs and wild canids such as the wolf possessed a metabolic scope three times greater than the general mammalian value (Langman et al., 1981), a 30-fold increase in oxygen consumption above the resting rate. This result has a significant bearing on the endurance of these carnivorans and influences their style of locomotion and preferred gaits. Such information remains largely beyond reach for extinct amphicyonids, yet if attainable would influence our evaluation of their locomotor pattern.

The species of *Borocyon* were not the first lineage of Carnivora to evolve limbs special-

ized for fore–aft motion and a lengthened stride. Temnocyonine amphicyonids developed elongate limbs and feet suggestive of a pursuit mode similar to that of living canids, yet the evidence of their postcranial anatomy is relatively sparse. Only five individuals are represented by skeletons that nonetheless convey a relatively complete picture of the anatomy of both fore- and hindlimbs. A few additional isolated bones from other localities can be directly compared with the more complete skeletons to provide a somewhat larger sample size. At least one partial postcranial skeleton assigned to each of the three currently recognized genera (*Temnocyon*, *Mammacyon*, and an undecribed genus) establishes that elongation of the limbs and feet was typical of end-member species of all of these lineages in the late Oligocene–early Miocene. Taken together, the species of *Borocyon* and the few temnocyonines represent the first Neogene experiments evolving a long-limbed, mid-sized to large carnivoran predator within North America.

DENTITION AND FEEDING

The dental formula of 3-1-4-3 in upper and lower jaws is consistent for nearly all species of North American amphicyonids except the temnocyonines, *Borocyon robustum*, and Clarendonian *Ischyrocyon*, which have lost M3. The migrant amphicyonines (*Amphicyon*, *Ysengrinia*, and *Cynelos*) that entered North America from Eurasia in the early Miocene all retain the full complement of molars (M1–M3/m1–m3) but reduce the size of their anterior premolars (P1–P3, p1–p3). North American daphoenine and temnocyonine amphicyonids retain well-developed premolar batteries in contrast to amphicyonines that live alongside them. Except for the presence of M3, the teeth of amphicyonids are similar in number and form to those of canids, so much so that they were for many years classified as Canidae (e.g., Simpson, 1945; Romer, 1966). Despite the similarity of the dentition, the morphology of the mandibular symphysis of daphoenine amphicyonids differs in some respects from Scapino's (1965) description of living *Canis*. However, as in canids, the symphysis of amphicyonids remains unfused, with the exception of some very old adults.

Jaw Registration

In *Daphoenodon superbus* the proportions of the holotype skull and mandibles (CM 1589) are only slightly distorted so that dental relationships during occlusion can be observed. Here, as in the wolf, the upper and lower toothrows are in contact in central occlusion yet the carnassials are not tightly registered. As the jaws are brought together in the wolf (*Canis lupus*), neuromuscular mechanisms first approximate the carnassial blades, followed by interlocking of the canines and I3 (Scapino, 1965; Mellet, 1981). Because canine contact is retarded relative to that of the carnassial pair, the wolf does not utilize the autocclusal bite mechanism described by Mellett (1984) in which the canines establish contact prior to the carnassials. In *Canis lupus* the canines do not come into firm contact until after the carnassials have begun to shear. However, in young *D. superbus*, the upper and lower canines make contact earlier in the bite, although not yet in a tightly locked relationship. As the carnassials wear over time, manual occlusion of the teeth in these beardogs suggests that interlocking of the canines eventually coincides with initial carnassial contact, suggesting that autocclusion employing the canines becomes more prevalent with age. This situation also apparently obtains in *Borocyon robustum* and *B. neomexicanus* where dental and mandibular dimensions correspond to those of the smaller *D. superbus*. Unfortunately, all skulls of *B. robustum* are distorted by crushing and lack canines so that the mandibles cannot be reliably occluded with the upper teeth. Nonetheless, certain aspects of its jaw mechanics can be described with some confidence.

In carnivorans with sectorial carnassials and a flexible mandibular symphysis, registration of the working-side mandible with the corresponding upper toothrow involves a lateral shift of the mandible as closure takes place. As the jaws close, the edges of the carnassials are brought into shearing registration by a slight lateral adjustment of the working mandible. Scapino (1965) described a coupling action in a canid between the zygomandibularis and medial pterygoid muscles of the working mandible that maintains

the carnassials in close registration. The precise registration of the carnassial blades, however, is facilitated by the shape of the craniomandibular joint and a flexible mandibular symphysis, which allows a final outward movement of the rear of the mandible to bring the m1–P4 into tight occlusion. At the end of the closing stroke, interlocking of the canines and I3 brings the mandibles into centric occlusion. As an individual ages, the molars and carnassials develop subhorizontal to flat wear surfaces in both canids (e.g., *Canis lupus*) and in amphicyonids. In old age, then, a precise occlusion was no longer possible or necessary because the shearing blades were worn away, leaving only broad crushing surfaces. At this point, some aged beardogs fused the mandibular symphysis and employed a jaw mechanism devoted entirely to crushing occlusion.

Mandibular Symphysis

Precise registration of the teeth is aided by a mobile mandibular symphysis in many species of Carnivora. The anatomy of the mandibular symphysis was analyzed in depth by Scapino (1965, 1981). Carnivoran symphyses were classified according to the way soft tissues in the symphyseal space related to the form of the mandibular symphyseal plates in histologic sections. Although in living Carnivora the form of the symphysis can differ with increasing body size and even within a species, the smallest species of *Daphoenodon* from the Great Plains and the largest *Borocyon* have similarly configured mandibular symphyses. These symphyses do not precisely correspond to any of Scapino's (1981) symphyseal types (Classes I–IV). However, the conjoined hemimandibles approximate his Class II symphysis where each symphyseal plate exhibits a smooth rectangular area anterosuperiorly and the remainder of the plate is characterized by numerous prominent, randomly oriented bony rugosities. The flat, non-rugose symphyseal plates of the wolf, considered a highly flexible Type I symphysis by Scapino, differ from these rugose, interdigitating plates evident in the symphyses of *Daphoenodon* and *Borocyon* species (fig. 38A, C).

The mandibular symphyseal plate of a female *B. robustum* (fig. 38A, UNSM 27002), in which the symphysis is well preserved, shows the anterosuperiorly placed, rectangular zone, with a smooth surface presumably for the attachment of a single, elongate fibrocartilage (length, 17.8 mm; width, 8.0 mm). In living carnivorans this fibrocartilage facilitates compression and expansion of the symphyseal joint. Below and posterior to the fibrocartilage zone, the remaining surface of the plate displays prominent interdigitating bony rugosities that show random alignment. These rugosities interlock with those of the opposing plate to prevent translation of the hemimandibles. The lower border of the mandible displays foramina leading into valleys between the rugosities, suggesting the possible presence of a venous network within the symphysis as described by Scapino (1981).

Additional intact mandibles of *B. robustum* (UNSM 25548, 25684, 26417) were carefully prepared and these exhibit a morphology of the symphyseal plates as in UNSM 27002. The mandibles of *Borocyon neomexicanus* (F:AM 49239) and *B. niobrarensis* (ACM 3452) that preserve an intact symphysis exhibit a similar morphology. Because the symphyseal plates in individuals of *Daphoenodon superbus* display the same pattern, this type of mandibular symphysis probably characterized the *Borocyon* lineage from its inception.

Of the carnivoran symphyses discussed and illustrated by Scapino (1981: fig. 3), the gross form of the symphysis of *B. robustum* seems at first to most closely approach *Ursus americanus* (fig. 38B). However, in *B. robustum* the fibrocartilage zone is larger and better developed than in the bear, and the robust, interdigitating rugosities lack the pronounced anteroposterior alignment evident in Scapino's (1981: fig. 3F) example of *Ursus* (some mandibles of *Borocyon robustum* do show an anteroposterior alignment of a few rugosities in the posterior symphyseal plate). The ursid symphyseal plate is elliptical in form, similar to that of *Borocyon robustum*, except that in ursids there is no evidence of a single, large anterosuperiorly placed fibrocartilage pad. In ursids the pad is narrow and irregular in form (Scapino, 1981) and lacks

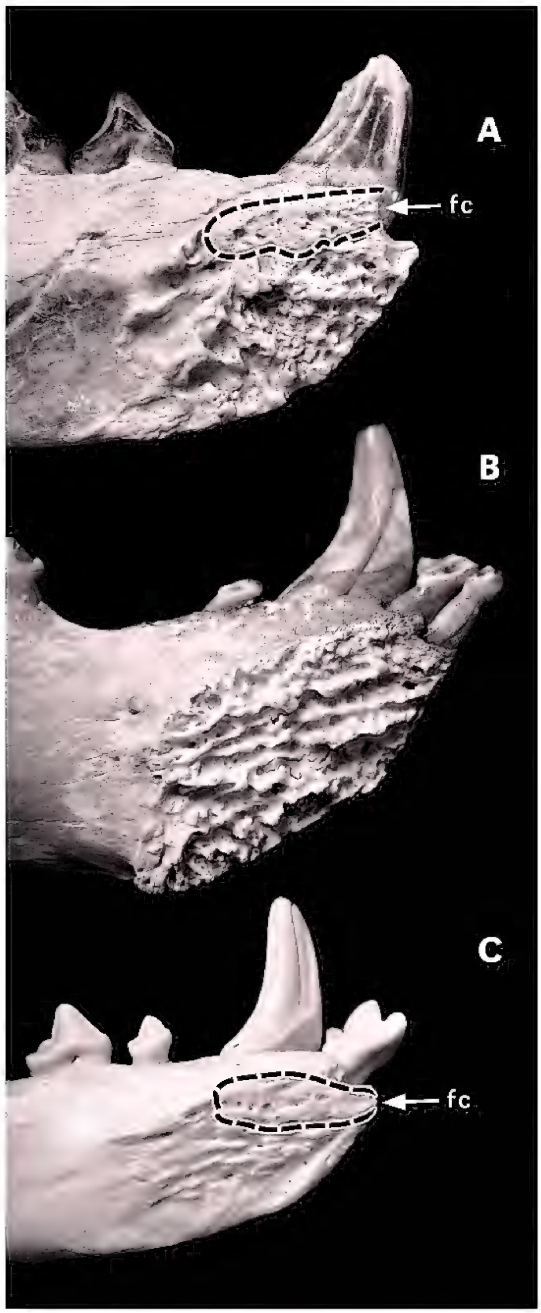

Fig. 38. Mandibular symphyses of (**A**) *Borocyon robustum*, (**B**) *Ursus americanus*, and (**C**) *Canis lupus*, in medial view, showing the symphyseal plate. Dashed line encloses the smooth bone for attachment of the subrectangular fibrocartilage pad (fc) in the wolf, which is inferred for *Borocyon robustum*. The symphyses of *Borocyon* and the wolf are considered to be flexible. The rugose, bony interdigitations of *B. robustum* symphyseal plates prevent translation of the hemimandibles more effectively than the smoother symphyseal plates of the wolf. The ursid lacks an extensive fibrocartilage and has a more rigid mandibular symphysis.

the smooth subrectangular surface situated along the upper part of the symphyseal plate that indicates its presence in the species of *Borocyon* and in *Daphoenodon superbus*.

Compression and expansion of the fibrocartilage pad contributed to flexibility of the symphyseal plates in *Borocyon*. In carnivorans with flexible symphyses, opening and closing of the posterior symphysis occurs about a vertical axis through the compressible fibrocartilage (Scapino, 1981). Slight rotation of the mandibles about their long axes, guided by the canines as the jaws close, also places the pad under compression as the carnassials are brought into contact during the bite. The fibrocartilage in *B. robustum*, just as in *Canis* (Scapino, 1965), probably accommodated movements of the mandible about its long axis during carnassial shear and crushing by the molars (m2–m3, M1–M2). The only articulating pair of hemimandibles of *B. robustum* belonging to a single individual (UNSM 25548, 25684) shows that rotation about a vertical axis through the symphysis results in opening of the posterior symphysis, and also permits slight rotation of these mandibles about their long axes. Furthermore, the presence of a single, large fibrocartilage pad clearly indicated in several individuals (UNSM 27002, 26417, 25548) indicates an ability for compression about a vertical axis through the pad and hence some symphyseal mobility.

The considerable height of the guiding canines and carnassials in *B. robustum* places a constraint on side-to-side shift of the jaws during the closing phase of the power stroke. Scapino (1981) described this action involving flexible symphyses of Types I and II, which is applicable in modified form to *B. robustum*. As the working mandible moves laterad, the posterior symphyseal space widens, with this action occurring around a vertical axis passing through the fibrocartilage pad. As the mandible comes to a stop,

constrained by the tissues of the craniomandibular joint, the carnassials are aligned but not yet in contact and the canines have met to guide the closure of the jaws. As the working mandible closes, it rotates inward slightly as m1 slides upward against P4. This compresses the fibrocartilage pad, which will return to its initial shape as the jaws open.

Scapino (1981) observed that a strongly interdigitated symphysis with limited or absent fibrocartilage pad was a stiff symphysis. He recognized this type of symphysis in large living felids and ursids. In ursids the interdigitating rugosities and various binding ligaments make dorsoventral or anteroposterior translational shear of the symphyseal plates impossible. However, manipulation of the hemimandibles of *Ursus americanus* shows that a very limited amount of rotation about the long axis of the mandible can occur. On the other hand, manipulation of the hemimandibles of *B. robustum* (UNSM 25548, 25684) demonstrates much more symphyseal mobility, involving rotation around the long axis of the mandible and also about a vertical axis through the fibrocartilage. Under Scapino's classification, a mandibular symphysis as seen in *B. robustum* would differ from those of ursids and should be similar to Class II with limited flexibility. The condition of the mandibular symphysis and dentition in *B. robustum* accords with Scapino's (1981: 370) summary analysis whereby a mobile symphysis and large carnassials might be expected in carnivorans processing hard materials such as bone. In durophagous carnivorans of large size, the complex interdigitating, rugose symphyseal plates prevent mandibular dislocation while interposed soft tissues still permit some flexibility.

In summary, the sample of mandibles of *Borocyon robustum* demonstrates the probable presence of a single, large fibrocartilage pad; of limited movement about the long axis of the mandible and around a vertical axis through the symphysis when hemimandibles are conjoined; and of foramina entering the rugose bone at the ventral border of the symphysis. These traits taken together suggest (1) a compressible symphyseal pad; (2) posterior opening and closing of the symphysis around a vertical axis through the pad; (3) the ability to adjust carnassial registration by limited mandibular axial rotation; and (4) perhaps incorporation of venous blood within the symphysis involved in volume adjustments (expansion–contraction) of symphyseal connective tissues. Some such movement at the symphysis is essential to precise registration of the large *Borocyon* carnassials, as evidenced by wear patterns on these teeth.

Scapino (1981) considered a flexible symphysis with a fibrocartilage pad, intermandibular cruciate ligaments, and a venous plexus as primitive for carnivorans. The mandibular symphysis in *Borocyon robustum* possibly still reflects this primitive condition, but with adjustment for increased body size, here considered to be the pronounced rugose interdigitation preventing translation of the symphyseal plates while still permitting some flexibility in the joint.

Dental Occlusion and Toothwear

It is possible to accurately describe dental occlusion and toothwear in several North American amphicyonids where adequate samples exist. A sample of *Daphoenodon superbus* from the den site at Agate Fossil Beds National Monument (Hunt et al., 1983), and from coeval waterhole deposits (Hunt, 1990), provides a series of ontogenetic stages from juveniles to aged adults, totaling at least 14 individuals. Mandibles of this species range in ontogenetic age from a young individual with only milk teeth in place to aged males with the molars nearly worn flat. Wear on the teeth, both premolars and molars, is consistent with patterns observed in other species of the genus—these species probably employed the teeth during feeding in the same manner.

As an individual of *D. superbus* ages, its teeth show the greatest degree of wear in two areas of the dentition: the canines and the carnassial/molar group. Incisors are gradually blunted by wear over time, yielding flat-surfaced pegs. Premolars (p1–p4, P1–P3) are not heavily worn, even in the oldest individuals in which wear is limited to blunting the principal cusp on each tooth (on p4, both the principal and posterior accessory cusps are eventually worn flat). The degree of wear increases as one proceeds backward in the

toothrow, culminating in heavily worn carnassials and molars. Thus, it is evident that food taken into the mouth was transferred to the rear where the focus of mastication occurred.

The dentition of both juveniles and adults of the species of *Borocyon* shows near identity of dental pattern and wear relative to the teeth of the *D. superbus* sample; a similar dental/mandibular function and ontogeny of tooth usage and wear is inferred for these species, presumably retained through descent from populations of late Arikareean *Daphoenodon*. Toothwear facets on the carnassials and molars in *D. superbus* provide evidence of shear as well as the blunting of cusps. The shearing blade of m1, formed by the labial surfaces of paraconid and protoconid, is nearly vertical in young adults in which wear has just been initiated (this wear surface forms a "V" on the labial face of the trigonid, the apex downward, ending at the cingulum). A reciprocal vertical wear surface on P4 appears on the inner surface of the metastylar blade and paracone. As m1 slides past P4 during shear, m1 is shifted slightly linguad as it moves along the inner face of P4 and the lingual surfaces of the M1 paracone and metacone.

Without food between the teeth, full closure of the jaws results in wear facets produced by direct contact of upper and lower canines, incisors, and p4–m3 with P4–M3. There are several contact points along the toothrow: (1) the interdigitating alignment of the canines and third incisors produces deeply grooved vertical facets on these teeth, but only flat wear surfaces appear on the blunted tips of the inner incisors; (2) insertion of m1 into the embrasure between P4 and M1 takes place without contact of the m1 protoconid with the maxilla—the upward trajectory of m1 is arrested by contact of its talonid basin with the M1 protocone, and by contact of m2–m3 with the posterior half of M2 and M3; and (3) the principal and accessory cusps of the large p4 produce a vertical facet on the anterior face of P4, and the principal p4 cusp also creates a facet on the inner heel of P3. The more anterior premolars usually do not directly occlude; food is trapped between their principal cusps and worked back to the carnassials and molars by the tongue—the horizontal, blunt wear surfaces limited to the principal cusps of the anterior premolars show that pressure contact with their tips is the principal cause of tooth wear.

Examination of an ontogenetic series of wolf (*Canis lupus*) dentitions shows that there is an established sequence of wear facets that develop on the carnassials, molars, and premolars as the animal ages. This sequential wear pattern is closely approximated by mandibles of *Daphoenodon*. Initially, in the wolf, only the tips of cusps are slightly blunted by wear, chiefly on the carnassials. Next, significant wear appears on the carnassial pair as a narrow strip of dentine where the enamel has been breached along the cutting edges of P4 and the m1 trigonid; this strip extends from paraconid to protoconid on m1, and from paracone to metastylar blade on P4. Wear on P4 is often pronounced in the carnassial notch itself. This wear pattern is consistent with the Every effect, the interlocking of upper and lower carnassials by resistant food material (Mellett, 1981). Other than the wear on P4 in the upper teeth, only the para- and metacone of M1 show flat wear facets from slight blunting of these cusps. This stage is followed by a confluence of horizontal facets from increased blunting of the cusps on m1 proto- and paraconids and the metaconid. P4 shows further wear on paracone and metastylar blade creating a planar surface that is slightly medially inclined. The paracone and metacone of M1 are next worn to more extensive flat surfaces but remain tall, and the principal cusps of the anterior premolars (p2–p4, P1–P3) now show initial wear. Finally, in late wear, the m1 protoconid and paraconid are heavily worn to a nearly continuous planar surface—hypoconid and entoconid are worn to a flat platform as is the m2 protoconid, producing a uniform crushing surface extending from the m1 talonid to include the entire m2. The P4 paracone is also heavily worn to form a lingually inclined surface that extends onto the metastylar blade. Wear on the para- and metacone of M1 has produced a continuous horizontal surface. Wear on the tips of the anterior premolars yields blunt cusps, with wear most extreme on the more posterior teeth (P3, p4).

If the mandibles of wolves are manually occluded at each of these various wear stages, it becomes evident that tooth-to-tooth contact involving carnassial shear during food processing is not the principal agency producing wear facets on the teeth. The only possible cause of this wear pattern during ontogeny is the processing of hard food objects that serve to blunt the teeth. It is well known that wolves will process and often consume bone of their prey along with meat (Mech, 1970; Mech et al., 1971; Haynes, 1982, 1983; Gazzola et al., 2005), and it is bone and other resistant connective tissues that are responsible for the blunting of the cusps over time. Young and Goldman (1944: 245) reported the contents of the stomach of a male Alaskan wolf that bears on this point: "The stomach was about half full of the hair, skin and leg bones of a Dall sheep. These bones had been bitten into small sections about one inch in length by the strong carnassial, or chopping teeth, of the wolf." Van Valkenburgh (1988) found that when processing hard materials, tooth breakage is a frequent occurrence among large living carnivores, with bone-processors most prone to tooth fracture. Of the eight *B. robustum* mandibles, two show damaged teeth subsequently abraded through later wear.

The same pattern of blunting of the cusps on carnassials, molars, and premolars of the wolf is evident in *Borocyon robustum*, the only species of *Borocyon* where the sample of mandibles is adequate to judge ontogenetic wear. However, in these *Borocyon* mandibles the m2 is lengthened relative to m2 of *Canis lupus*, creating a longer, more developed crushing platform that extends from the m1 talonid to m3. This platform in *B. robustum* is 35%–36% (N = 6) of the functional toothrow length (p2–m3). It is ~26% in the wolf (N = 7). It is this platform that serves as the locus for bone processing in the African hunting canid *Lycaon pictus* (Van Valkenburgh, 1996). Thus, the wear pattern of the dentition, the presence of a crushing platform at the rear of the toothrow, the structure of the mandibular symphysis and craniomandibular joint, as well as the robust skull with massive temporomandibular musculature suggest that durophagy was probably important in food processing by these large, mobile carnivorans.

Scapino (1981) considered a flexible symphysis to be a practical adaptation in large durophagous carnivorans crunching hard bone, allowing the teeth to avoid sudden damaging impacts when breaking hard material, a behavior made possible by a compensating rotation of the mandible about its long axis. *Borocyon robustum* represents an end-member of a lineage that came to rely on carnassial/molar crushing for the processing of hard materials.

The method of Therrien (2005) was used to create a mandibular force profile for *Borocyon robustum* (table 7). The hemimandible (UNSM 25684) that best occluded with the paratype cranium (see frontispiece) was measured because of the lack of distortion of its mandibular corpus and dentition. This is a large individual (UNSM 25684), probably male, but not the largest of the available hemimandibles of the species. Bite force calculated at successive points along the length of the mandible reflects adaptation to load-bearing (Biknevicius and Ruff, 1992a, 1992b). Bending strength is represented by the section modulus (Z) calculated from measurements of mandibular depth and width at these points.

Therrien (2005) argued that the mandibular force profile derived from these values for jaw depth and width contributed insight into feeding behavior. He applied beam theory to the hemimandible, which was modeled in cross-section as a solid ellipse of bone. Biknevicius and Ruff (1992a) developed a similar model that accounted for the absence of bone within the mandibular cylinder (medullary space), a method requiring planar radiographs of the mandible to measure cortical bone thickness.

The mandibular force profile for *B. robustum* (fig. 39) was compared to those for canid, felid, and hyaenid carnivores presented by Therrien (2005: figs. 3–7). Mandibular depth and width were measured at the same interdental loci utilized by Therrien (2005: fig. 2). Bending strength in the dorsoventral (Zx) and labiolingual (Zy) planes was calculated from these measurements as well as relative mandibular force (Zx/Zy). The values for Zx and Zy, relative to the distance (L) from the articular condyle to each interdigital locus, allow a comparison among

TABLE 7
Mandibular Force Profile for *Borocyon robustum* (UNSM 25684) Calculated According to Therrien's (2005) Method of Beam Analysis

	Section Modulus		Distance (cm) from Articular Condyle	Measure of Bending Strength		
	Zx	Zy		Log Zx/L[a]	Log Zy/L[b]	Zx/Zy[c]
Canine	6.08	5.06	21.80	−0.55	−0.63	1.20
P3–P4	3.61	1.62	16.90	−0.67	−1.02	2.23
P4–M1	4.23	1.75	14.80	−0.54	−0.93	2.41
M1–M2	5.71	2.23	11.54	−0.31	−0.71	2.56
M2–M3	5.87	2.04	9.57	−0.21	−0.67	2.88
Post M3	7.22	2.17	8.50	−0.07	−0.59	3.33

[a]Dorsoventral force.
[b]Labiolingual force.
[c]Relative force.

carnivore species of the magnitude of bending strength along the length of the mandible.

Zx/Zy values are proportional to the ratio of the depth and width diameters. Ratios >1.00 demonstrate resistance to dorsoventral loading (a deep, narrow mandible); a ratio <1.00 indicates a resistance to labiolingual torsion or bending. Therrien (2005) suggested that the ability to tolerate high dorsoventral loading enabled the animal to exert considerable bite force on its prey. Resistance to labiolingual forces permitted the carnivore to withstand strong torsional and transverse forces that result from the processing of hard materials or from the violent actions of struggling prey.

The mandibular force profile of *B. robustum* closely corresponds to those of living canids such as the grey (*Canis lupus*) and dire wolves (*Canis dirus*), but it parallels living hyenas in the strength of the symphyseal region (fig. 39). Therrien (2005) considered that the high Zx/Zy values of hyaenids (~1.20) at the canine reflect a well-buttressed symphysis, on occasion involved in bone processing in *Crocuta*. The Zx/Zy value for *B. robustum* at the canine is also 1.20 but it is unlikely that the symphyseal region was routinely involved in bone processing. Although the highly interdigitated, rugose bone of the *Borocyon* symphysis attests to its strength relative to that of the wolf, the force profile suggests that durophagous processing was accomplished by the post-carnassial battery that forms the crushing platform at the back of the mandible. As in canids studied by Therrien, the slope for the dorsoventral force values (Zx/L) was steeper than that for the relatively uniform labiolingual values (Zy/L, table 7), indicating that dorsoventral bending strength is pronounced beneath the posterior cheek teeth. The Zx/Zy values similarly indicate increased dorsoventral buttressing of the mandible beneath the crushing molars.

A deep mandibular corpus beneath the molars was interpreted by Therrien (2005) as an adaptation for bone processing, and it supports the inference that *B. robustum* was a durophagous feeder (note the marked increase in Zx/Zy behind the carnassial from 2.56 to 3.33, which is similar to *Canis lupus* at 2.66 to 3.24). When considering labiolingual forces (Zy/L) applied to the mandible during torsion and the application of transverse stresses, the mandible of *B. robustum* is apparently equally strong at the canine and in the post-carnassial region, reflecting that the emphasis in mandibular reinforcement is principally focused on a highly developed resistance to dorsoventral bending in the postcarnassial mandibular corpus.

Application of Therrien's method to *B. robustum* does not provide absolute values for bite force but yields a useful relative comparison with living carnivores that suggests a feeding style involving quick, shallow but powerful bites, a strongly buttressed mandibular symphysis, and the processing of hard materials by the posterior cheek teeth, hence a composite of canid and hyaenid attributes, and in overview the possibility of a pack hunting lifestyle. No

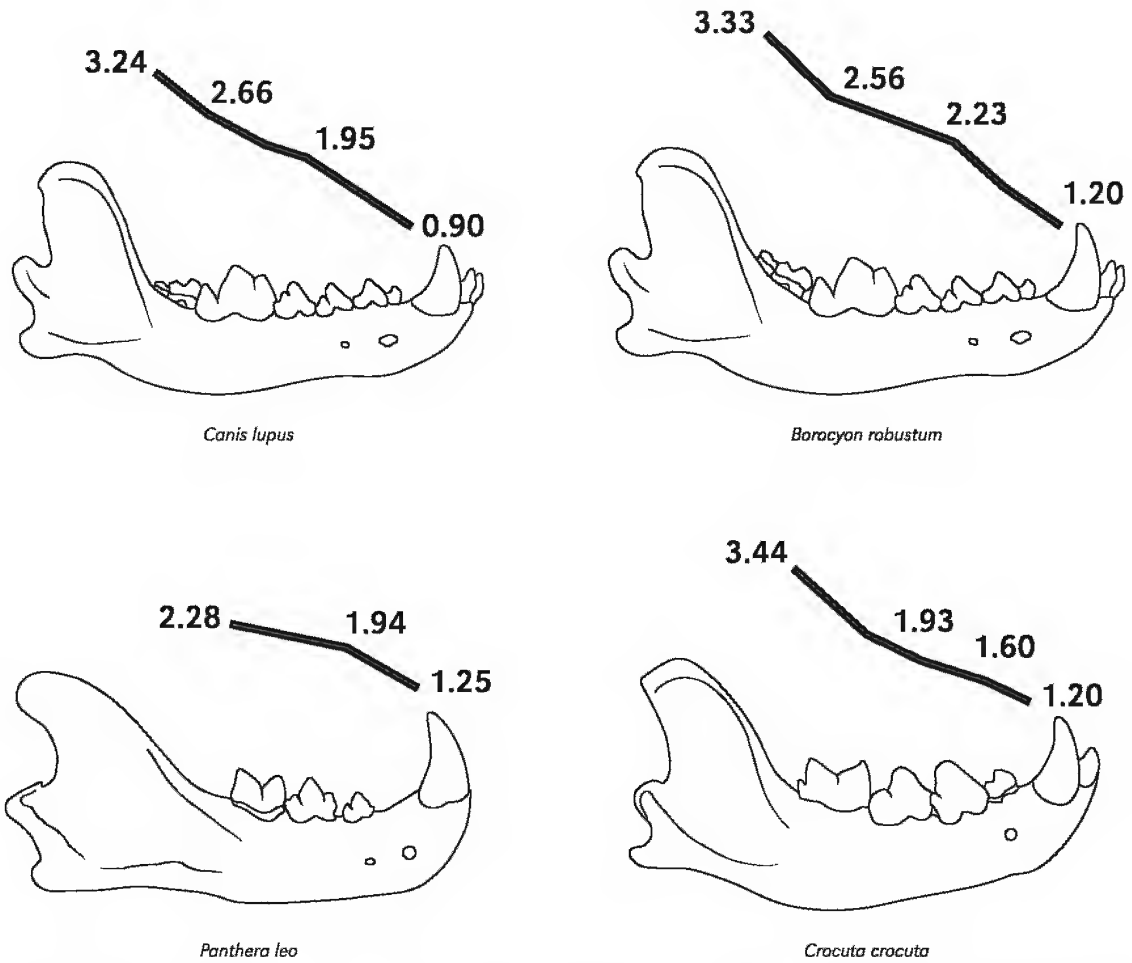

Fig. 39. Mandibular force profiles of large living carnivorans and the amphicyonid *Borocyon robustum* (in part from Therrien, 2005). Values represent relative mandibular force (Zx/Zy).

large living carnivore is an exact comparator to *Borocyon robustum* in its mandibular morphology and force profiles—its feeding style appears to have combined adaptations distributed today among large canids and hyaenids. Perhaps most striking, however, is that the forces generated by its mandibular biomechanics were indeed formidable.

In the totality of its mandibular and dental characteristics, *Borocyon robustum* remains somewhat outside the morphologic spectrum represented by living large carnivorans, a predator whose anatomical mosaic of craniodental and postcranial traits existed only briefly in the North American early Miocene interval.

CONCLUSIONS

The daphoenine amphicyonid *Borocyon robustum* was the dominant long-limbed predatory carnivoran of the North American early Miocene. The species occurs from the Pacific Northwest through the Great Plains to the Florida Gulf Coast, a geographic range made known only recently. Although previously unrecognized as a keystone species of its predator guild, due to scarcity of fossil remains, currently available craniodental and postcranial material provide a nearly complete account of the skeleton. The principal skeletal modifications evolved within the *Borocyon* lineage were identified by compar-

ison with the plesiomorphic species *Daphoenodon superbus* and *D. notionastes*, which are both "short-legged" daphoenine amphicyonids.

Borocyon robustum represents the conclusion of a remarkable experiment within the daphoenine Amphicyonidae, evolving a long-limbed pursuit predator, capable of securing its prey through enhanced muscular strength and an economic gait that probably emphasized endurance over speed. The lengthened forelimb, equaling proportions of efficient living runners such as wolves, attests to this. The forelimb is remarkable for an early Miocene amphicyonid, and its musculoskeletal characteristics are distinct from all New World amphicyonines. Elongation of the distal forelimb is most similar to that of living wolves and cheetahs and is more pronounced than seen in living lions and tigers. The hindlimbs, adapted for forward thrust with a parasagittal alignment, powered the engine of locomotion. A proportional increase in stride length, together with limb elements emphasizing efficient fore–aft motion, suggests a capability for stamina and even speed in pursuit of prey.

Craniodental morphology of *B. robustum* includes a canid-like dentition with well-developed canines, premolars, carnassials, and crushing post-carnassial molars. The wear pattern of these teeth gives evidence of processing hard food materials while retaining a capability for carnassial shearing during the early and prime periods of the carnivore's lifespan. In old age the crushing function predominated, based on the tendency for molars and carnassials to be worn to blunted, flat subhorizontal surfaces. The form of the mandibular symphysis suggests a degree of mobility during mastication, with this flexibility adjusting the jaws for processing durophagous materials such as bone.

Borocyon robustum, as the terminal species of the lineage, emerges as a mosaic of craniodental and postcranial traits not evident in any other extinct or living large carnivoran. This predator evolved skeletal features that precede similar parallel adaptations seen today in several of the large canid and felid lines. Yet the total array of skeletal features occurring in *B. robustum* represents its own unique adaptive solution to the environments of the North American early Miocene. Among the large predatory Carnivora of the Oligocene and early Miocene, *Borocyon robustum* and the temnocyonine amphicyonids are the closest anatomical parallels to the longer-limbed pursuit predators of the Pleistocene and Recent.

The species of *Borocyon* frequented semiarid terrain of New Mexico and the Great Plains in the early Miocene and it seems probable that the lengthened limbs and anatomical adaptations for an economy of gait evolved in response to the drying climate and more open terrain of the North American midcontinent in the late Arikareean–early Hemingfordian interval. Its size and efficiency as a dominant member of its predator guild surely contributed to its subsequent appearance in the Pacific Northwest and the Gulf Coast.

ACKNOWLEDGMENTS

Curators at the following instutitions generously loaned material for this study: M.C. Coombs, ACM; R.H. Tedford and M.C. McKenna, AMNH; M.R. Dawson, CM; Ted Fremd, John Day National Monument; L.D. Martin and C.D. Frailey, KU; W.A. Clemens and A.D. Barnosky, UCMP; B.J. MacFadden, UF; P. Freeman, UNSM; J.A. Lillegraven and M. Cassiliano, UW. The late Ted Galusha (AMNH) discovered and collected the important and only known sample of *Borocyon neomexicanus* from New Mexico in 1947. Galusha and R.H. Tedford brought the sample to my attention and introduced me to Standing Rock Quarry. I extend my thanks to Mary Dawson (CM), who allowed access over many years to Peterson's specimens of amphicyonids, as well as to field notes and specimen labels that established the site of collection of the *Borocyon* holotype. To the landowners of western Nebraska and Oregon who granted us access during this study, I am particularly appreciative.

Most illustrations are the work of UNSM staff artist Angie Fox. Without her talent and attention to detail this report would not have been possible. Some illustrations were completed in the 1960s by the late Ray Gooris of

the American Museum. Preparation of much of the UNSM material of *Borocyon* was initially undertaken by the Frick Laboratory of the American Museum from the 1930s to 1960s. Recently collected specimens were prepared by Ellen Stepleton and Rob Skolnick (UNSM), who discovered additional unprepared material of *Borocyon* in the UNSM collections that contributed signficantly to the study. I benefited from a careful reading of the manuscript and suggestions for improvement by M.C. Coombs and two anonymous reviewers. Funding has been provided by the Harriet Meek Fund (UNSM) and by National Science Foundation DBI-0535316.

REFERENCES

Alexander, R.M. 1988. Elastic mechanisms in animal movement. Cambridge and New York: Cambridge University Press, 141 pp.

Alexander, R.M. 2003. Principles of animal locomotion. Princeton: Princeton University Press, 370 pp.

Alexander, R.M., M.B. Bennett, and R.F. Ker. 1986. Mechanical properties and function of the paw pads of some mammals. Journal of the Zoological Society of London 209: 405–419.

Anyonge, W. 1993. Body mass in large extant and extinct carnivores. Journal of the Zoological Society of London 231: 339–350.

Bertram, J.E., and A.A. Biewener. 1990. Differential scaling of the long bones in the terrestrial Carnivora and other mammals. Journal of Morphology 204: 157–169.

Biewener, A.A. 1989a. Scaling body support in mammals: limb posture and muscle mechanics. Science 245: 45–48.

Biewener, A.A. 1989b. Mammalian terrestrial locomotion and size: mechanical design principles define limits. Bioscience 39: 776–783.

Biewener, A.A. 1990. Biomechanics of mammalian terrestrial locomotion. Science 250: 1097–1103.

Biknevicius, A.R., and C.B. Ruff. 1992a. The structure of the mandibular corpus and its relationship to feeding behaviors in extant carnivorans. Journal of the Zoological Society of London 228: 479–507.

Biknevicius, A.R., and C.B. Ruff. 1992b. Use of biplanar radiographs for estimating cross-sectional geometric properties of mandibles. Anatomical Record 232: 157–163.

Carrano, M.T. 1999. What, if anything, is a cursor? Categories versus continua for determining locomotor habit in mammals and dinosaurs. Journal of the Zoological Society of London 247: 29–42.

Cassiliano, M. 1980. Stratigraphy and vertebrate paleontology of the Horse Creek-Trail Creek area, Laramie County, Wyoming. Contributions to Geology University of Wyoming 19: 25–68.

Christiansen, P. 1999. Scaling of the limb bones to body mass in terrestrial mammals. Journal of Morphology 239: 167–190.

Christiansen, P., and J.S. Adolfssen. 2005. Bite forces, canine strength, and skull allometry in carnivores (Mammalia, Carnivora). Journal of the Zoological Society of London 266: 133–151.

Davis, D.D. 1949. The shoulder architecture of bears and other carnivores. Fieldiana Zoology 31: 285–305.

Davis, D.D. 1964. The giant panda: a morphological study of evolutionary mechanisms. Fieldiana Zoology, Memoirs 3: 1–339.

English, A.W. 1978. Functional analysis of the shoulder girdle of cats during locomotion. Journal of Morphology 156: 279–292.

Evans, H.E. 1993. Miller's Anatomy of the dog. 3rd ed. Philadelphia: W.B. Saunders, 1113 pp.

Fisher, R.V., and J.M. Rensberger. 1972. Physical stratigraphy of the John Day Formation, central Oregon. University of California Publications in Geological Sciences 101: 1–33.

Frailey, D. 1979. The large mammals of the Buda local fauna (Arikareean: Alachua County, Florida). Bulletin of the Florida State Museum 24(2): 123–173.

Galusha, T. 1966. The Zia Sand Formation, new early to medial Miocene beds in New Mexico. American Museum Novitates 2271: 1–12.

Galusha, T. 1975. Stratigraphy of the Box Butte Formation, Nebraska. Bulletin of the American Museum of Natural History 156(1): 1–68.

Gawne, C. 1981. Sedimentology and stratigraphy of the Miocene Zia Sand of New Mexico. Geological Society of America Bulletin 92: 999–1007.

Gazzola, A., I. Bertelli, E. Avanzinelli, A. Tolosano, P. Bertotto, and M. Apollonio. 2005. Predation by wolves (*Canis lupus*) on wild and domestic ungulates of the western Alps, Italy. Journal of the Zoological Society of London 266: 205–213.

Gingerich, P.D. 1990. Prediction of body mass in mammalian species from long bone lengths and diameters. Contributions from the University of Michigan Museum of Paleontology 28(4): 79–92.

Ginsburg, L. 1961. Plantigradie et digitigradie chez les carnivores fissipedes. Mammalia 25(1): 1–21.

Ginsburg, L. 1977. *Cynelos lemanensis* (Pomel), carnivore ursidé de l'Aquitanien d'Europe. Annales de Paléontologie 63(1): 57–104.

Gonyea, W., and R. Ashworth. 1977. The form and function of retractile claws in the Felidae and other representative carnivorans. Journal of Morphology 145: 229–238.

Goslow, G.E., Jr., H.J. Seeherman, C.R. Taylor, M.N. McCutchin, and N.C. Heglund. 1981. Electrical activity and relative length changes of dog limb muscles as a function of speed and gait. Journal of Experimental Biology 94: 15–42.

Haynes, G. 1982. Utilization and skeletal disturbances of North American prey carcasses. Arctic 35(2): 266–281.

Haynes, G. 1983. A guide for differentiating mammalian carnivore taxa responsible for gnaw damage to herbivore limb bones. Paleobiology 9(2): 164–172.

Hemmingsen, A.M. 1960. Energy metabolism as related to body size and respiratory surfaces, and its evolution. Report of the Steno Memorial Hospital (Copenhagen) 9: 1–110.

Hunt, R.M., Jr. 1990. Taphonomy and sedimentology of Arikaree (lower Miocene) fluvial, eolian, and lacustrine paleoenvironments, Nebraska and Wyoming: a paleobiota entombed in fine-grained volcaniclastic rocks. Geological Society of America Special Paper 244: 69–111.

Hunt, R.M., Jr. 1996. Amphicyonidae (Chap. 23). *In* D. Prothero and R.J. Emry (editors), The terrestrial Eocene-Oligocene transition in North America: 476–485. Cambridge and New York: Cambridge University Press.

Hunt, R.M., Jr. 2001. Small Oligocene amphicyonids from North America (*Paradaphoenus*, Mammalia, Carnivora). American Museum Novitates 3331: 1–20.

Hunt, R.M., Jr. 2002a. Intercontinental migration of Neogene amphicyonids (Mammalia, Carnivora): appearance of the Eurasian beardog *Ysengrinia* in North America. American Museum Novitates 3384: 1–53.

Hunt, R.M., Jr. 2002b. New amphicyonid carnivorans (Mammalia, Daphoeninae) from the early Miocene of southeastern Wyoming. American Museum Novitates 3385: 1–41.

Hunt, R.M., Jr. 2003. Intercontinental migration of large mammalian carnivores: earliest occurrence of the Old World beardog *Amphicyon* (Carnivora, Amphicyonidae) in North America. *In* L.J. Flynn (editor), Vertebrate fossils and their context: contributions in honor of Richard H. Tedford. Bulletin of the American Museum of Natural History 279: (chap. 4) 77–115.

Hunt, R.M., Jr. 2004. Global climate and the evolution of large mammalian carnivores during the later Cenozoic in North America. *In* G.C. Gould and S.K. Bell (editors), Tributes to Malcolm C. McKenna: his students, his legacy. Bulletin of the American Museum of Natural History 285: (chap. 11) 139–156.

Hunt, R.M., Jr. 2005. An early Miocene dome-skulled chalicothere from the "Arikaree" conglomerates of Darton: calibrating the ages of High Plains paleovalleys against Rocky Mountain tectonism. American Museum Novitates 3486: 1–45.

Hunt, R.M., Jr., and E. Stepleton. 2004. Geology and paleontology of the upper John Day beds, John Day River Valley, Oregon: lithostratigraphic and biochronologic revision in the Haystack Valley and Kimberly areas (Kimberly and Mt. Misery quadrangles). Bulletin of the American Museum of Natural History 282: 1–90.

Hunt, R.M., Jr., and E. Stepleton. 2006. Biochronologic and lithostratigraphic reappraisal of the upper John Day Formation, north-central Oregon. Paleobios 26(2): 21–25.

Hunt, R.M., Jr., X.-X. Xue, and J. Kaufman. 1983. Miocene burrows of extinct beardogs: indication of early denning behavior of large mammalian carnivores. Science 221: 364–366.

International Commission on Zoological Nomenclature. 1985. International Code of Zoological Nomenclature, 3rd ed., adopted by the International Union of Biological Sciences. London: International Trust for Zoological Nomenclature.

Jenkins, F.A., Jr., 1973. The functional anatomy and evolution of the mammalian humero-ulnar articulation. American Journal of Anatomy 137(3): 281–298.

Jenkins, F.A., Jr., and S.M. Camazine. 1977. Hip structure and locomotion in ambulatory and cursorial carnivores. Journal of the Zoological Society of London 181: 351–370.

Langman, V.A., R.V. Baudinette, and C.R. Taylor. 1981. Maximum aerobic capacity of wild and domestic canids compared. Federation Proceedings 40: 432.

Loomis, F.B. 1936. Three new Miocene dogs and their phylogeny. Journal of Paleontology 10(1): 44–52.

MacFadden, B.J., and R.M. Hunt, Jr. 1998. Magnetic polarity stratigraphy and correlation of the Arikaree Group, Arikareean (late Oligocene-early Miocene) of northwestern Nebraska. Geological Society of America Special Paper 325: 143–165.

McNab, B.K. 1990. The physiological significance of body size. *In* J. Damuth and B.J. MacFadden (editors), Body size in mammalian paleontology: 11–23. Cambridge and New York: Cambridge University Press.

Mech, L.D. 1970. The wolf: ecology and behavior of an endangered species. New York: Natural History Press, 384 pp.

Mech, L.D., L.D. Frenzel, R.R. Ream, and J.W. Winship. 1971. Movements, behavior, and ecology of timber wolves in northeastern Minnestota. *In* L.D. Mech and L.D. Frenzel (editors), Ecological studies of the timber wolf in northeastern Minnesota. U.S. Forest Service Research Paper NC-52: 1–35.

Mellett, J.S. 1981. Mammalian carnassial function and the "Every Effect". Journal of Mammalogy 62: 164–166.

Mellett, J.S. 1984. Autocclusal mechanisms in the carnivore dentition. Australian Mammalogy 8: 233–238.

Merriam, J.C. 1901. A contribution to the geology of the John Day Basin. University of California Publications in Geological Sciences 2(9): 269–314.

Myers, M.J., and K. Steudel. 1985. Effect of limb mass and its distribution on the energetic cost of running. Journal of Experimental Biology 116: 363–373.

Nowak, R.M. 1991. Walker's Mammals of the world. 5th ed. Baltimore: Johns Hopkins University Press, 1629 pp.

Ohale, L.O.C., and H.B. Groenewald. 2003. The morphological chacteristics of the antebrachiocarpal joint of the cheetah (*Acinonyx jubatus*). Onderstepoort Journal of Veterinary Research 70(1): 15–20.

Peterson, O.A. 1907. The Miocene beds of western Nebraska and eastern Wyoming and their vertebrate faunae. Annals of the Carnegie Museum 4(1): 21–72.

Peterson, O.A. 1909. A new genus of carnivores from the Miocene of western Nebraska. Science 29(746): 620–621.

Peterson, O.A. 1910. Description of new carnivores from the Miocene of western Nebraska. Memoir of the Carnegie Museum 4(5): 205–278.

Romer, A.S. 1966. Vertebrate paleontology. 3rd ed. Chicago: University of Chicago Press, 468 pp.

Scapino, R. 1965. The third joint of the canine jaw. Journal of Morphology 116: 23–50.

Scapino, R. 1981. Morphological investigation into functions of the jaw symphysis in carnivorans. Journal of Morphology 167: 339–375.

Schaller, G.B. 1973. Golden shadows, flying hooves. New York: Alfred Knopf, 287 pp.

Schmidt-Nielsen, K. 1984. Scaling: why is animal size so important. Cambridge and New York: Cambridge University Press, 241 pp.

Schramm, E.F., and H.J. Cook. 1921. The Agate anticline, Sioux County, Nebraska. Bulletin A, Kanoka Petroleum Company, Lincoln, Nebraska, 38 pp.

Simpson, G.G. 1945. The principles of classification and a classification of mammals. Bulletin of the American Museum of Natural History 85: i–xvi, 1–350.

Stein, B.R., and A. Casinos. 1997. What is a cursorial mammal? Journal of the Zoological Society of London 242: 185–192.

Taylor, C.R., G.M. Maloiy, E.R. Weibel, V.A. Langman, J.M. Kamau, H.J. Seeherman, and N.C. Heglund. 1981. Design of the mammalian respiratory system. III. Scaling maximum aerobic capacity to body mass: wild and domestic mammals. Respiratory Physiology 44: 25–37.

Taylor, M.E. 1989. Locomotor adaptations by carnivores. *In* J.L. Gittleman (editor), Carnivore behavior, ecology and evolution: 382–409. Ithaca: Cornell University Press.

Tedford, R.H. 1981. Mammalian biochronology of the late Cenozoic basins of New Mexico. Geological Society of America Bulletin 92: 1008–1022.

Tedford, R.H. 1982. Neogene stratigraphy of the northwestern Albuquerque Basin. *In* New Mexico Geological Society Guidebook, 33rd Field Conference, Albuquerque Country II: 273–278.

Tedford, R.H., L.B. Albright, A.D. Barnosky, I. Ferrusquia-Villafranca, R.M. Hunt, Jr., J.E. Storer, C.C. Swisher, M.R. Voorhies, S.D. Webb, and D.P. Whistler. 2004. Mammalian biochronology of the Arikareean through Hemphillian interval (late Oligocene through early Pliocene epochs). *In* M.O. Woodburne (editor), Late Cretaceous and Cenozoic mammals of North America: 169–231. New York: Columbia University Press.

Therrien, F. 2005. Mandibular force profiles of extant carnivorans and implications for the feeding behavior of extinct predators. Journal of the Zoological Society of London 267: 249–270.

Tokuriki, M. 1973a. Electromyographic and joint mechanical studies in quadrupedal locomotion. I. Walk. Japanese Journal of Veterinary Science 35: 433–448.

Tokuriki, M. 1973b. Electromyographic and joint mechanical studies in quadrupedal locomotion. II. Trot. Japanese Journal of Veterinary Science 35: 525–535.

Van Valkenburgh, B. 1987. Skeletal indicators of locomotor behavior in living and extinct carnivores. Journal of Vertebrate Paleontology 7: 162–182.

Van Valkenburgh, B. 1988. Incidence of tooth breakage among large predatory mammals. American Naturalist 131(2): 291–302.

Van Valkenburgh, B. 1996. Feeding behavior in free-ranging large African carnivores. Journal of Mammalogy 77(1): 240–254.

Wang, X. 1993. Transformation from plantigrady to digitigrady: functional morphology of locomotion in *Hesperocyon* (Canidae: Carnivora). American Museum Novitates 3069: 1–23.

Yalden, D.W. 1970. The functional morphology of the carpal bones in carnivores. Acta Anatomica 77: 481–500.

Young, S.P., and E.A. Goldman. 1944. The wolves of North America (Part I). New York: Dover, 385 pp.

APPENDIX 1

Limb Bone Lengths (in mm) and Proportions of Daphoenine and Amphicyonine Amphicyonids, Living Ursids, Felids, and Canids

	Humerus	Radius	R/H[a]	Femur	Tibia	T/F[b]
AMPHICYONIDAE						
Daphoenus vetus						
F:AM 50329	168	129	76.8	193	172	89.1
F:AM 25451	142	119	83.8			
AMNH 11857	165	138	83.6		178	
CM 492	185	135	73.0	201	179	89.0
YPM PU 13792	165	129	78.2	184	167	90.8
USNM 17847	160	125	78.1			
F:AM 76206	159	125	78.6			
Daphoenodon superbus						
CM 1589	210	182	86.7	230	205	89.1
Borocyon neomexicanus						
F:AM 68241	241					
F:AM 68242		234	97.0[e]	282		90.8[f]
F:AM Jemez 7-105		240	99.6[e]			
F:AM 68243				302		
F:AM Jemez 6-86				306		
F:AM Jemez 7-106					256	
Borocyon niobrarensis						
ACM 3452	270	265	98.1			
UNSM 25555	263					
UW 10004	264	250	94.7	319	271	85.0
Borocyon cf. *B. robustum*						
KU 113751	280					
KU 113706		255				
KU 113645				322		
Borocyon robustum						
UNSM 26260	286					
UNSM 26210	339[g]		95.8[g]			
UNSM 25877		275				
UNSM 25595		290				
UNSM 26426		291				
UNSM 25554		299				
UNSM 26297		302				
UNSM 25553		316				
UNSM 26425		319				
UNSM 44721		317				
UNSM 26435				380		
UNSM 26343				356[h]		
UNSM 25558					321	84.5[i]
UNSM 26360					314	88.2[i]
Ysengrinia americana						
CM 2400	300					
UNSM 44606	287					
F:AM 54147	270	241[h]	89.3			
USNM 186993				351	280	79.8
UNSM 44600		260				
UNSM 44601		250				
UNSM 44691		252				
UNSM 44624				364		
UNSM 44690				353		
UNSM 44620					287	
UNSM 44621					297	

APPENDIX 1
(Continued)

	Humerus	Radius	R/H[a]	Femur	Tibia	T/F[b]
UNSM 44622					287	
UNSM 44623					288	
Cynelos lemanensis[c]	220	197	89.5	282	240	85.1
Adilophontes brachykolos	222	199	89.6			
URSIDAE						
Ursus arctos						
CNHM 43744[d]	304	247	81.2	355	248	69.9
CNHM 47419[d]	312	255	81.7	377	253	68.2
CNHM 84467[d]	204	162	79.4	249	179	71.9
Ursus arctos (Kodiak)						
ZM 17888	405	334	82.5	448	331	73.9
ZM 19565	395	329	83.3	451	325	72.1
CNHM 63802[d]	415	345	83.1	519	355	68.4
CNHM 27268[d]	386	305	79.0	464	315	67.9
CNHM 63803[d]	327	268	82.0	390	275	70.5
Ursus americanus						
UNSM 16986	268	240	89.6	299	239	79.9
UNSM 283	288	259	89.9	330	261	79.1
UNSM 15112	247	221	89.5	278	229	82.4
UNSM 3253	250	231	92.4	282	229	81.2
AM 24157	334	282	84.4	370	281	75.9
KU 12725m	328	269	82.0	358	282	78.8
KU 2232	297	266	89.5	343	262	76.4
KU 158714	243	224	92.1	285	220	77.2
Thalarctos maritimus						
AM 75244	394	340	86.3	465	346	74.4
AM 75245	385	325	84.4	453	335	73.9
ZM 16938	396	339	85.6	477	346	72.5
Helarctos malayanus						
ZM 27897	228	193	84.6	247	182	73.7
ZM 13875	180	153	85.0	194	144	74.2
FELIDAE						
Felis concolor						
UNSM 19688	231	192	83.1	270	256	94.8
KU 73932	218	183	83.9	260	244	93.8
KU 155308m	225	185	82.2	264	242	91.7
Panthera tigris						
ZM 14343	296	242	81.8	334	285	85.3
ZM 14602	270	225	83.3	314	262	83.4
ZM 14603	274	221	80.7	—	—	—
AM 217100	301	260	86.4	345	296	85.8
AM 14030	267	226	84.6	301	261	86.7
AM 14032	298	250	83.9	340	291	85.6
AM 85404	344	289	84.0	398	347	87.2
AM 85396	345	287	83.2	398	349	87.6
AM 135846	313	265	84.7	348	300	86.2
Panthera leo						
AM 85140	324	298	94.0	361	307	85.0
AM 85142	303	285	94.0	350	298	85.1
AM 85143	323	300	92.9	369	309	83.7
AM 85144	328	295	90.0	369	317	85.9
AM 85145	296	278	93.9	344	297	86.3
AM 85147	289	265	91.7	323	275	85.1

APPENDIX 1
(Continued)

	Humerus	Radius	R/H[a]	Femur	Tibia	T/F[b]
AM 85149	330	302	91.5	368	322	87.5
AM 52078	369	333	90.2	404	339	83.9
AM 80609	332	311	93.7	372	320	86.0
AM 54995	322	293	91.0	360	320	88.9
KU 164623	302	278	92.1	339	302	89.1
KU 9432	339	311	91.7	377	324	85.9
KU 8413	280	260	92.9	319	279	87.5
KU 2768	300	280	93.3	331	291	87.9
KU 157340	349	314	90.0	382	328	85.9
AM 54996	301	273	90.7	338	302	89.3
Neofelis nebulosa						
UNSM 16951	141	116	82.2	157	150	95.5
KU 143489m	174	144	82.7	189	182	96.3
KU 158656f	143	114	79.7	158	148	93.7
Acinonyx jubatus						
UNSM 16913	263	252	95.8	285	287	100.7
UNSM 15518	236	235	99.6	254	260	102.3
UNSM 15552	253	250	98.8	279	280	100.3
UNSM 16019	—	—	—	244	244	100.0
CANIDAE						
Canis lupus						
CNHM 21207[d]	209	213	101.9	234	233	99.6
CNHM 51772[d]	228	227	99.6	255	246	96.5
CNHM 51773[d]	216	210	97.2	241	233	96.7
CNHM 54015[d]	209	207	99.0	230	232	100.9
UNSM 15596	230	230	100.0	244	261	106.9
UNSM 17458	—	—	—	244	253	103.7
UNSM 17459	233	232	99.6	253	260	102.8
UNSM 12641	222	226	101.8	238	253	106.3
KU 157331m	239	239	100.0	245	269	109.8
KU 2137	237	234	98.7	251	266	106.0
Canis latrans						
UNSM 14166	170	173	101.7	184	194	105.4
UNSM 14180	166	173	104.2	181	194	107.1
UNSM 14246	155	160	103.2	172	178	103.4
UNSM 14459	165	172	104.2	176	183	104.0
UNSM 713	161	164	101.9	175	184	105.1
UNSM 2382	160	164	102.5	175	183	104.6
UNSM 3392	159	166	104.4	177	186	105.1
KU 16087m	167	170	101.8	179	189	105.6
Chrysocyon brachyurus						
Davis, 1964: 35[d]	—	—	108.1 (2)[j]	—	—	107.8 (2)[j]

m indicates male; f, female.

[a]Humeroradial index (Davis, 1964).

[b]Femorotibial index (Davis, 1964).

[c]From Ginsburg (1977).

[d]From Davis (1964).

[e]234/241 mm and 240/241 mm, the range of estimated R/H ratios.

[f]256/282 mm, the most probable T/F ratio.

[g]Estimated length, calculated using proportions of an incomplete humerus. An R/H of 96.5 was determined for *Borocyon robustum* using an average humerus length of 312 mm and an average radius length of 301 mm.

[h]Estimated.

[i]321/380 mm (Hemingford Quarries) and 314/356 mm (Bridgeport Quarries), the estimated T/F ratios.

[j]Sample size.

APPENDIX 2
Metapodial Lengths (in mm) of North American Daphoenine Amphicyonids

	MC2	MC3	MC4	MC5	MT2	MT3	MT4	MT5	MC1 or MT1
Daphoenodon superbus									
CM 1589	51	62	60	47	59	70	73	62	32 (MC1)
									42 (MT1)
CM 1589C					63.1	73.3	77.3	68.3	42.3 (MT1)
CM 2774		60.5							
AMNH 81055								68.5	
CM 1599					57.7			69.4	
CM 1589A						72.4			
CM 1589B[a]	58.4	68.3				73.6			
FMNH UC1362						72.5	76.6		
Daphoenodon skinneri									
None									
Daphoenodon falkenbachi									
None									
Borocyon neomexicanus									
F:AM 68241	63.6							71[b]	38.5 (MC1)
F:AM 68240A	72.5								
F:AM 68242			78.5	67.2	76.9	85.0	91.5		
F:AM 68244			78.3						48.2 (MT1)
Borocyon robustum									
Runningwater Fm.									
UNSM 25574	82.1								
UNSM 26432	79.8								
UNSM 25564		96.7							
UNSM 26434		96.7							
UNSM 26433		95.0							
F:AM 68263			82.3						
F:AM 68264				76.0					
F:AM 68264A				84.2					
UNSM 25572				79.1					
UNSM 26444					87.0				
UNSM 26443					90.1				
UNSM 25562						106.9			
UNSM 26446						100.6			
UNSM 26445						108.3			
UNSM 26447							115.4		
UNSM 26448							109.6		
UNSM 25563							108.2		
F:AM H275-2716							110.2		
F:AM 68265							105.7		
F:AM 68265A								86.5	
UNSM 26450								92.7	
UNSM 26449								80.0	
CM 1918									49.7 (MC1)
Borocyon robustum									
Bridgeport Quarries									
UNSM 26460									53.4 (MC1)
UNSM 26461									50.6 (MC1)
UNSM 26462	84.1								
UNSM 26463	84.3								
UNSM 26464	82.4								
UNSM 26465	79.1								
UNSM 26466	77.4								

APPENDIX 2
(Continued)

	MC2	MC3	MC4	MC5	MT2	MT3	MT4	MT5	MC1 or MT1
UNSM 26467		93.3							
UNSM 26468		98.9							
UNSM 28469		88.7							
UNSM 26470		92.6							
UNSM 26471		98.8							
UNSM 26472		97.5							
UNSM 26473			102.0						
UNSM 26474			100.0						
UNSM 26475			95.1						
UNSM 26476			100.6						
UNSM 26477				78.1					
UNSM 26478				76.2					
UNSM 26479				77.0					
UNSM 26480				78.0					
UNSM 26408					92.0				
UNSM 26409					89.8				
UNSM 26410					89.7				
UNSM 26411						105.8			
UNSM 26412						102.6			
UNSM 26413						103.3			
UNSM 26414							108.0		
UNSM 44700								97.6	
UNSM 44701								100.2	
Zia Sand Fm. (Chamisa Mesa Mbr.)									
F:AM 68254			94.4	76.4					
Borocyon niobrarensis									
Runningwater Fm. (lower part)									
ACM 3452	72.4	85.3	85.3	70.8					44.8 (MC1)
ACM 34-58		82.2	84.0						
UNSM 44702	71.2	86.4	87.6						
F:AM 107601	69.6								
F:AM 68269							104.9		
Unnamed rock unit									
UW 10004			85.5	68.5	79.2	92.3	97.0		
Borocyon cf. *B. robustum*									
Suwannee River, Florida									
KU 118496		86.3							
KU 118495		78.2							
KU 118488						91.9			
KU 118486							100.5[b]		
KU 118484								82.5	
KU 118502									42.2 (MC1)
Adilophontes brachykolos									
Anderson Ranch Fm.									
F:AM 54140						74.0	78.9		

MC indicates metacarpal; MT, metatarsal.
[a]Metapodials may not belong to one individual.
[b]Estimated measurement.

APPENDIX 3
Metapodial Lengths (in mm) of Living Canids, Felids, Ursids, and Hyaenids

	MC2	MC3	MC4	MC5	MT2	MT3	MT4	MT5	MC1	MT1
CANIDAE										
Canis lupus										
UNSM 15596	90.0	100.9	101.8	88.3	97.3	109.9	114.2	103.1	33.2	
UNSM 17459	84.2	96.7	96.1	83.7	94.1	106.1	109.0	99.8	33.4	
UNSM 17431	—	—	—	—	96.9	111.7	115.1	100.4	—	
KU 83463f	81.9	91.5	91.5	79.9	90.7	102.7	103.3	92.4	30.5	
KU 157331m	89.5	100.5	100.3	86.0	99.2	111.0	112.8	100.9	32.9	
Canis latrans										
UNSM 14459	59.7	68.0	66.8	56.4	67.3	74.3	75.4	67.9	22.6	
UNSM 14246	59.8	67.7	67.4	57.6	67.9	75.4	76.7	67.0	—	
UNSM 14166	65.5	73.4	74.5	62.2	74.2	82.6	83.7	74.6	—	
UNSM 14180	59.5	66.5	66.6	56.6	69.0	75.0	77.0	69.1	—	
UNSM 3392	62.1	70.5	68.6	57.6	70.9	77.9	79.0	68.1	—	
KU 16087m	61.8	70.1	69.1	59.0	71.2	79.8	80.9	72.8	—	9.5
FELIDAE										
Felis concolor										
UNSM 19688	75.1	84.2	79.7	62.4	93.9	103.1	100.4	89.1	28.6	
UNSM 25870	79.2	86.5	82.8	64.6	94.2	105.6	104.2	92.4	—	
KU 12722f	72.0	79.5	72.6	58.2	85.5	96.0	94.4	82.1	25.8	11.4
KU 155308m	68.5	77.5	72.7	58.1	90.8	103.5	99.7	85.6	25.9	
Neofelis nebulosa										
UNSM 16951	37.5	44.6	43.0	34.6	51.7	56.9	58.6	54.5	17.5	
KU 143489m	46.8	54.2	52.0	41.8	60.0	67.3	68.7	62.0	22.3	
Acinonyx jubatus										
UNSM 16913	75.7	90.8	87.8	69.3	102.2	117.6	116.7	97.1	24.6	
UNSM 16019	—	—	—	—	89.3	101.7	100.1	85.4	13.6	
UNSM 15518	71.3	87.1	84.0	67.2	98.1	109.7	109.7	94.5	14.1	
UNSM 15552	74.2	89.0	86.6	67.6	100.1	116.6	116.1	97.1	24.8	
UNSM 15479	57.9	69.5	68.7	53.1	82.7	98.1	97.4	82.0	19.8	
UNSM 15603	65.7	77.8	75.6	60.1	—	—	—	—	21.8	
Panthera onca										
UNSM 16919	55.5	62.0	59.6	47.4	64.9	73.8	73.6	66.2	24.5	
Panthera pardus										
UNSM 21000	60.2	69.7	67.0	53.8	74.6	83.3	83.2	76.3	21.1	
KU 127982f	54.9	63.5	60.7	47.6	69.3	78.7	77.9	70.3	21.2	11.5
KU 41253f	56.1	67.3	65.6	50.9	72.5	84.6	86.0	75.0	23.1	11.9
Panthera leo										
UNSM 15480	98.6	109.3	102.1	83.9	—	—	—	—	—	
KU 164623	95.2	109.0	105.5	85.9	109.6	123.3	123.6	108.8	42.1	18.2
KU 9432m	111.1	122.4	118.4	99.5	124.8	138.6	137.3	123.5	—	21.9
KU 2753m	99.0	115.5	113.2	88.9	117.2	133.7	136.4	121.2	—	
KU 163781f	95.5	111.7	106.8	86.2	113.1	123.8	124.7	113.0	38.1	20.8
KU 8413f	92.7	105.3	102.1	82.4	108.8	119.7	118.2	106.9	40.6	23.6
KU 12102f	94.8	108.7	104.0	85.4	110.8	123.4	123.5	108.4	38.7	22.0
KU 2768	91.2	104.7	101.4	84.7	110.3	123.8	124.2	112.0	39.4	
Panthera tigris (Siberia)										
UNSM 16656	103.5	118.0	113.8	88.9	—	—	—	—	42.7	
FMNH 159999f	95.4	110.8	105.6	82.3	109.2	125.3	121.2	105.7	40.9	19.6
Panthera tigris (So. Asia)										
FMNH 60760f	93.0	108.0	101.0	82.0	107.8	123.0	119.2	104.0	36.2	

APPENDIX 3
(Continued)

	MC2	MC3	MC4	MC5	MT2	MT3	MT4	MT5	MC1	MT1
FMNH 57172	95.8	111.6	105.4	83.8	110.9	125.4	122.7	111.1	39.7	
FMNH 134496m	94.7	108.1	104.8	83.4	109.8	123.1	121.5	108.1	42.5	
FMNH 165401	83.0	97.2	93.1	74.3	95.0	110.0	109.2	96.6	35.4	
Panthera tigris (Sumatra)										
UNSM 14602	83.1	94.4	90.1	70.1	96.5	109.2	106.8	95.3	33.2	
UNSM 14343	89.1	101.1	97.9	75.1	—	—	—	—	37.1	
URSIDAE										
Ursus americanus										
UNSM 1870	60.8	65.3	65.7	64.0	60.9	65.3	65.7	64.6	50.4	46.7
UNSM 15112	59.1	62.3	62.9	63.0	56.4	60.5	67.0	66.4	—	
KU 158714f	55.4	58.5	60.6	60.0	51.8	57.5	64.3	64.0	45.0	42.3
KU 2232	67.8	70.5	73.0	73.8	65.6	71.2	78.4	77.3	56.9	53.3
Ursus arctos (Kodiak)										
ZM 17888	98.6	101.0	103.9	105.9	95.0	102.2	110.2	114.1	93.0	84.1
HYAENIDAE										
Crocuta crocuta										
UNSM 16471	86.1	97.9	96.0	81.4	80.8	89.6	89.0	76.3		
UNSM 16470	90.3	103.8	98.1	76.1	84.1	94.6	89.8	71.0		
Hyaena brunnea										
UNSM 15506	86.0	97.9	95.0	82.2	80.4	87.7	85.3	75.9		

MC indicates metacarpal; MT, metatarsal; m, male; f, female.

APPENDIX 4
Comparative Length (in %) of Paraxonic Metatarsals 3–4 Relative to Metacarpals 3–4 of Living Canids, Felids, Ursids, Hyaenids, and the Amphicyonid *Borocyon*

	%MT3 > MC3	%MT4 > MC4
AMPHICYONIDAE		
Daphoenodon superbus		
CM 1589	12.9	21.7
Borocyon neomexicanus[a]	—	16.6
Borocyon niobrarensis[b]	9.1	13.3
Borocyon robustum[c]	9.4	10.2
CANIDAE		
Canis lupus		
UNSM 15596	8.9	12.2
UNSM 17459	9.7	13.4
KU 83463f	12.2	12.9
KU 157331m	10.4	12.5
Canis latrans		
UNSM 14459	9.3	12.9
UNSM 14246	11.4	13.8
UNSM 14166	12.5	12.3
UNSM 14180	12.8	15.6
UNSM 3392	10.5	15.2
KU 16087m	13.8	17.0
FELIDAE		
Felis concolor		
UNSM 19688	22.4	26.0
UNSM 25870	22.1	25.8
KU 12722f	20.8	30.0
KU 155308m	33.5	37.1
Neofelis nebulosa		
UNSM 16951	27.6	36.3
KU 143489m	24.1	32.1
Acinonyx jubatus		
UNSM 16913	29.5	32.9
UNSM 15518	25.9	30.6
UNSM 15552	31.0	34.0
UNSM 15479	41.1	41.8
Panthera onca		
UNSM 16919	19.0	23.5
Panthera pardus		
UNSM 21000	19.5	24.1
KU 127982f	23.9	28.3
KU 41253f	25.7	31.1
Panthera leo		
KU 164623	13.1	17.2
KU 9432m	13.2	16.0
KU 2753m?	15.8	20.5
KU 163781f	10.8	16.8
KU 8413f	13.7	15.8
KU 12102f	13.5	18.8
KU 2768	18.2	22.5
Panthera tigris		
UNSM 14602	15.7	18.5
FMNH 57172	12.4	16.4
FMNH 60760	13.9	18.0
FMNH 159999	13.1	14.8
FMNH 134496	13.9	15.9
FMNH 165401	13.2	17.3
URSIDAE		
Ursus americanus		
UNSM 1870	0.0	0.0
UNSM 15112	−3.0	6.5
KU 158714f	−1.7	6.1
KU 2232	1.0	7.4
Ursus arctos (Kodiak)		
ZM 17888	1.2	6.1
HYAENIDAE		
Crocuta crocuta		
UNSM 16471	−9.3	−7.9
UNSM 16470	−9.7	−9.2
Hyaena brunnea		
UNSM 15506	−11.6	−11.4

APPENDIX 4
(Continued)

MT indicates metatarsal; MC, metacarpal; m, male; f, female.

[a]Not certainly from one individual but from the same quarry.

[b]Based on two individuals of similar body size, one with MC3–MC4, the other with MT3–MT4.

[c]Based on averages from multiple individuals.